



Search for a resonance decaying into a scalar particle and a Higgs boson in final states with leptons and two photons in proton–proton collisions at $\sqrt{s} = 13$ TeV with the ATLAS detector

The ATLAS Collaboration

A search for a hypothetical heavy scalar particle, X , decaying into a singlet scalar particle, S , and a Standard Model Higgs boson, H , using 140 fb^{-1} of proton–proton collision data at the centre-of-mass energy of 13 TeV recorded with the ATLAS detector at the LHC is presented. The explored mass range is $300 \leq m_X \leq 1000 \text{ GeV}$ and $170 \leq m_S \leq 500 \text{ GeV}$. The signature of this search is one or two leptons (e or μ) from the decay of vector bosons originating from the S particle, $S \rightarrow W^\pm W^\mp / ZZ$, and two photons from the Higgs boson decay, $H \rightarrow \gamma\gamma$. No significant excess is observed above the expected Standard Model background. The observed (expected) upper limits at the 95% confidence level on the cross-section for $gg \rightarrow X \rightarrow SH$, assuming the same $S \rightarrow WW/ZZ$ branching ratios as for a SM-like heavy Higgs boson, are between 530 (800) fb and 120 (170) fb.

Contents

1	Introduction	2
2	ATLAS detector	4
3	Data and simulation samples	5
3.1	Data Samples	5
3.2	Monte Carlo simulated samples	5
4	Object and event selection	8
4.1	Object selection	8
4.2	Event selection	9
4.3	Boosted Decision Tree strategy	10
5	Background estimation	13
6	Systematic uncertainties	14
6.1	Theoretical uncertainties	14
6.2	Experimental uncertainties	15
6.3	Continuum background modelling uncertainty	15
7	Results	16
8	Conclusion	20

1 Introduction

The Higgs boson was discovered by the ATLAS [1] and CMS [2] Collaborations in 2012 [3, 4]. Since then, an important goal has been to determine the Higgs boson properties and to perform precision measurements using proton–proton (pp) collision data from the Large Hadron Collider (LHC). Up until now, all measured properties are consistent with the Standard Model (SM) Higgs boson predictions [5, 6]. This discovery not only demonstrates the existence of the Higgs boson, but it also opens up new frontiers in particle physics that aim to address the limitations of the SM. There are a variety of beyond-the-SM scenarios that introduce additional scalar bosons such as the Next-to-Minimal Supersymmetric Standard Model (NMSSM) [7, 8], the Two-Real-Singlet Model (TRSM) [9, 10] or two-Higgs-Doublet Models (2HDM) [11].

The 2HDM+S model [12] extends the 2HDM hypothesis by considering the production of a heavy CP-even scalar boson (X) that could decay into an SM Higgs boson (H) and a hypothetical scalar singlet (S). A representative diagram of the $X \rightarrow SH$ production via gluon–gluon fusion is shown in Figure 1. The $X \rightarrow SH$ branching ratio is assumed to be 100%.

Searches inspired by the 2HDM+S probing $X \rightarrow SS \rightarrow WW^*WW^*$ [13], $X \rightarrow SH \rightarrow b\bar{b}\gamma\gamma$ [14] and $X \rightarrow SH \rightarrow VV\tau\tau$ [15], where V can be either a W^\pm or Z boson, have been performed by the ATLAS Collaboration. For the latter, no significant excess is observed above the expected SM processes, and 95% confidence level (CL) upper limits are set on the signal production cross-section between 542 fb and 72 fb in the mass ranges $500 \leq m_X \leq 1500$ GeV and $200 \leq m_S \leq 500$ GeV [15]. The $X \rightarrow SH$ search in the

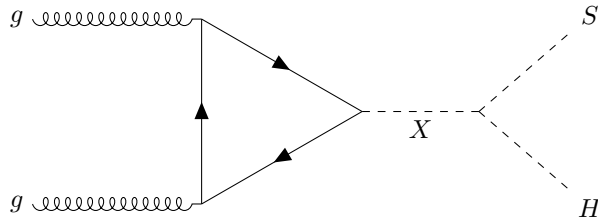


Figure 1: Illustrative Feynman diagram for $X \rightarrow SH$ production via gluon–gluon fusion.

$bb\gamma\gamma$ final state [14] set upper limits on the cross-section times the branching ratio ranging from 39 fb to 0.09 fb, over the mass ranges $170 \leq m_X \leq 1000$ GeV and $15 \leq m_S \leq 500$ GeV. The CMS Collaboration has also performed searches for $X \rightarrow SH$ in the $bb\gamma\gamma$ [16], $bb\tau\tau$ [17], and $4b$ [18] decay modes. In the diphoton plus two b -quarks search, the upper limits on the product of the production cross-section and the decay branching ratios of the signal process lie in the range of 0.9 – 0.04 fb [16], in the explored mass ranges $300 \leq m_X \leq 1000$ GeV and $90 \leq m_S \leq 800$ GeV. For the search with a pair of tau leptons and b -quarks in the final state, limits are set on the production cross-section ranging from 125 fb to 2.7 fb in the mass ranges $240 \leq m_X \leq 3000$ GeV and $60 \leq m_S \leq 2800$ GeV [17]. Comparable limits are found in the search involving four b -quarks in the final state, ranging from 150 to 0.1 fb in the mass ranges $0.9 \leq m_X \leq 4$ TeV and $60 \leq m_S \leq 600$ GeV [18]. All these results are obtained assuming for the S boson the same mass-dependent branching ratios as for the SM Higgs boson [19] (denoted SM-like branching ratios in the following).

This paper is focused on the search for $X \rightarrow SH \rightarrow VV\gamma\gamma$. The final state of interest is characterised by two photons from the SM Higgs boson decay ($H \rightarrow \gamma\gamma$), and one or two leptons (electrons or muons) originating from the vector bosons produced in the $S \rightarrow VV$ decays. This signature benefits from a good diphoton mass ($m_{\gamma\gamma}$) resolution [20] and the $m_{\gamma\gamma}$ distribution is used as the final discriminant. The requirement of at least one lepton rejects some SM background processes and therefore increases the signal-to-background ratio. The events are classified by the number and flavour of the leptons (electrons and muons) in the final state and multivariate analysis techniques are used to enhance the sensitivity of the search. The algorithm is trained to distinguish between the dominant SM backgrounds (multi-jet processes and vector bosons produced in association with a pair of photons) and the $X \rightarrow SH \rightarrow VV\gamma\gamma$ signal. This search is performed over the mass ranges $300 \leq m_X \leq 1000$ GeV and $170 \leq m_S \leq 500$ GeV. It allows to explore lower mass ranges than other final states with b -quarks where the signal becomes boosted at low m_S values, and suffer from low energetic b -quarks falling below the reconstructed threshold in the low m_X region. In the interpretation of the search results, the S boson is assumed to have SM-like branching ratios. Two additional scenarios wherein the S boson decays with a 100% branching ratio into a pair of W^\pm or Z bosons, $S \rightarrow W^+W^-/ZZ$, are also considered.

This paper is organised as follows. A brief description of the ATLAS detector is given in Section 2. Data and simulation samples are described in Section 3. The object reconstruction and event selection are outlined in Section 4. The background estimation and the systematic uncertainties are described in Section 5 and Section 6, respectively. Section 7 presents the results of this search, which are summarised in Section 8.

2 ATLAS detector

The ATLAS detector [1] at the LHC covers nearly the entire solid angle around the collision point.¹ It consists of an inner tracking detector surrounded by a thin superconducting solenoid, electromagnetic and hadronic calorimeters, and a muon spectrometer incorporating three large superconducting air-core toroidal magnets.

The inner-detector system (ID) is immersed in a 2 T axial magnetic field and provides charged-particle tracking in the range $|\eta| < 2.5$. The high-granularity silicon pixel detector covers the vertex region and typically provides four measurements per track, the first hit generally being in the insertable B-layer (IBL) installed before Run 2 [21, 22]. It is followed by the SemiConductor Tracker (SCT), which usually provides eight measurements per track. These silicon detectors are complemented by the transition radiation tracker (TRT), which enables radially extended track reconstruction up to $|\eta| = 2.0$. The TRT also provides electron identification information based on the fraction of hits (typically 30 in total) above a higher energy-deposit threshold corresponding to transition radiation.

The calorimeter system covers the pseudorapidity range $|\eta| < 4.9$. Within the region $|\eta| < 3.2$, electromagnetic calorimetry is provided by barrel and endcap high-granularity lead/liquid-argon (LAr) calorimeters, with an additional thin LAr presampler covering $|\eta| < 1.8$ to correct for energy loss in material upstream of the calorimeters. Hadronic calorimetry is provided by the steel/scintillator-tile calorimeter, segmented into three barrel structures within $|\eta| < 1.7$, and two copper/LAr hadronic endcap calorimeters. The solid angle coverage is completed with forward copper/LAr and tungsten/LAr calorimeter modules optimised for electromagnetic and hadronic energy measurements respectively.

The muon spectrometer (MS) comprises separate trigger and high-precision tracking chambers measuring the deflection of muons in a magnetic field generated by the superconducting air-core toroidal magnets. The field integral of the toroids ranges between 2.0 and 6.0 T m across most of the detector. Three layers of precision chambers, each consisting of layers of monitored drift tubes, cover the region $|\eta| < 2.7$, complemented by cathode-strip chambers in the forward region, where the background is highest. The muon trigger system covers the range $|\eta| < 2.4$ with resistive-plate chambers in the barrel, and thin-gap chambers in the endcap regions.

The luminosity is measured mainly by the LUCID-2 [23] detector that records Cherenkov light produced in the quartz windows of photomultipliers located close to the beampipe.

Events are selected by the first-level trigger system implemented in custom hardware, followed by selections made by algorithms implemented in software in the high-level trigger [24]. The first-level trigger accepts events from the 40 MHz bunch crossings at a rate below 100 kHz, which the high-level trigger further reduces in order to record complete events to disk at about 1 kHz.

A software suite [25] is used in data simulation, in the reconstruction and analysis of real and simulated data, in detector operations, and in the trigger and data acquisition systems of the experiment.

¹ ATLAS uses a right-handed coordinate system with its origin at the nominal interaction point (IP) in the centre of the detector and the z -axis along the beam pipe. The x -axis points from the IP to the centre of the LHC ring, and the y -axis points upwards. Polar coordinates (r, ϕ) are used in the transverse plane, ϕ being the azimuthal angle around the z -axis. The pseudorapidity is defined in terms of the polar angle θ as $\eta = -\ln \tan(\theta/2)$ and is equal to the rapidity $y = \frac{1}{2} \ln \left(\frac{E+p_z c}{E-p_z c} \right)$ in the relativistic limit. Angular distance is measured in units of $\Delta R \equiv \sqrt{(\Delta y)^2 + (\Delta \phi)^2}$.

3 Data and simulation samples

3.1 Data Samples

The data used were collected with the ATLAS detector during 2015–2018, from pp collisions at a centre-of-mass energy $\sqrt{s} = 13$ TeV, corresponding to an integrated luminosity of 140 fb^{-1} with an uncertainty of 0.83% [26] after data quality requirements [27]. Events were recorded using diphoton triggers that require two reconstructed photon candidates with minimum transverse energies of 35 GeV and 25 GeV [28]. During the 2015–2016 data taking period, a *Loose* identification requirement was applied for this diphoton trigger while it was replaced by the *Medium* selection criteria to keep a tolerable trigger rate in 2017–2018 due to the increased instantaneous luminosity.

3.2 Monte Carlo simulated samples

3.2.1 Signal samples

The Monte Carlo (MC) simulated signal samples were produced with the PYTHIA 8 generator [29] with the matrix element calculation at leading order (LO) accuracy in quantum chromodynamics (QCD), followed by parton showering, hadronisation and underlying event modelling using the A14 set of tuned parameters (“tune”) [30] and the NNPDF2.3_{LO} parton distribution functions (PDF) [31]. During the sample generation, both X and S were assumed to have a narrow width compared with the experimental resolution, and their widths are fixed to 10 MeV. A total of 20 signal samples for various m_X and m_S were generated. The X boson was required to decay into S and H with S only decaying into a pair of W or Z bosons and H decaying into a pair of photons. By considering leptonic decays of W or Z bosons, the following three final state samples were produced for each m_X and m_S combination: $WW(\ell\nu q\bar{q}') + \gamma\gamma$, $WW(\ell\nu\ell\nu) + \gamma\gamma$, and $ZZ(\ell\ell q\bar{q}/\ell\ell\nu\nu) + \gamma\gamma$, where $\ell = e, \mu, \text{ or } \tau$. The $ZZ(4\ell) + \gamma\gamma$ decay sample is excluded due to its negligible contribution. To achieve a better signal generation efficiency, the samples were produced by requiring to have at least one lepton with transverse momentum (p_T) greater than 7 GeV and pseudorapidity $|\eta| < 3$ at the generator level.

3.2.2 Background samples

The main background contributions result from SM single and double-Higgs boson production, forming a resonance on the diphoton mass ($m_{\gamma\gamma}$) spectrum, and other SM processes giving a smoothly falling $m_{\gamma\gamma}$ spectrum (continuum background). The corresponding events were generated with MC simulation.

Simulated events for single Higgs boson production via gluon–gluon fusion (ggF) were produced with the POWHEG BOX v2 generator [32–36] at next-to-next-to-leading order (NNLO) accuracy in QCD and interfaced with PYTHIA 8. The NNLO accuracy for arbitrary inclusive $gg \rightarrow H$ observables was achieved by reweighting the Higgs boson rapidity spectrum in HJ-MiNLO [37–39] to that of HNNLO [40]. The PDF4LHC15_{NNLO} PDF set [41] and the AZNLO tune [42] of PYTHIA 8 were used and the decays of b - and c -hadrons were modelled by the EVTGEN 1.6.0 programme [43]. These events were normalised using the NNLO cross-section in QCD plus electroweak corrections at next-to-leading order (NLO) [19, 44–53].

Simulated single Higgs boson events produced via vector-boson fusion (VBF) were generated with POWHEG BOX v2 at NLO accuracy in QCD and interfaced with PYTHIA 8. The PDF4LHC15_{NLO} PDF

set and AZNLO tune were used. Simulated events were normalised using an approximate-NNLO QCD cross-section with NLO electroweak corrections [54–56].

Events of single Higgs boson produced in association with a vector boson (VH , $V = W/Z$) were simulated using POWHEG Box v2 and interfaced with PYTHIA 8. The POWHEG prediction is accurate to NLO in QCD for $VH+1$ jet distributions by using the MiNLO [57] prescription. The loop-induced $gg \rightarrow ZH$ process was generated separately at LO. The PDF4LHC15_{NLO} PDF set and the AZNLO tune were used. Cross-sections calculated at NNLO in QCD with NLO electroweak corrections for $q\bar{q}/qg \rightarrow VH$ and at NLO and next-to-leading-logarithm accuracy in QCD for $gg \rightarrow ZH$ [58–64] were used for the normalisation of the MC samples.

Events corresponding to Higgs boson production in association with a pair of top or bottom quarks ($t\bar{t}H$ or $b\bar{b}H$) were simulated using POWHEG Box v2 at NLO with the NNPDF3.0_{NLO} PDF set [65]. The events were interfaced with PYTHIA 8 using the A14 tune and the NNPDF2.3_{LO} PDF set. The decays of bottom and charm hadrons were performed with EVTGEN 1.6.0.

Finally, events for single Higgs boson production in association with a single top quark were simulated with the MADGRAPH_AMC@NLO 2.3.3 [66] generator at NLO with the NNPDF3.0_{NLO} PDF set. The events were interfaced with PYTHIA 8 using the A14 tune and the NNPDF2.3_{LO} PDF set.

In addition to the single Higgs boson processes, events corresponding to the SM double Higgs boson ggF and VBF production modes are also considered. Those events were generated with POWHEG Box v2 at NLO accuracy in QCD using the PDF4LHC15_{NLO} PDF set and interfaced with PYTHIA 8. During the sample generation, one of the Higgs bosons was required to decay into two photons and the other Higgs boson was required to decay into WW , ZZ or $\tau\tau$, giving a final state with a pair of electrons or muons, or with one electron and one muon. Leptons were required to have $p_T > 7$ GeV and $|\eta| < 3$ at the generator level.

The normalisation of all Higgs boson samples accounts for the decay branching ratios calculated with HDECAY [67–69] and PROPHECY4F [70–72].

Continuum background from $\gamma\gamma$ +jets, $V+\gamma\gamma$, and $t\bar{t}+\gamma\gamma$ processes is considered. Their contributions are described with corresponding MC simulated samples that are exclusively used for the event selection optimisation. These samples were normalised with cross-sections as predicted by their corresponding MC generators.

Events from $\gamma\gamma$ +jets production were simulated using the SHERPA 2.2.4 generator [73] at NLO accuracy in QCD with up to one additional parton and at LO with up to three additional partons. The matrix elements of these events were calculated with the Comix [74] and OPENLOOPS [75, 76] libraries and then matched to the SHERPA parton shower [77] using the MEPS@NLO prescription [78–81]. The NNPDF3.0_{NNLO} PDF set [65] was used to describe the parton distributions in the incoming protons. A generator-level selection was applied to these events with the requirement of the invariant mass of the two photons to be between 90 GeV and 175 GeV.

The $V + \gamma\gamma$ events were generated using SHERPA 2.2.4 at NLO accuracy in QCD with up to one additional parton and up to three extra partons at LO. The calculation procedure is the same as in $\gamma\gamma$ +jets event generation. Events were generated separately according to their final states as listed: $ee+\gamma\gamma$, $\mu\mu+\gamma\gamma$, $\tau\tau+\gamma\gamma$, $e\nu+\gamma\gamma$, $\mu\nu+\gamma\gamma$, $\tau\nu+\gamma\gamma$, and $\nu\nu+\gamma\gamma$. The generator-level photon p_T was required to be greater than 17 GeV and the invariant mass of the two photons should be larger than 80 GeV for these events.

Table 1: Summary of MC simulated samples used in this analysis.

Process	Generator	PDF	Tune
Signal			
$X \rightarrow SH \rightarrow VV + \gamma\gamma$	PYTHIA 8	NNPDF2.3 _{LO}	A14
SM Single and double Higgs boson production			
ggF H	POWHEG+PYTHIA 8	PDF4LHC15 _{NNLO}	AZNLO
VBF H	POWHEG+PYTHIA 8	PDF4LHC15 _{NLO}	AZNLO
WH	POWHEG+PYTHIA 8	PDF4LHC15 _{NLO}	AZNLO
$qq \rightarrow ZH$	POWHEG+PYTHIA 8	PDF4LHC15 _{NLO}	AZNLO
$gg \rightarrow ZH$	POWHEG+PYTHIA 8	PDF4LHC15 _{NLO}	AZNLO
$t\bar{t}H$	POWHEG+PYTHIA 8	NNPDF3.0 _{NLO}	A14
$b\bar{b}H$	POWHEG+PYTHIA 8	NNPDF3.0 _{NLO}	A14
$tHbj$	MADGRAPH_AMC@NLO+PYTHIA 8	NNPDF3.0 _{NLO}	A14
tHW	MADGRAPH_AMC@NLO+PYTHIA 8	NNPDF3.0 _{NLO}	A14
ggF $HH \rightarrow VV + \gamma\gamma$	POWHEG+PYTHIA 8	PDF4LHC15 _{NLO}	A14
VBF $HH \rightarrow VV + \gamma\gamma$	POWHEG+PYTHIA 8	PDF4LHC15 _{NLO}	A14
Continuum background			
$\gamma\gamma + \text{jets}$	SHERPA	NNPDF3.0 _{NNLO}	–
$V + \gamma\gamma$	SHERPA	NNPDF3.0 _{NNLO}	–
$t\bar{t}\gamma\gamma$	MADGRAPH_AMC@NLO+PYTHIA 8	NNPDF3.0 _{NLO}	A14
Lepton-dependence samples			
$\gamma\gamma + 0\ell + \text{jets}$	MADGRAPH_AMC@NLO+PYTHIA 8	NNPDF3.0 _{NLO}	A14
$\gamma\gamma + 1\ell + \text{jets}$	MADGRAPH_AMC@NLO+PYTHIA 8	NNPDF3.0 _{NLO}	A14
$\gamma\gamma + 2\ell + \text{jets}$	MADGRAPH_AMC@NLO+PYTHIA 8	NNPDF3.0 _{NLO}	A14

The $t\bar{t} + \gamma\gamma$ process is simulated with the MADGRAPH5_AMC@NLO generator at LO and interfaced with PYTHIA 8. The NNPDF2.3_{LO} PDF set and A14 tune were used for this production. The decays of bottom and charm hadrons were performed with EVTGEN 1.6.0.

In addition, dedicated samples (donated “lepton-dependence samples”) corresponding to final states of $\gamma\gamma + 0\ell + \text{jets}$, $\gamma\gamma + 1\ell + \text{jets}$, and $\gamma\gamma + 2\ell + \text{jets}$ are generated to study the $m_{\gamma\gamma}$ distribution difference for cases with different lepton multiplicity at the generator level. These samples were produced with MADGRAPH5_AMC@NLO interfaced with PYTHIA 8. All possible SM processes with described final states except for those with $H \rightarrow \gamma\gamma$ were included in the event generation.

All simulated events except for the signals, $\gamma\gamma + \text{jets}$ and lepton-dependence samples were passed through a detailed detector simulation of the ATLAS detector implemented with GEANT4 [82, 83]. The remaining samples were simulated using ATLFastII [83], which employs GEANT4 except for a parameterisation of the calorimeter response [84]. The effect of multiple interactions in the same and neighbouring bunch crossings (pile-up) was modelled by overlaying the simulated hard-scattering event with inelastic pp events generated with PYTHIA 8 [85] using the NNPDF2.3_{LO} PDF set and the A3 tune [86]. A summary of MC simulated samples can be found in Table 1.

4 Object and event selection

4.1 Object selection

Vertices from pp collisions are reconstructed if they have associated at least two ID tracks with $p_T > 0.5$ GeV. The diphoton primary vertex (PV) is chosen by using a neural network algorithm that uses information about the ID tracks as well as the photon candidates [87].

Photons are reconstructed based on a dynamic, topological cell clustering-based algorithm from the energy deposits in the electromagnetic calorimeter in the region $|\eta| < 2.37$, excluding the transition region between the barrel and endcap calorimeters $1.37 < |\eta| < 1.52$ [88]. The photon identification criteria is constructed using information from the shower shapes and the primary identification criteria is labelled as *Tight*. The photon isolation criteria quantifies the activity near the photons from the tracks of nearby charged particles, or from energy deposits in the calorimeter [88]. This analysis considers events by selecting photon candidates which are required to satisfy a set of preselection criteria. The two photons with the highest transverse momentum, referred to as leading (γ_1) and subleading (γ_2) photons, must satisfy $p_T > 22$ GeV and $|\eta| < 2.37$, excluding the transition region between the barrel and endcap calorimeters $1.37 < |\eta| < 1.52$. Photon candidates are separated from multi-jet backgrounds by applying *Tight* identification and further isolation requirements to suppress jets misidentified as photons.

Electrons are reconstructed and identified based on clusters built from energy deposits in the electromagnetic calorimeter, which are matched to a track in the inner detector [88]. The muon reconstruction is performed using information from the inner detector and muon spectrometer, as well as the electromagnetic and hadronic calorimeters [89]. In this search, electron candidates are required to have $p_T > 10$ GeV and $|\eta| < 2.47$, excluding the transition region between the barrel and endcap calorimeters $1.37 < |\eta| < 1.52$. Muon candidates should have $p_T > 10$ GeV and $|\eta| < 2.7$. Leptons must satisfy *Medium* identification and *Loose* isolation [88, 89], and a set of requirements based on the longitudinal and transverse impact parameters relative to the vertex and the beam axis.

Jets are reconstructed using a particle flow algorithm [90] from noise-suppressed positive-energy topological clusters [91] in the calorimeter using the anti- k_r algorithm [92, 93] with a radius parameter $R = 0.4$. The jet energy scale calibration restores the jet p_T , energy, and mass to that of jets reconstructed at particle level [94]. In this search, jets are required to have $p_T > 25$ GeV and to be in the central region of the detector, $|\eta| < 2.5$. To suppress jets from pileup, a jet-vertex-tagger multivariate discriminant [95] is applied to jets with $p_T < 60$ GeV. Jets containing b -hadrons are identified (b -tagged) using the 77% efficiency working point of the DL1r b -tagging algorithm [96].

An overlap removal procedure is performed to avoid double-counting objects. First, electrons overlapping with any of the two selected photons ($\Delta R < 0.4$) are removed. Jets overlapping with the selected photons ($\Delta R < 0.4$) or electrons ($\Delta R < 0.2$) are removed. Electrons overlapping with the remaining jets ($\Delta R < 0.4$) are removed to match the requirements imposed when measuring isolated electron efficiencies. Finally, muons overlapping with photons or jets ($\Delta R < 0.4$) are removed.

The missing transverse momentum, with magnitude E_T^{miss} , is defined as the negative vector sum of the transverse momenta of the selected photon, electron, muon, and jet objects, as well as of the transverse momenta of remaining low- p_T particles estimated by using tracks associated with the diphoton primary vertex but not assigned to any of the selected objects [97].

The above requirements constitute the event preselection of this search.

Table 2: Event selection and classification strategy.

Preselection	Two photon candidates and no b -tagged jets			
Region	1ℓ	$e\mu$	$2\ell(WW)$	$2\ell(ZZ)$
Number of leptons	1	2	2	2
Total electric charge	–	0	0	0
Same flavour leptons	–	No	Yes	Yes
$ m_{\ell\ell} - m_Z $ [GeV]	–	–	> 10	< 10
Number of jets	≥ 2	–	–	≥ 2
Strategy	BDT	Cut-based	BDT	Cut-based
Number of signal regions	2	1	2	1
$m_{\gamma\gamma}$ region	[105, 160] GeV			

4.2 Event selection

This search selects events with two photons from the Higgs boson decay, and one or two leptons coming from the vector bosons originated from the $S \rightarrow VV$ process. Events are required to pass diphoton triggers as described in Section 3. Moreover, photons are required to have $p_T^{\gamma^{1(2)}}/m_{\gamma\gamma} > 0.35$ (0.25) [20]. Selected events must contain one or two additional leptons (e or μ) with $p_T > 10$ GeV. To suppress backgrounds with top quarks, events are rejected if there is any b -tagged jet.

The events are classified into four different regions depending on the number and flavour of leptons originating from the vector boson decays in the $S \rightarrow W^+W^-$ and $S \rightarrow ZZ$ processes. Events in the one-lepton (1ℓ) region are required to have one lepton and at least two jets. The other regions account for events with two leptons with opposite electric charge. Events with two leptons of different flavour are targeted in the $e\mu$ region. Events having two leptons of same flavour (SF) are further split by checking the compatibility of the dilepton invariant mass with the Z -mass pole. Events with at least two jets and satisfying $|m_{\ell\ell} - 91.2 \text{ GeV}| < 10 \text{ GeV}$ are classified in the $2\ell(ZZ)$ region, which targets the $S \rightarrow ZZ \rightarrow \ell\ell$ +jets process. The remaining SF events are included in the $2\ell(WW)$ region.

Two optimisation strategies are adopted. For each of the 1ℓ and $2\ell(WW)$ regions, a Boosted Decision Tree (BDT) is used to enhance the analysis sensitivity. The 1ℓ and $2\ell(WW)$ regions further split the events by dividing the BDT output distribution into the loose (low BDT score) and tight (high BDT score) signal regions. The $e\mu$ and $2\ell(ZZ)$ signal regions are limited in statistics and have higher signal-over-background ratios than the BDT-based regions. Due to this, the $e\mu$ and $2\ell(ZZ)$ signal regions follow an inclusive cut-based strategy and events are not further split into sub-regions. This analysis strategy results in six signal regions.

The final discriminant of this search is the diphoton invariant mass spectrum. To be consistent with the $H \rightarrow \gamma\gamma$ process and to exclude the region of the Z -boson resonance, the range of $m_{\gamma\gamma}$ is limited to the [105, 160] GeV region. The signal region is defined as the $m_{\gamma\gamma}$ within [120, 130] GeV. Events outside the signal region, referred to as sideband events, are used to estimate the main background processes as described in Section 5. After all selections described above are applied, the combined acceptance and selection efficiency for the signal production ranges from 11% to 25%, which increases for higher m_X hypotheses. Table 2 summarises the event selection and strategy for each of the signal regions.

4.3 Boosted Decision Tree strategy

The dominant signal process in this search is the $S \rightarrow W^+W^-$ decay given the larger branching ratio compared with the $S \rightarrow ZZ$ process for the explored m_S range. In the 1ℓ region one of the W bosons decays leptonically and the other decays hadronically. In the $e\mu$ and $2\ell(WW)$ regions both W bosons decay leptonically resulting into a pair of leptons with different and same flavour, respectively. Two BDTs are built based on the kinematic observables from the final-state objects in the 1ℓ and $2\ell(WW)$ regions. The different signal samples are grouped according to the S mass into four groups: $m_S = 170$ GeV, $m_S = 200$ GeV, $m_S = 300$ GeV and $m_S = 400, 500$ GeV. These groups contain from four to six signal samples depending on the m_X values in each group. The BDT algorithms are trained for each group against the total background from MC simulation using the parameterised BDT method [98].

Twelve and nine variables for the 1ℓ and $2\ell(WW)$ regions respectively are used to train each BDT, as listed in Table 3. The BDT input variables list excludes $m_{\gamma\gamma}$ as it is used as the main discriminant; these variables are selected to have small correlation with $m_{\gamma\gamma}$. The BDT variable with the highest separation power is the transverse momentum of the pairs of photons from the SM Higgs boson decay ($p_T^{\gamma\gamma}$). The comparison of the $p_T^{\gamma\gamma}$ distributions for data, the expected SM background processes and the $(m_X, m_S) = (1000, 500)$ GeV signal from simulation is shown in Figure 2 for the 1ℓ and $2\ell(WW)$ regions.

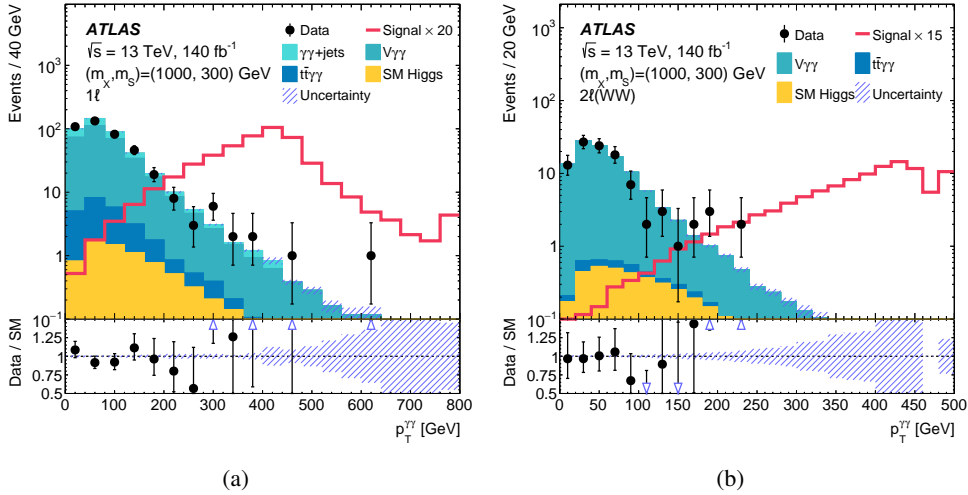


Figure 2: Transverse momentum of the diphoton system, $p_T^{\gamma\gamma}$, in the (a) 1ℓ and (b) $2\ell(WW)$ regions for data and the expected SM background from simulation after the event selection is applied. The $V\gamma\gamma$ and $\gamma\gamma$ +jets simulated background is scaled to match the data yield excluding the $120 < m_{\gamma\gamma} < 130$ GeV region. The contribution from the SM single and double Higgs boson processes (denoted “SM Higgs”), which is estimated from the MC simulation, is also shown. The signal prediction (open red histogram) for the scenario of SM-like $\mathcal{B}(S \rightarrow WW/ZZ)$ is also shown, normalised to a cross-section corresponding to the 95% CL upper limit shown in Figure 6. An additional normalisation factor, as indicated in the legend, is applied to scale the signal for visibility. The last bin in each distribution contains the overflow.

Figure 3 shows the BDT output distributions for data, the expected SM background processes and the $(m_X, m_S) = (1000, 500)$ GeV signal from simulation. The BDT output discriminant is used to further split events in loose and tight BDT regions: 1ℓ loose and 1ℓ tight regions are defined for the 1ℓ region, as well as 2ℓ loose and 2ℓ tight signal regions for the $2\ell(WW)$ region. The BDT score threshold values used

Table 3: Variables used as inputs to the BDT in the 1ℓ and $2\ell(WW)$ regions. The highest- p_T (leading) lepton is denoted ℓ_1 , and the subleading lepton is denoted ℓ_2 . The numbers indicate the ranking of each input variable, with 1 corresponding to the most highly ranked variable.

Variable	Description	BDT-based regions	
		1ℓ	$2\ell(WW)$
$\Delta R(\gamma\gamma, \ell\nu jj)$	ΔR between the diphoton system and the $\ell + E_T^{\text{miss}} jj$ system	10	
$\Delta R(\gamma\gamma, \ell\nu\ell\nu)$	ΔR between the diphoton system and the $\ell\ell + E_T^{\text{miss}}$ system		9
$\Delta R(jj, \ell\nu)$	ΔR between the dijet system and the $\ell + E_T^{\text{miss}}$ system	9	
$\Delta R(\ell_1\nu, \ell_2)$	ΔR between leading lepton + E_T^{miss} and subleading lepton		8
$p_T^{\ell+E_T^{\text{miss}} jj}$	p_T of the $\ell + E_T^{\text{miss}} jj$ system	2	
$p_T^{\gamma\gamma}$	p_T of the diphoton system	1	2
$\Delta\phi(\gamma\gamma, \ell_{(1)})$	$\Delta\phi$ between the diphoton system and the (leading) lepton	12	7
$\Delta R(\ell, E_T^{\text{miss}})$	ΔR between the lepton and the E_T^{miss}	8	
$p_T^{\ell_{(1)}}$	p_T of the (leading) lepton	4	4
$p_T^{\ell_1+E_T^{\text{miss}}}$	p_T of the leading lepton and E_T^{miss} system		3
$m_T(\ell_{(1)} E_T^{\text{miss}})$	Transverse mass of the (leading) lepton and E_T^{miss}	11	5
$m_{\ell\ell}$	Invariant mass of the dilepton system		6
E_T^{miss}	Missing transverse energy	3	1
$\Delta R(j, j)$	ΔR between the two jets with closest mass to m_W	6	
p_T^{jj}	p_T of the the two jets with closest mass to m_W	5	
m_{jj}	Invariant mass of the dijet system with closest mass to m_W	7	

range from -0.1 to 0.2 depending on the signal mass hypothesis, and result from a scan using the root square of the signal significance in each region added in quadrature: $Z_{\text{comb}} = \sqrt{Z_{\text{loose}}^2 + Z_{\text{tight}}^2}$, being

$$Z_{\text{loose/tight}} = \sqrt{2 \times \left[(s+b) \times \left(\ln \frac{s+b}{b} \right) - s \right]_{\text{loose/tight}}}, \quad (1)$$

where s represents the signal event yields and b is the background yield in each BDT region. Both signal and background yields are calculated by considering events in the region of $120 < m_{\gamma\gamma} < 130$ GeV. The selected threshold values are established by maximising Z_{comb} under the requirement of the presence of at least one sideband data event in the tight BDT regions. Table 4 shows the SM expected event yields, estimated as detailed in Section 5, and the observed data for each of the analysis regions. The expected signal yields for $(m_X, m_S) = (1000, 300)$ GeV, considering a $gg \rightarrow X \rightarrow SH$ production cross-section of 1 pb, are provided for comparison. The S scalar boson is assumed to decay into other SM particles with the same mass-dependent branching ratios of the SM Higgs boson.

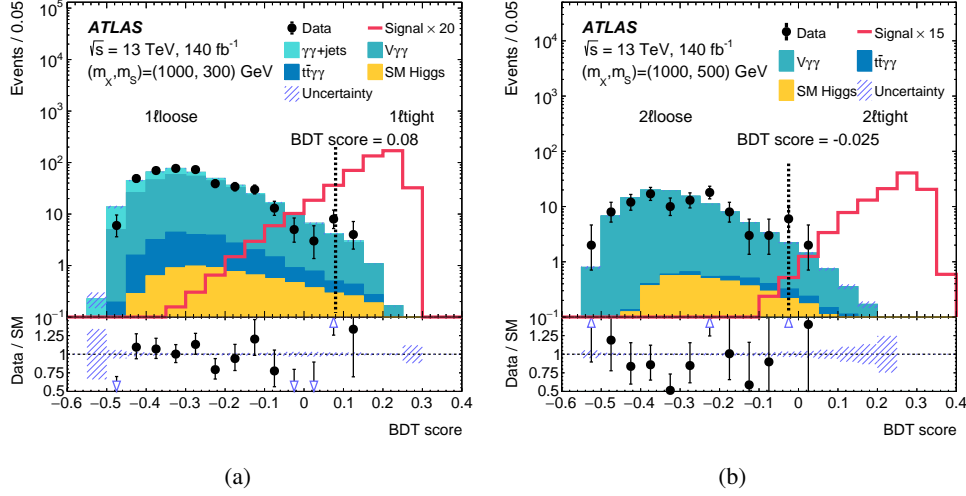


Figure 3: BDT output distributions in the (a) 1ℓ and (b) $2\ell(WW)$ regions for data and the expected SM background from simulation after the event selection is applied. The $V\gamma\gamma$ and $\gamma\gamma$ +jets simulated background is scaled to match the data yield excluding the $120 < m_{\gamma\gamma} < 130$ GeV region. The contribution from the SM single and double Higgs boson processes (denoted “SM Higgs”), which is estimated from the MC simulation, is also shown. The signal prediction (open red histogram) for the scenario of SM-like $\mathcal{B}(S \rightarrow WW/ZZ)$ is also shown, normalised to a cross-section corresponding to the 95% CL upper limit shown in Figure 6. An additional normalisation factor, as indicated in the legend, is applied to scale the signal for visibility. The BDT score threshold values are represented by the dashed vertical lines. The shaded band represents the statistical uncertainty on the background prediction. The last bin in each distribution contains the overflow.

Table 4: Observed data and expected event yields for the different analysis regions after the full selection from Table 2 is applied. The continuum background includes the $V\gamma\gamma$, $\gamma\gamma$ +jets and $t\bar{t}\gamma\gamma$ processes estimated as described in Section 5. The contribution from the SM single and double Higgs boson processes (denoted “SM Higgs”) is estimated from simulation. The uncertainties include all sources of systematic uncertainty described in Section 6. Event yields for the $(m_X, m_S) = (1000, 300)$ GeV signal are also shown assuming $\sigma(gg \rightarrow X \rightarrow SH) = 1$ pb and SM-like $\mathcal{B}(S \rightarrow WW/ZZ)$.

	BDT-based regions				Cut-based regions	
	1ℓtight	1ℓloose	2ℓtight	2ℓloose	2ℓ(ZZ)	$e\mu$
Continuum	6.0 ± 2.4	405 ± 20	2.0 ± 1.4	100 ± 10	2.0 ± 1.4	2.0 ± 1.4
SM Higgs	0.55 ± 0.08	6.8 ± 0.9	0.46 ± 0.06	3.35 ± 0.46	0.52 ± 0.08	0.24 ± 0.03
Total background	6.6 ± 2.8	412 ± 23	2.46 ± 1.6	103 ± 11	2.52 ± 1.6	2.24 ± 1.5
Signal (m_X, m_S) (1000, 300) GeV	20.9 ± 2.4	2.90 ± 0.34	2.96 ± 0.35	0.016 ± 0.002	2.03 ± 0.24	2.08 ± 0.24
Data	6	405	2	100	2	2

5 Background estimation

Background processes can be classified into “resonant” or “continuum” based on their $m_{\gamma\gamma}$ spectrum. The SM Higgs boson single and pair production events form the resonant background component. These processes are purely estimated from MC simulation.

The continuum background component arises mostly from multi-jet processes associated with two photons ($\gamma\gamma$ +jets), and vector boson or top-antitop-quark production in association with a pair of photons ($V + \gamma\gamma$ and $t\bar{t}\gamma\gamma$). Contributions from these processes are checked with the MC simulated samples as described in Section 3.2.2 and used for the event selection optimisation. No dedicated MC simulated events are produced for processes with small contribution such as $VV+\gamma\gamma$ or processes with jets or leptons misidentified as photons. Their contributions are included in the data-driven background, which accounts for all possible processes. The contribution from the continuum background is estimated from a fit to the data $m_{\gamma\gamma}$ distribution in the sideband region with a template. This template is generated from an analytic function that is obtained from a fit to $m_{\gamma\gamma}$ distribution in a dedicated data control region due to low statistics of sideband data in the signal region. These control regions are defined by requiring zero leptons and at least two photons passing looser identification and isolation criteria but failing the signal region photon selections as described in Section 4.1. Two different control samples are defined based on the number of leptons in each signal region using the selected jet to mimic the lepton behaviour. The control sample for the $\gamma\gamma + 1\ell$ region selects events with a pair of photons accompanied by one jet. For the other signal regions with a pair of leptons in the final state, the control sample requires the presence of at least two jets. A schematic diagram presenting the definitions of different regions is shown in Figure 4. The fitted $m_{\gamma\gamma}$ shape difference between the signal region and control region is considered as a systematic uncertainty in the background shape estimation. In addition, the $m_{\gamma\gamma}$ shape difference related to the number of leptons in the generator-level is also evaluated and included as a systematic uncertainty. This uncertainty is estimated by comparing the fit results to the full $m_{\gamma\gamma}$ mass range distributions in the control region and the validation region using dedicated lepton-dependence MC samples as described in Section 3.2.2, where the validation region is defined by applying almost the same event selections as the signal region but inverting identification and isolation requirements as same as in the control region.

Three types of analytic functions are explored: exponential function, exponential function of a 2nd order polynomial, and a Chebyshev polynomial of order $n = 1, \dots, 5$. The functional form is chosen via a spurious signal test as described in Ref. [99]. The spurious signal is extracted by performing a signal-plus-background fit to the data $m_{\gamma\gamma}$ distribution in the control region (denoted “background-only” template), which is assumed to only include contributions from continuum background processes. The selection criteria follow the strategy as documented in Ref. [20]. The spurious signal should be less than 20% of the background uncertainty. In addition to the spurious signal requirement, the goodness of the fit with background functional form to the background-only template is evaluated with a χ^2 test and the corresponding p -value is required to be greater than 5%. When multiple functions pass the criteria, the one with the smallest degrees of freedom is chosen. The corresponding spurious signal for the selected function is treated as the systematic uncertainty due to background modelling with the analytic function. In total 80 continuum background functions are estimated corresponding to various signal regions. Of these 80 functions, 78 are exponential functions of 2nd order polynomials and the remaining two are simple exponential functions. Due to the low statistics in the $e\mu$ and $2\ell(ZZ)$ signal regions and the fact that the $m_{\gamma\gamma}$ distribution shows a negligible dependence on the flavour of leptons, the continuum background shape estimated in the 2ℓ tight region is also applied to these two regions.

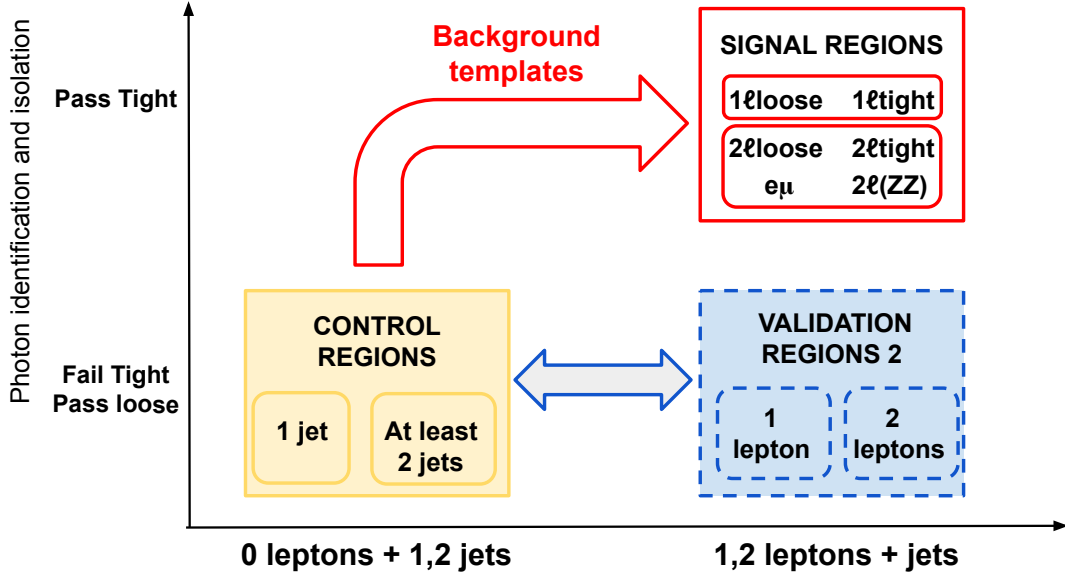


Figure 4: Definition of signal and control regions. The red arrow represents the $m_{\gamma\gamma}$ template generated in the 0-lepton control region which is applied to the signal regions. The systematic uncertainty in the background shape, obtained from differences between the control and the validation regions, is indicated by the blue arrow.

6 Systematic uncertainties

Systematic uncertainties arise from the theory modelling of signal and background, the detector simulation and instrumental effects, and the estimation of the continuum background.

6.1 Theoretical uncertainties

Theoretical uncertainties are considered for signal and the SM single and double Higgs boson backgrounds. Uncertainties from six sources are considered: from PDF set and strong coupling constant α_S , from the QCD factorisation and renormalisation scales (μ_F and μ_R), and from the parton shower parameters and hadronisation models.

To evaluate the impact of varying the PDF set choice and α_S value, event weights corresponding to alternative PDF sets and α_S values are generated for each event along with the nominal weight. Effects on signal region yields are considered as systematic uncertainties. Variations on signal and SM Higgs boson yields are found to be 6% and 4% respectively.

The systematic uncertainty due to higher-order QCD effects is estimated by independently varying the QCD factorisation and renormalisation scales up and down from their nominal values by a factor of two, taking the envelope of the 7-point variation. Their impacts on signal and SM Higgs boson background yields are about 9% and 13% respectively.

The uncertainty due to the parton shower and hadronisation model is estimated by comparing the yields from the nominal MC samples using PYTHIA 8, with alternative samples using instead HERWIG 7. The corresponding uncertainties in the signal and Higgs boson background yields are 5% and 3% respectively.

6.2 Experimental uncertainties

Systematic uncertainties arising from the luminosity determination, pileup modelling, and trigger, reconstruction and selection efficiencies, as well as energy scales and resolutions, are considered for signal, single and double Higgs boson processes. Their impacts on both the normalisation and shape are included in the statistical analysis for the final results.

The uncertainty in the integrated luminosity for 2015–2018 data taking period is 0.83% [26], obtained using the LUCID-2 detector for the primary luminosity measurement, complemented by measurements using the inner detector and calorimeters.

The uncertainty in the modelling of the pileup distribution in the simulation is estimated to have 2%–3% impacts on yields of signal, single and double Higgs boson events.

The photon reconstruction, identification and isolation efficiencies are measured using three data-driven techniques as mentioned in Ref. [100]. Their effects on yields and shapes are estimated by varying the measured efficiency scale factors between data and simulation, resulting in less than 2% variations for signal yields. Uncertainties in the photon energy scale and resolution described in Ref. [88] are considered as well. These uncertainties affect the signal yield less than 0.5%; a similar impact is found for single Higgs boson and double Higgs bosons events. The uncertainty in the photon trigger efficiency is also considered and its impact on event yields is found to be negligible.

Uncertainties in the electron reconstruction, identification and isolation efficiencies are reported in Ref. [100]. They affect the signal and SM Higgs boson yields by about 2%. Uncertainties in electron energy scale and resolution are also evaluated and found to have a negligible impact.

In addition, uncertainties in muon reconstruction, identification, isolation efficiencies as well as the muon momentum scale and resolution [89], and uncertainties in the jet energy scale and resolution [94] are also considered. Furthermore, uncertainties arising from jet property selections: jet-vertex-tagger [95] and b -jet tagging [101–103] are included. Finally, the uncertainty related to E_T^{miss} resulting from tracks not associated with the selected objects [97] is considered. All these uncertainties were found to have a negligible impact on the signal and SM Higgs boson yields.

6.3 Continuum background modelling uncertainty

The continuum background estimation (see Section 5) assumes no significant shape differences between the control region (events with no leptons) and the signal region (events with at least one lepton). An uncertainty (called lepton-dependence uncertainty) associated with the background modelling is evaluated by comparing the shape of the $m_{\gamma\gamma}$ distribution in $\gamma\gamma + 0\ell$ events with that in $\gamma\gamma + \ell\nu jj$ and $\gamma\gamma + \ell\nu\ell\nu$ events from dedicated MC simulated samples (see Section 3.2.2). The variations between diphoton events with and without leptons are computed using the $m_{\gamma\gamma}$ distribution in the [105, 160] GeV range. The average variation over all bins is about 2% for all signal regions. In addition to lepton-dependence uncertainty, a 2% uncertainty arises from the comparison of the shape of the $m_{\gamma\gamma}$ distribution in the control and the signal

regions. The systematic uncertainty arising from a potential bias from the background shape functional form choice is accounted by the spurious signal uncertainty (see Section 5).

7 Results

The contribution of a potential signal in the data is extracted through a simultaneous fit to the $m_{\gamma\gamma}$ distributions in all six signal regions, which is implemented with the RooFIT [104] and RooSTATS [105] frameworks. The fit is performed with a binned likelihood model built from the product of the Poission distribution in each bin and region, and including Gaussian distributions to describe the effect of systematic uncertainties. For each $m_{\gamma\gamma}$ distribution, 22 equal width bins in a range of 105 GeV to 160 GeV are used in the fit. The parameter-of-interest is $\sigma(gg \rightarrow X) \times \mathcal{B}(X \rightarrow SH)$ and is left unconstrained in the fit. The shape of the signal for each individual region is obtained from simulated events. Contributions from the single and double Higgs boson processes are estimated from MC simulated samples with their normalisation fixed to SM predictions. Theoretical and experimental uncertainties corresponding to both the signal and the Higgs boson backgrounds are included in the fit and controlled by the nuisance parameters. For the continuum background, the shape is estimated with the method described in Section 5 and kept fixed in the fit, while its normalisation is left unconstrained. In total four individual normalisation factors are included corresponding to 1ℓ tight, 1ℓ loose, 2ℓ tight and 2ℓ loose, respectively. The $e\mu$ and $2\ell(ZZ)$ regions share the same normalisation factor for continuum background as the 2ℓ tight region. Background shape uncertainty and the spurious signal uncertainty are also considered in the fit and described by the corresponding nuisance parameters. To improve the robustness of the fit, any systematic uncertainty with less than 0.5% impact on either shape or yield is removed from the fit model. With such requirement, only uncertainties related to photon and electron, pileup reweighting, theory, and continuum background estimation are left, and others are ignored during the fit.

Three scenarios are considered for the final results corresponding to three hypotheses on the $S \rightarrow WW/ZZ$ branching ratios: SM-like $\mathcal{B}(S \rightarrow WW/ZZ)$ [19], $\mathcal{B}(S \rightarrow WW) = 100\%$, and $\mathcal{B}(S \rightarrow ZZ) = 100\%$.

Figure 5 presents the $m_{\gamma\gamma}$ distributions in the six signal regions after performing the signal-plus-background fit corresponding to a signal with $m_X = 1000$ GeV and $m_S = 300$ GeV for the SM-like $\mathcal{B}(S \rightarrow WW/ZZ)$ scenario. Other branching-ratio scenarios and signal-mass hypotheses are also tested and no deviation with respect to the SM background expectation is observed. Consequently, 95% CL upper limits are set on $\sigma(gg \rightarrow X) \times \mathcal{B}(X \rightarrow SH)$ for each branching-ratio scenario and signal-mass hypothesis using the profile likelihood ratio technique with the asymptotic approximation [106] and the CL_s [107, 108] method. The results are validated using pseudo-experiments and found to agree within 20%.

Figure 6 shows the 95% CL observed and expected limits on $\sigma(gg \rightarrow X) \times \mathcal{B}(X \rightarrow SH)$ as a function of m_X and m_S for the SM-like $\mathcal{B}(S \rightarrow WW/ZZ)$ scenario. The observed (expected) limit ranges from 530 fb (800 fb) to 120 fb (170 fb) depending on the scalar masses. The results are dominated by the 1ℓ tight region, with the other regions contributing with comparably lower sensitivity. In the 1ℓ tight region, a slight deficit in the data yield compared to the background expectation is observed across all mass hypotheses, which leads to a better observed limit than the expected one for every mass point.

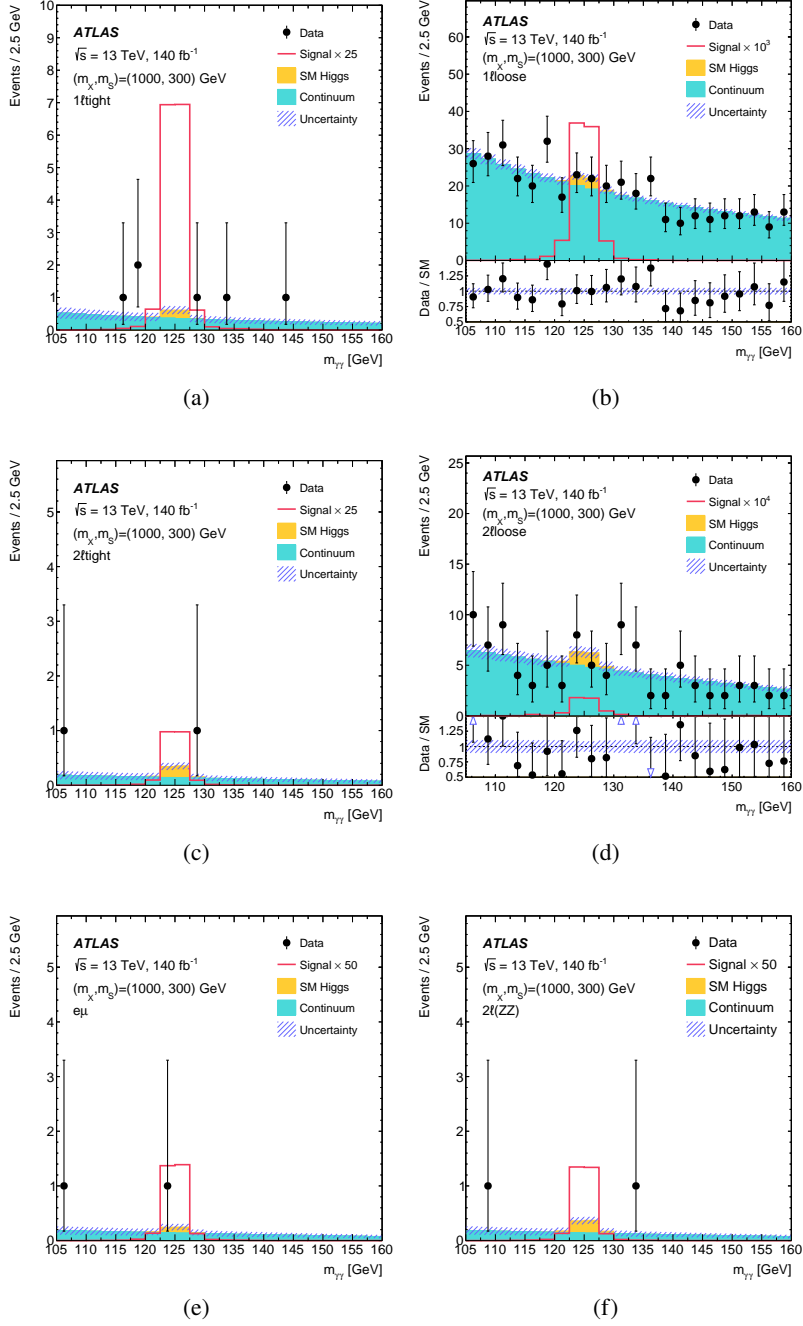


Figure 5: Distribution of $m_{\gamma\gamma}$ after the signal-plus-background fit to data in the (a) $1\ell_{\text{tight}}$, (b) $1\ell_{\text{loose}}$, (c) $2\ell_{\text{tight}}$, (d) $2\ell_{\text{loose}}$, (e) $e\mu$ and (f) $2\ell(ZZ)$ regions. The contribution from the SM single and double Higgs boson processes (denoted “SM Higgs”), which is estimated from the MC simulation, is shown added on top of the continuum background distribution. The signal prediction (open red histogram) for the scenario of SM-like $\mathcal{B}(S \rightarrow WW/ZZ)$ is also shown, normalised to a cross-section corresponding to the 95% CL upper limit shown in Figure 6. An additional normalisation factor, as indicated in the legend, is applied to scale the signal for visibility.

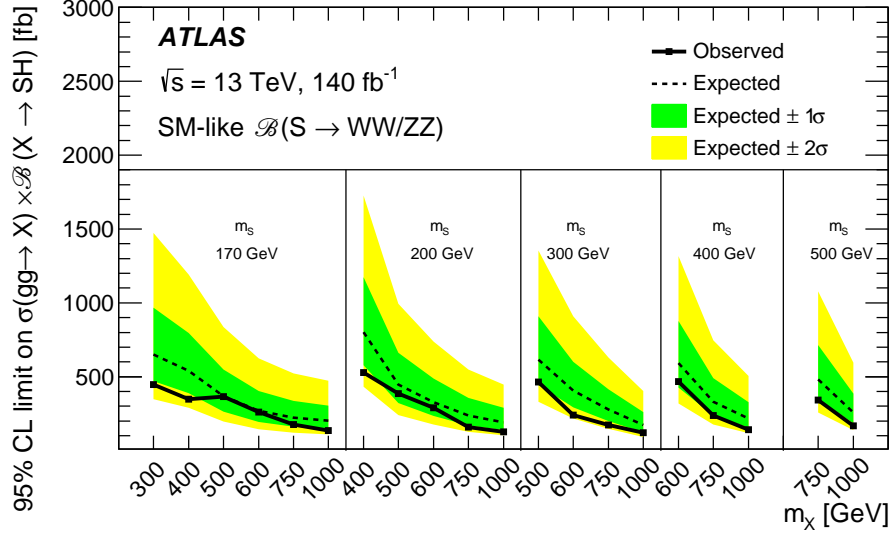


Figure 6: Observed (solid line) and expected (dashed line) 95% CL upper limits on $\sigma(gg \rightarrow X) \times \mathcal{B}(X \rightarrow SH)$ as a function of m_X and m_S , under the assumption of SM-like $\mathcal{B}(S \rightarrow WW/ZZ)$. The green and yellow shaded areas indicate the ± 1 and ± 2 standard deviations around the expected limit.

Limits corresponding to assumptions of the scalar S with a 100% decay branching ratio to WW or ZZ are derived and presented in Figure 7 and 8. Under the assumption that $\mathcal{B}(S \rightarrow WW) = 100\%$, the observed limit varies from 470 fb to 91 fb whereas the expected limit ranges from 610 fb to 120 fb. The upper limits under the scenario $\mathcal{B}(S \rightarrow ZZ) = 100\%$ are significantly higher: from 1530 fb to 360 fb for observed limits and from 2160 fb to 510 fb for expected limits. The analysis sensitivity is limited by the statistical uncertainty, with systematic uncertainties degrading the expected limits by about 2%.

These results are comparable to the $X \rightarrow SH \rightarrow VV\tau\tau$ [15] search, which observes an upper limit on the production cross-section from 540 fb to 72 fb, assuming SM-like $\mathcal{B}(S \rightarrow WW/ZZ)$. Under the $\mathcal{B}(S \rightarrow WW) = 100\%$ and $\mathcal{B}(S \rightarrow ZZ) = 100\%$ scenarios, the upper limits on the production cross-section and decay branching ratio are in the ranges 26 – 3 fb and 33 – 6 fb, respectively. By correcting by the $\mathcal{B}(H \rightarrow \tau\tau)$, these results can be expressed in upper limits on the $X \rightarrow SH$ production cross-section, and compared to those obtained by this analysis. These upper limits are set in the ranges 410 – 47 fb and 520 – 95 fb for $\mathcal{B}(S \rightarrow WW) = 100\%$ and $\mathcal{B}(S \rightarrow ZZ) = 100\%$, respectively.

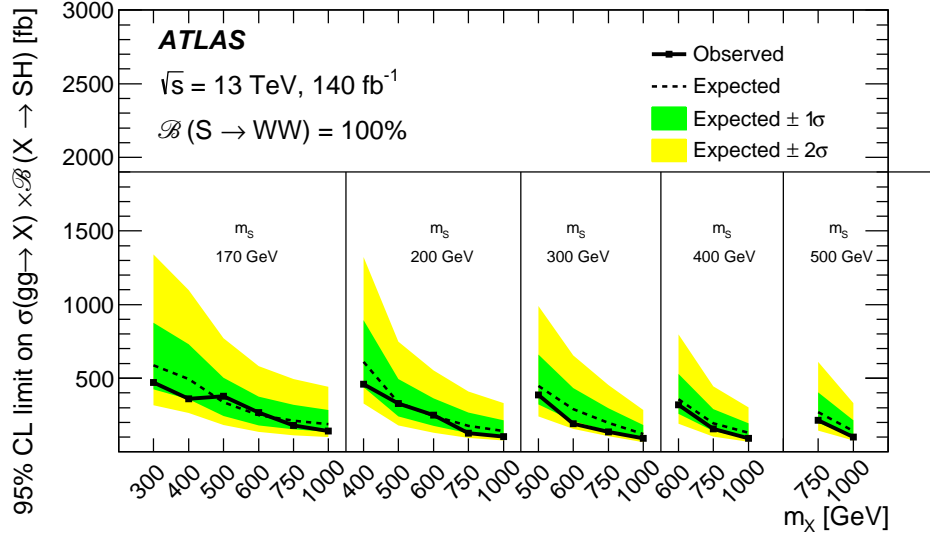


Figure 7: Observed (solid line) and expected (dashed line) 95% CL upper limits on $\sigma(gg \rightarrow X) \times \mathcal{B}(X \rightarrow SH)$ as a function of m_X and m_S , under the assumption of $\mathcal{B}(S \rightarrow WW) = 100\%$. The green and yellow shaded areas indicate the ± 1 and ± 2 standard deviations around the expected limit.

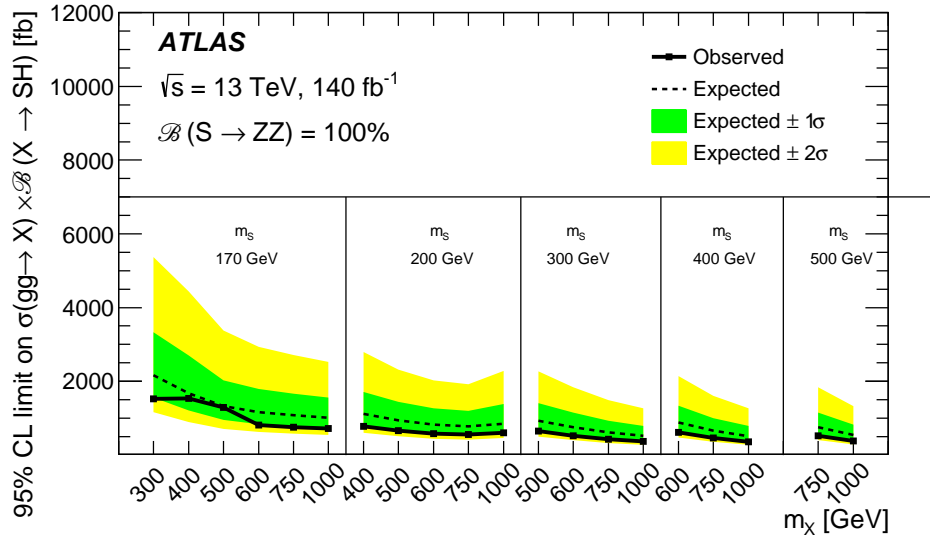


Figure 8: Observed (solid line) and expected (dashed line) 95% CL upper limits on $\sigma(gg \rightarrow X) \times \mathcal{B}(X \rightarrow SH)$ as a function of m_X and m_S , under the assumption of $\mathcal{B}(S \rightarrow ZZ) = 100\%$. The green and yellow shaded areas indicate the ± 1 and ± 2 standard deviations around the expected limit.

8 Conclusion

This paper presents the first search for the $X \rightarrow SH \rightarrow VV\gamma\gamma$ process by selecting events with a pair of photons accompanied by one or two leptons (electrons or muons). The analysis is based on 140 fb^{-1} of proton–proton collision data at $\sqrt{s} = 13 \text{ TeV}$ recorded with the ATLAS detector at the LHC. The $X \rightarrow SH \rightarrow VV\gamma\gamma$ signal is searched for over the $300 \leq m_X \leq 1000 \text{ GeV}$ and $170 \leq m_S \leq 500 \text{ GeV}$ mass ranges, probing lower m_X values than the ATLAS $SH \rightarrow VV\tau\tau$ search, and complementing the ATLAS $X \rightarrow SH \rightarrow bb\gamma\gamma$ search by testing a different S -boson decay mode.

No excess of events above the expected SM background is observed and 95% CL upper limits are set on the cross-section times branching ratio, $\sigma(gg \rightarrow X) \times \mathcal{B}(X \rightarrow SH)$, under different assumptions for the $S \rightarrow WW/ZZ$ branching ratios. The observed (expected) upper limits lie in the range of 530–120 fb (800–170 fb) under the assumption that $\mathcal{B}(S \rightarrow WW/ZZ)$ corresponding to those the SM Higgs boson would have at the mass of the S particle. The corresponding observed (expected) upper limits on the cross-section are in the range of 470–91 fb (610–120 fb) under the assumption of $\mathcal{B}(S \rightarrow WW) = 100\%$. Alternatively, under the assumption of $\mathcal{B}(S \rightarrow ZZ) = 100\%$, the observed (expected) limits are in the range of 1530–360 fb (2160–510 fb).

Acknowledgements

We thank CERN for the very successful operation of the LHC and its injectors, as well as the support staff at CERN and at our institutions worldwide without whom ATLAS could not be operated efficiently.

The crucial computing support from all WLCG partners is acknowledged gratefully, in particular from CERN, the ATLAS Tier-1 facilities at TRIUMF/SFU (Canada), NDGF (Denmark, Norway, Sweden), CC-IN2P3 (France), KIT/GridKA (Germany), INFN-CNAF (Italy), NL-T1 (Netherlands), PIC (Spain), RAL (UK) and BNL (USA), the Tier-2 facilities worldwide and large non-WLCG resource providers. Major contributors of computing resources are listed in Ref. [109].

We gratefully acknowledge the support of ANPCyT, Argentina; YerPhI, Armenia; ARC, Australia; BMWFW and FWF, Austria; ANAS, Azerbaijan; CNPq and FAPESP, Brazil; NSERC, NRC and CFI, Canada; CERN; ANID, Chile; CAS, MOST and NSFC, China; Minciencias, Colombia; MEYS CR, Czech Republic; DNRF and DNSRC, Denmark; IN2P3-CNRS and CEA-DRF/IRFU, France; SRNSFG, Georgia; BMBF, HGF and MPG, Germany; GSRI, Greece; RGC and Hong Kong SAR, China; ISF and Benoziy Center, Israel; INFN, Italy; MEXT and JSPS, Japan; CNRST, Morocco; NWO, Netherlands; RCN, Norway; MNiSW, Poland; FCT, Portugal; MNE/IFA, Romania; MESTD, Serbia; MSSR, Slovakia; ARRS and MIZŠ, Slovenia; DSI/NRF, South Africa; MICINN, Spain; SRC and Wallenberg Foundation, Sweden; SERI, SNSF and Cantons of Bern and Geneva, Switzerland; MOST, Taipei; TENMAK, Türkiye; STFC, United Kingdom; DOE and NSF, United States of America.

Individual groups and members have received support from BCKDF, CANARIE, CRC and DRAC, Canada; CERN-CZ, FORTE and PRIMUS, Czech Republic; COST, ERC, ERDF, Horizon 2020, ICSC-NextGenerationEU and Marie Skłodowska-Curie Actions, European Union; Investissements d’Avenir Labex, Investissements d’Avenir Idex and ANR, France; DFG and AvH Foundation, Germany; Herakleitos, Thales and Aristeia programmes co-financed by EU-ESF and the Greek NSRF, Greece; BSF-NSF and MINERVA, Israel; NCN and NAWA, Poland; La Caixa Banking Foundation, CERCA Programme Generalitat de

Catalunya and PROMETEO and GenT Programmes Generalitat Valenciana, Spain; Göran Gustafssons Stiftelse, Sweden; The Royal Society and Leverhulme Trust, United Kingdom.

In addition, individual members wish to acknowledge support from Armenia: Yerevan Physics Institute (FAPERJ); CERN: European Organization for Nuclear Research (CERN PJAS); Chile: Agencia Nacional de Investigación y Desarrollo (FONDECYT 1230812, FONDECYT 1230987, FONDECYT 1240864); China: National Natural Science Foundation of China (NSFC - 12175119, NSFC 12275265, NSFC-12075060); Czech Republic: Czech Science Foundation (GACR - 24-11373S), Ministry of Education Youth and Sports (FORTE CZ.02.01.01/00/22_008/0004632), PRIMUS Research Programme (PRIMUS/21/SCI/017); European Union: European Research Council (ERC - 948254, ERC 101089007), Horizon 2020 Framework Programme (MUCCA - CHIST-ERA-19-XAI-00), European Union, Future Artificial Intelligence Research (FAIR-NextGenerationEU PE00000013), Italian Center for High Performance Computing, Big Data and Quantum Computing (ICSC, NextGenerationEU); France: Agence Nationale de la Recherche (ANR-20-CE31-0013, ANR-21-CE31-0013, ANR-21-CE31-0022), Investissements d'Avenir Labex (ANR-11-LABX-0012); Germany: Baden-Württemberg Stiftung (BW Stiftung-Postdoc Eliteprogramme), Deutsche Forschungsgemeinschaft (DFG - 469666862, DFG - CR 312/5-2); Italy: Istituto Nazionale di Fisica Nucleare (ICSC, NextGenerationEU); Japan: Japan Society for the Promotion of Science (JSPS KAKENHI JP22H01227, JSPS KAKENHI JP22H04944, JSPS KAKENHI JP22KK0227); Netherlands: Netherlands Organisation for Scientific Research (NWO Veni 2020 - VI.Veni.202.179); Norway: Research Council of Norway (RCN-314472); Poland: Polish National Agency for Academic Exchange (PPN/PPO/2020/1/00002/U/00001), Polish National Science Centre (NCN 2021/42/E/ST2/00350, NCN OPUS nr 2022/47/B/ST2/03059, NCN UMO-2019/34/E/ST2/00393, UMO-2020/37/B/ST2/01043, UMO-2021/40/C/ST2/00187, UMO-2022/47/O/ST2/00148, UMO-2023/49/B/ST2/04085); Slovenia: Slovenian Research Agency (ARIS grant J1-3010); Spain: Generalitat Valenciana (Artemisa, FEDER, IDIFEDER/2018/048), Ministry of Science and Innovation (MCIN & NextGenEU PCI2022-135018-2, MICIN & FEDER PID2021-125273NB, RYC2019-028510-I, RYC2020-030254-I, RYC2021-031273-I, RYC2022-038164-I), PROMETEO and GenT Programmes Generalitat Valenciana (CIDEAGENT/2019/027); Sweden: Swedish Research Council (Swedish Research Council 2023-04654, VR 2018-00482, VR 2022-03845, VR 2022-04683, VR 2023-03403, VR grant 2021-03651), Knut and Alice Wallenberg Foundation (KAW 2018.0157, KAW 2018.0458, KAW 2019.0447, KAW 2022.0358); Switzerland: Swiss National Science Foundation (SNSF - PCEFP2_194658); United Kingdom: Leverhulme Trust (Leverhulme Trust RPG-2020-004), Royal Society (NIF-R1-231091); United States of America: U.S. Department of Energy (ECA DE-AC02-76SF00515), Neubauer Family Foundation.

References

- [1] ATLAS Collaboration, *The ATLAS Experiment at the CERN Large Hadron Collider*, [JINST 3 \(2008\) S08003](#).
- [2] CMS Collaboration, *The CMS Experiment at the CERN LHC*, [JINST 3 \(2008\) S08004](#).
- [3] ATLAS Collaboration, *Observation of a new particle in the search for the Standard Model Higgs boson with the ATLAS detector at the LHC*, [Phys. Lett. B 716 \(2012\) 1](#), arXiv: [1207.7214 \[hep-ex\]](#).
- [4] CMS Collaboration, *Observation of a new boson at a mass of 125 GeV with the CMS experiment at the LHC*, [Phys. Lett. B 716 \(2012\) 30](#), arXiv: [1207.7235 \[hep-ex\]](#).
- [5] ATLAS Collaboration, *A detailed map of Higgs boson interactions by the ATLAS experiment ten years after the discovery*, [Nature 607 \(2022\) 52](#), arXiv: [2207.00092 \[hep-ex\]](#), Erratum: [Nature 612 \(2022\) E24](#).
- [6] CMS Collaboration, *A portrait of the Higgs boson by the CMS experiment ten years after the discovery*, [Nature 607 \(2022\) 60](#), arXiv: [2207.00043 \[hep-ex\]](#), Erratum: [Nature 623 \(2023\) E4](#).
- [7] U. Ellwanger, C. Hugonie and A. M. Teixeira, *The Next-to-Minimal Supersymmetric Standard Model*, [Phys. Rept. 496 \(2010\) 1](#), arXiv: [0910.1785 \[hep-ph\]](#).
- [8] M. Maniatis, *The Next-to-Minimal Supersymmetric extension of the Standard Model reviewed*, [Int. J. Mod. Phys. A 25 \(2010\) 3505](#), arXiv: [0906.0777 \[hep-ph\]](#).
- [9] T. Robens, T. Stefaniak and J. Wittbrodt, *Two-real-scalar-singlet extension of the SM: LHC phenomenology and benchmark scenarios*, [Eur. Phys. J. C 80 \(2020\) 151](#), arXiv: [1908.08554 \[hep-ph\]](#).
- [10] T. Robens, *Two-Real-Singlet-Model Benchmark Planes*, [Symmetry 15 \(2023\) 27](#), arXiv: [2209.10996 \[hep-ph\]](#).
- [11] G. C. Branco et al., *Theory and phenomenology of two-Higgs-doublet models*, [Phys. Rept. 516 \(2012\) 1](#), arXiv: [1106.0034 \[hep-ph\]](#).
- [12] S. Baum and N. R. Shah, *Two Higgs doublets and a complex singlet: disentangling the decay topologies and associated phenomenology*, [JHEP 12 \(2018\) 044](#), arXiv: [1808.02667 \[hep-ph\]](#).
- [13] ATLAS Collaboration, *Search for Higgs boson pair production in the $WW^{(*)}WW^{(*)}$ decay channel using ATLAS data recorded at $\sqrt{s} = 13$ TeV*, [JHEP 05 \(2019\) 124](#), arXiv: [1811.11028 \[hep-ex\]](#).
- [14] ATLAS Collaboration, *Search for a resonance decaying into a scalar particle and a Higgs boson in the final state with two bottom quarks and two photons in proton-proton collisions at a center of mass energy of 13 TeV with the ATLAS detector*, (2024), arXiv: [2404.12915 \[hep-ex\]](#).
- [15] ATLAS Collaboration, *Search for a new heavy scalar particle decaying into a Higgs boson and a new scalar singlet in final states with one or two light leptons and a pair of τ -leptons with the ATLAS detector*, [JHEP 10 \(2023\) 009](#), arXiv: [2307.11120 \[hep-ex\]](#).

- [16] CMS Collaboration, *Search for a new resonance decaying into two spin-0 bosons in a final state with two photons and two bottom quarks in proton–proton collisions at $\sqrt{s} = 13$ TeV*, (2023), arXiv: [2310.01643 \[hep-ex\]](#).
- [17] CMS Collaboration, *Search for a heavy Higgs boson decaying into two lighter Higgs bosons in the $\tau\tau bb$ final state at 13 TeV*, *JHEP* **11** (2021) 057, arXiv: [2106.10361 \[hep-ex\]](#).
- [18] CMS Collaboration, *Search for a massive scalar resonance decaying to a light scalar and a Higgs boson in the four b quarks final state with boosted topology*, *Phys. Lett. B* **842** (2023) 137392, arXiv: [2204.12413 \[hep-ex\]](#).
- [19] D. de Florian et al., *Handbook of LHC Higgs Cross Sections: 4. Deciphering the Nature of the Higgs Sector*, (2017), arXiv: [1610.07922 \[hep-ph\]](#).
- [20] ATLAS Collaboration, *Measurements of the Higgs boson inclusive and differential fiducial cross-sections in the diphoton decay channel with pp collisions at $\sqrt{s} = 13$ TeV with the ATLAS detector*, *JHEP* **08** (2022) 027, arXiv: [2202.00487 \[hep-ex\]](#).
- [21] ATLAS Collaboration, *ATLAS Insertable B-Layer: Technical Design Report*, ATLAS-TDR-19; CERN-LHCC-2010-013, 2010, URL: <https://cds.cern.ch/record/1291633>, Addendum: ATLAS-TDR-19-ADD-1; CERN-LHCC-2012-009, 2012, URL: <https://cds.cern.ch/record/1451888>.
- [22] B. Abbott et al., *Production and integration of the ATLAS Insertable B-Layer*, *JINST* **13** (2018) T05008, arXiv: [1803.00844 \[physics.ins-det\]](#).
- [23] G. Avoni et al., *The new LUCID-2 detector for luminosity measurement and monitoring in ATLAS*, *JINST* **13** (2018) P07017.
- [24] ATLAS Collaboration, *Performance of the ATLAS trigger system in 2015*, *Eur. Phys. J. C* **77** (2017) 317, arXiv: [1611.09661 \[hep-ex\]](#).
- [25] ATLAS Collaboration, *Software and computing for Run 3 of the ATLAS experiment at the LHC*, (2024), arXiv: [2404.06335 \[hep-ex\]](#).
- [26] ATLAS Collaboration, *Luminosity determination in pp collisions at $\sqrt{s} = 13$ TeV using the ATLAS detector at the LHC*, *Eur. Phys. J. C* **83** (2023) 982, arXiv: [2212.09379 \[hep-ex\]](#).
- [27] ATLAS Collaboration, *ATLAS data quality operations and performance for 2015–2018 data-taking*, *JINST* **15** (2020) P04003, arXiv: [1911.04632 \[physics.ins-det\]](#).
- [28] ATLAS Collaboration, *Performance of electron and photon triggers in ATLAS during LHC Run 2*, *Eur. Phys. J. C* **80** (2020) 47, arXiv: [1909.00761 \[hep-ex\]](#).
- [29] T. Sjöstrand et al., *An introduction to PYTHIA 8.2*, *Comput. Phys. Commun.* **191** (2015) 159, arXiv: [1410.3012 \[hep-ph\]](#).
- [30] ATLAS Collaboration, *ATLAS Pythia 8 tunes to 7 TeV data*, ATL-PHYS-PUB-2014-021, 2014, URL: <https://cds.cern.ch/record/1966419>.
- [31] NNPDF Collaboration, R. D. Ball et al., *Parton distributions with LHC data*, *Nucl. Phys. B* **867** (2013) 244, arXiv: [1207.1303 \[hep-ph\]](#).

- [32] K. Hamilton, P. Nason, E. Re and G. Zanderighi, *NNLOPS simulation of Higgs boson production*, [JHEP **10** \(2013\) 222](#), arXiv: [1309.0017 \[hep-ph\]](#).
- [33] K. Hamilton, P. Nason and G. Zanderighi, *Finite quark-mass effects in the NNLOPS POWHEG+MiNLO Higgs generator*, [JHEP **05** \(2015\) 140](#), arXiv: [1501.04637 \[hep-ph\]](#).
- [34] S. Alioli, P. Nason, C. Oleari and E. Re, *A general framework for implementing NLO calculations in shower Monte Carlo programs: the POWHEG BOX*, [JHEP **06** \(2010\) 043](#), arXiv: [1002.2581 \[hep-ph\]](#).
- [35] P. Nason, *A new method for combining NLO QCD with shower Monte Carlo algorithms*, [JHEP **11** \(2004\) 040](#), arXiv: [hep-ph/0409146](#).
- [36] S. Frixione, P. Nason and C. Oleari, *Matching NLO QCD computations with parton shower simulations: the POWHEG method*, [JHEP **11** \(2007\) 070](#), arXiv: [0709.2092 \[hep-ph\]](#).
- [37] K. Hamilton, P. Nason and G. Zanderighi, *MINLO: multi-scale improved NLO*, [JHEP **10** \(2012\) 155](#), arXiv: [1206.3572 \[hep-ph\]](#).
- [38] J. M. Campbell et al., *NLO Higgs boson production plus one and two jets using the POWHEG BOX, MadGraph4 and MCFM*, [JHEP **07** \(2012\) 092](#), arXiv: [1202.5475 \[hep-ph\]](#).
- [39] K. Hamilton, P. Nason, C. Oleari and G. Zanderighi, *Merging H/W/Z + 0 and 1 jet at NLO with no merging scale: a path to parton shower + NNLO matching*, [JHEP **05** \(2013\) 082](#), arXiv: [1212.4504 \[hep-ph\]](#).
- [40] S. Catani and M. Grazzini, *Next-to-Next-to-Leading-Order Subtraction Formalism in Hadron Collisions and its Application to Higgs-Boson Production at the Large Hadron Collider*, [Phys. Rev. Lett. **98** \(2007\) 222002](#), arXiv: [hep-ph/0703012 \[hep-ph\]](#).
- [41] J. Butterworth et al., *PDF4LHC recommendations for LHC Run II*, [J. Phys. G **43** \(2016\) 023001](#), arXiv: [1510.03865 \[hep-ph\]](#).
- [42] ATLAS Collaboration, *Measurement of the Z/ γ^* boson transverse momentum distribution in pp collisions at $\sqrt{s} = 7$ TeV with the ATLAS detector*, [JHEP **09** \(2014\) 145](#), arXiv: [1406.3660 \[hep-ex\]](#).
- [43] D. J. Lange, *The EvtGen particle decay simulation package*, [Nucl. Instrum. Meth. A **462** \(2001\) 152](#).
- [44] C. Anastasiou et al., *High precision determination of the gluon fusion Higgs boson cross-section at the LHC*, [JHEP **05** \(2016\) 058](#), arXiv: [1602.00695 \[hep-ph\]](#).
- [45] C. Anastasiou, C. Duhr, F. Dulat, F. Herzog and B. Mistlberger, *Higgs Boson Gluon-Fusion Production in QCD at Three Loops*, [Phys. Rev. Lett. **114** \(2015\) 212001](#), arXiv: [1503.06056 \[hep-ph\]](#).
- [46] F. Dulat, A. Lazopoulos and B. Mistlberger, *iHixs 2 – Inclusive Higgs cross sections*, [Comput. Phys. Commun. **233** \(2018\) 243](#), arXiv: [1802.00827 \[hep-ph\]](#).
- [47] R. V. Harlander and K. J. Ozeren, *Finite top mass effects for hadronic Higgs production at next-to-next-to-leading order*, [JHEP **11** \(2009\) 088](#), arXiv: [0909.3420 \[hep-ph\]](#).

- [48] R. V. Harlander and K. J. Ozeren,
Top mass effects in Higgs production at next-to-next-to-leading order QCD: Virtual corrections,
[Phys. Lett. B **679** \(2009\) 467](#), arXiv: [0907.2997 \[hep-ph\]](#).
- [49] R. V. Harlander, H. Mantler, S. Marzani and K. J. Ozeren,
Higgs production in gluon fusion at next-to-next-to-leading order QCD for finite top mass,
[Eur. Phys. J. C **66** \(2010\) 359](#), arXiv: [0912.2104 \[hep-ph\]](#).
- [50] A. Pak, M. Rogal and M. Steinhauser,
Finite top quark mass effects in NNLO Higgs boson production at LHC, [JHEP **02** \(2010\) 025](#),
arXiv: [0911.4662 \[hep-ph\]](#).
- [51] S. Actis, G. Passarino, C. Sturm and S. Uccirati,
NLO electroweak corrections to Higgs boson production at hadron colliders,
[Phys. Lett. B **670** \(2008\) 12](#), arXiv: [0809.1301 \[hep-ph\]](#).
- [52] S. Actis, G. Passarino, C. Sturm and S. Uccirati,
NNLO computational techniques: The cases $H \rightarrow \gamma\gamma$ and $H \rightarrow gg$, [Nucl. Phys. B **811** \(2009\) 182](#),
arXiv: [0809.3667 \[hep-ph\]](#).
- [53] M. Bonetti, K. Melnikov and L. Tancredi, *Higher order corrections to mixed QCD-EW contributions to Higgs boson production in gluon fusion*, [Phys. Rev. D **97** \(2018\) 056017](#),
arXiv: [1801.10403 \[hep-ph\]](#), Erratum: [Phys. Rev. D **97** \(2018\) 099906\(E\)](#).
- [54] M. Ciccolini, A. Denner and S. Dittmaier, *Strong and Electroweak Corrections to the Production of a Higgs Boson + 2 Jets via Weak Interactions at the Large Hadron Collider*,
[Phys. Rev. Lett. **99** \(2007\) 161803](#), arXiv: [0707.0381 \[hep-ph\]](#).
- [55] M. Ciccolini, A. Denner and S. Dittmaier,
Electroweak and QCD corrections to Higgs production via vector-boson fusion at the CERN LHC,
[Phys. Rev. D **77** \(2008\) 013002](#), arXiv: [0710.4749 \[hep-ph\]](#).
- [56] P. Bolzoni, F. Maltoni, S.-O. Moch and M. Zaro,
Higgs Boson Production via Vector-Boson Fusion at Next-to-Next-to-Leading Order in QCD,
[Phys. Rev. Lett. **105** \(2010\) 011801](#), arXiv: [1003.4451 \[hep-ph\]](#).
- [57] G. Luisoni, P. Nason, C. Oleari and F. Tramontano, *$HW^\pm/HZ + 0$ and 1 jet at NLO with the POWHEG BOX interfaced to GoSam and their merging within MiNLO*, [JHEP **10** \(2013\) 083](#),
arXiv: [1306.2542 \[hep-ph\]](#).
- [58] M. L. Ciccolini, S. Dittmaier and M. Krämer,
Electroweak radiative corrections to associated WH and ZH production at hadron colliders,
[Phys. Rev. D **68** \(2003\) 073003](#), arXiv: [hep-ph/0306234 \[hep-ph\]](#).
- [59] O. Brein, A. Djouadi and R. Harlander,
NNLO QCD corrections to the Higgs-strahlung processes at hadron colliders,
[Phys. Lett. B **579** \(2004\) 149](#), arXiv: [hep-ph/0307206](#).
- [60] O. Brein, R. V. Harlander, M. Wiesemann and T. Zirke,
Top-quark mediated effects in hadronic Higgs-Strahlung, [Eur. Phys. J. C **72** \(2012\) 1868](#),
arXiv: [1111.0761 \[hep-ph\]](#).
- [61] L. Altenkamp, S. Dittmaier, R. V. Harlander, H. Rzehak and T. J. E. Zirke,
Gluon-induced Higgs-strahlung at next-to-leading order QCD, [JHEP **02** \(2013\) 078](#),
arXiv: [1211.5015 \[hep-ph\]](#).

- [62] A. Denner, S. Dittmaier, S. Kallweit and A. Mück, *HAWK 2.0: A Monte Carlo program for Higgs production in vector-boson fusion and Higgs strahlung at hadron colliders*, [Comput. Phys. Commun.](#) **195** (2015) 161, arXiv: [1412.5390 \[hep-ph\]](#).
- [63] O. Brein, R. V. Harlander and T. J. E. Zirke, *vh@nnlo – Higgs Strahlung at hadron colliders*, [Comput. Phys. Commun.](#) **184** (2013) 998, arXiv: [1210.5347 \[hep-ph\]](#).
- [64] R. V. Harlander, A. Kulesza, V. Theeuwes and T. Zirke, *Soft gluon resummation for gluon-induced Higgs Strahlung*, [JHEP](#) **11** (2014) 082, arXiv: [1410.0217 \[hep-ph\]](#).
- [65] NNPDF Collaboration, R. D. Ball et al., *Parton distributions for the LHC run II*, [JHEP](#) **04** (2015) 040, arXiv: [1410.8849 \[hep-ph\]](#).
- [66] J. Alwall et al., *The automated computation of tree-level and next-to-leading order differential cross sections, and their matching to parton shower simulations*, [JHEP](#) **07** (2014) 079, arXiv: [1405.0301 \[hep-ph\]](#).
- [67] A. Djouadi, J. Kalinowski and M. Spira, *HDECAY: a program for Higgs boson decays in the Standard Model and its supersymmetric extension*, [Comput. Phys. Commun.](#) **108** (1998) 56, arXiv: [hep-ph/9704448](#).
- [68] M. Spira, *QCD effects in Higgs physics*, [Fortsch. Phys.](#) **46** (1999) 203, arXiv: [hep-ph/9705337](#).
- [69] A. Djouadi, M. M. Mühlleitner and M. Spira, *Decays of Supersymmetric Particles: the Program SUSY-HIT (SUSpect-SdecaY-Hdecay-InTerface)*, [Acta Phys. Polon. B](#) **38** (2007) 635, arXiv: [hep-ph/0609292](#).
- [70] A. Bredenstein, A. Denner, S. Dittmaier and M. M. Weber, *Radiative corrections to the semileptonic and hadronic Higgs-boson decays $H \rightarrow WW/ZZ \rightarrow 4$ fermions*, [JHEP](#) **02** (2007) 080, arXiv: [hep-ph/0611234](#).
- [71] A. Bredenstein, A. Denner, S. Dittmaier and M. M. Weber, *Precise predictions for the Higgs-boson decay $H \rightarrow WW/ZZ \rightarrow 4$ leptons*, [Phys. Rev. D](#) **74** (2006) 013004, arXiv: [hep-ph/0604011 \[hep-ph\]](#).
- [72] A. Bredenstein, A. Denner, S. Dittmaier and M. M. Weber, *Precision calculations for the Higgs decays $H \rightarrow ZZ/WW \rightarrow 4$ leptons*, [Nucl. Phys. B Proc. Suppl.](#) **160** (2006) 131, ed. by J. Blumlein, S. Moch and T. Riemann, arXiv: [hep-ph/0607060](#).
- [73] E. Bothmann et al., *Event generation with Sherpa 2.2*, [SciPost Phys.](#) **7** (2019) 034, arXiv: [1905.09127 \[hep-ph\]](#).
- [74] T. Gleisberg and S. Höche, *Comix, a new matrix element generator*, [JHEP](#) **12** (2008) 039, arXiv: [0808.3674 \[hep-ph\]](#).
- [75] F. Cascioli, P. Maierhöfer and S. Pozzorini, *Scattering Amplitudes with Open Loops*, [Phys. Rev. Lett.](#) **108** (2012) 111601, arXiv: [1111.5206 \[hep-ph\]](#).
- [76] A. Denner, S. Dittmaier and L. Hofer, *Collier: A fortran-based complex one-loop library in extended regularizations*, [Comput. Phys. Commun.](#) **212** (2017) 220, arXiv: [1604.06792 \[hep-ph\]](#).
- [77] S. Schumann and F. Krauss, *A parton shower algorithm based on Catani-Seymour dipole factorisation*, [JHEP](#) **03** (2008) 038, arXiv: [0709.1027 \[hep-ph\]](#).

- [78] S. Catani, F. Krauss, B. R. Webber and R. Kuhn, *QCD Matrix Elements + Parton Showers*, **JHEP** **11** (2001) 063, arXiv: [hep-ph/0109231](#).
- [79] S. Höche, F. Krauss, S. Schumann and F. Siegert, *QCD matrix elements and truncated showers*, **JHEP** **05** (2009) 053, arXiv: [0903.1219 \[hep-ph\]](#).
- [80] S. Höche, F. Krauss, M. Schönherr and F. Siegert, *A critical appraisal of NLO+PS matching methods*, **JHEP** **09** (2012) 049, arXiv: [1111.1220 \[hep-ph\]](#).
- [81] S. Höche, F. Krauss, M. Schönherr and F. Siegert, *QCD matrix elements + parton showers. The NLO case*, **JHEP** **04** (2013) 027, arXiv: [1207.5030 \[hep-ph\]](#).
- [82] S. Agostinelli et al., *GEANT4 – a simulation toolkit*, **Nucl. Instrum. Meth. A** **506** (2003) 250.
- [83] ATLAS Collaboration, *The ATLAS Simulation Infrastructure*, **Eur. Phys. J. C** **70** (2010) 823, arXiv: [1005.4568 \[physics.ins-det\]](#).
- [84] ATLAS Collaboration, *The simulation principle and performance of the ATLAS fast calorimeter simulation FastCaloSim*, ATL-PHYS-PUB-2010-013, 2010, URL: <https://cds.cern.ch/record/1300517>.
- [85] T. Sjöstrand, S. Mrenna and P. Skands, *A brief introduction to PYTHIA 8.1*, **Comput. Phys. Commun.** **178** (2008) 852, arXiv: [0710.3820 \[hep-ph\]](#).
- [86] ATLAS Collaboration, *The Pythia 8 A3 tune description of ATLAS minimum bias and inelastic measurements incorporating the Donnachie–Landshoff diffractive model*, ATL-PHYS-PUB-2016-017, 2016, URL: <https://cds.cern.ch/record/2206965>.
- [87] ATLAS Collaboration, *Measurement of Higgs boson production in the diphoton decay channel in pp collisions at center-of-mass energies of 7 and 8 TeV with the ATLAS detector*, **Phys. Rev. D** **90** (2014) 112015, arXiv: [1408.7084 \[hep-ex\]](#).
- [88] ATLAS Collaboration, *Electron and photon performance measurements with the ATLAS detector using the 2015–2017 LHC proton–proton collision data*, **JINST** **14** (2019) P12006, arXiv: [1908.00005 \[hep-ex\]](#).
- [89] ATLAS Collaboration, *Muon reconstruction and identification efficiency in ATLAS using the full Run 2 pp collision data set at $\sqrt{s} = 13$ TeV*, **Eur. Phys. J. C** **81** (2021) 578, arXiv: [2012.00578 \[hep-ex\]](#).
- [90] ATLAS Collaboration, *Jet reconstruction and performance using particle flow with the ATLAS Detector*, **Eur. Phys. J. C** **77** (2017) 466, arXiv: [1703.10485 \[hep-ex\]](#).
- [91] ATLAS Collaboration, *Topological cell clustering in the ATLAS calorimeters and its performance in LHC Run 1*, **Eur. Phys. J. C** **77** (2017) 490, arXiv: [1603.02934 \[hep-ex\]](#).
- [92] M. Cacciari, G. P. Salam and G. Soyez, *FastJet user manual*, **Eur. Phys. J. C** **72** (2012) 1896, arXiv: [1111.6097 \[hep-ph\]](#).
- [93] M. Cacciari, G. P. Salam and G. Soyez, *The anti- k_t jet clustering algorithm*, **JHEP** **04** (2008) 063, arXiv: [0802.1189 \[hep-ph\]](#).

- [94] ATLAS Collaboration, *Jet energy scale and resolution measured in proton–proton collisions at $\sqrt{s} = 13$ TeV with the ATLAS detector*, *Eur. Phys. J. C* **81** (2021) 689, arXiv: [2007.02645 \[hep-ex\]](#).
- [95] ATLAS Collaboration, *Performance of pile-up mitigation techniques for jets in pp collisions at $\sqrt{s} = 8$ TeV using the ATLAS detector*, *Eur. Phys. J. C* **76** (2016) 581, arXiv: [1510.03823 \[hep-ex\]](#).
- [96] ATLAS Collaboration, *ATLAS flavour-tagging algorithms for the LHC Run 2 pp collision dataset*, *Eur. Phys. J. C* **83** (2023) 681, arXiv: [2211.16345 \[physics.data-an\]](#).
- [97] ATLAS Collaboration, *The performance of missing transverse momentum reconstruction and its significance with the ATLAS detector using 140fb^{-1} of $\sqrt{s} = 13$ TeV pp collisions*, (2024), arXiv: [2402.05858 \[hep-ex\]](#).
- [98] P. Baldi, K. Cranmer, T. Faucett, P. Sadowski and D. Whiteson, *Parameterized neural networks for high-energy physics*, *Eur. Phys. J. C* **76** (2016) 235, arXiv: [1601.07913 \[hep-ex\]](#).
- [99] ATLAS Collaboration, *Recommendations for the Modeling of Smooth Backgrounds*, ATL-PHYS-PUB-2020-028, 2020, URL: <https://cds.cern.ch/record/2743717>.
- [100] ATLAS Collaboration, *Electron and photon efficiencies in LHC Run 2 with the ATLAS experiment*, (2023), arXiv: [2308.13362 \[hep-ex\]](#).
- [101] ATLAS Collaboration, *ATLAS b-jet identification performance and efficiency measurement with $t\bar{t}$ events in pp collisions at $\sqrt{s} = 13$ TeV*, *Eur. Phys. J. C* **79** (2019) 970, arXiv: [1907.05120 \[hep-ex\]](#).
- [102] ATLAS Collaboration, *Measurement of the c-jet mistagging efficiency in $t\bar{t}$ events using pp collision data at $\sqrt{s} = 13$ TeV collected with the ATLAS detector*, *Eur. Phys. J. C* **82** (2022) 95, arXiv: [2109.10627 \[hep-ex\]](#).
- [103] ATLAS Collaboration, *Calibration of the light-flavour jet mistagging efficiency of the b-tagging algorithms with Z+jets events using 139fb^{-1} of ATLAS proton–proton collision data at $\sqrt{s} = 13$ TeV*, *Eur. Phys. J. C* **83** (2023) 728, arXiv: [2301.06319 \[hep-ex\]](#).
- [104] W. Verkerke and D. Kirkby, *The RooFit toolkit for data modeling*, 2003, arXiv: [physics/0306116 \[physics.data-an\]](#).
- [105] L. Moneta et al., *The RooStats Project*, *PoS ACAT2010* (2010) 057, ed. by T. Speer et al., arXiv: [1009.1003 \[physics.data-an\]](#).
- [106] G. Cowan, K. Cranmer, E. Gross and O. Vitells, *Asymptotic formulae for likelihood-based tests of new physics*, *Eur. Phys. J. C* **71** (2011) 1554, arXiv: [1007.1727 \[physics.data-an\]](#), Erratum: *Eur. Phys. J. C* **73**, 2501 (2013).
- [107] A. L. Read, *Presentation of search results: the CL_s technique*, *J. Phys. G* **28** (2002) 2693, ed. by M. R. Whalley and L. Lyons.
- [108] T. Junk, *Confidence level computation for combining searches with small statistics*, *Nucl. Instrum. Meth. A* **434** (1999) 435, arXiv: [hep-ex/9902006](#).
- [109] ATLAS Collaboration, *ATLAS Computing Acknowledgements*, ATL-SOFT-PUB-2023-001, 2023, URL: <https://cds.cern.ch/record/2869272>.

The ATLAS Collaboration

G. Aad [ID](#)¹⁰⁴, E. Aakvaag [ID](#)¹⁷, B. Abbott [ID](#)¹²³, S. Abdelhameed [ID](#)^{119a}, K. Abeling [ID](#)⁵⁶, N.J. Abicht [ID](#)⁵⁰, S.H. Abidi [ID](#)³⁰, M. Aboeela [ID](#)⁴⁵, A. Aboulhorma [ID](#)^{36e}, H. Abramowicz [ID](#)¹⁵⁴, H. Abreu [ID](#)¹⁵³, Y. Abulaiti [ID](#)¹²⁰, B.S. Acharya [ID](#)^{70a,70b,1}, A. Ackermann [ID](#)^{64a}, C. Adam Bourdarios [ID](#)⁴, L. Adamczyk [ID](#)^{87a}, S.V. Addepalli [ID](#)²⁷, M.J. Addison [ID](#)¹⁰³, J. Adelman [ID](#)¹¹⁸, A. Adiguzel [ID](#)^{22c}, T. Adye [ID](#)¹³⁷, A.A. Affolder [ID](#)¹³⁹, Y. Afik [ID](#)⁴⁰, M.N. Agaras [ID](#)¹³, J. Agarwala [ID](#)^{74a,74b}, A. Aggarwal [ID](#)¹⁰², C. Agheorghiesei [ID](#)^{28c}, F. Ahmadov [ID](#)^{39,y}, W.S. Ahmed [ID](#)¹⁰⁶, S. Ahuja [ID](#)⁹⁷, X. Ai [ID](#)^{63e}, G. Aielli [ID](#)^{77a,77b}, A. Aikot [ID](#)¹⁶⁶, M. Ait Tamlhat [ID](#)^{36e}, B. Aitbenkikh [ID](#)^{36a}, M. Akbiyik [ID](#)¹⁰², T.P.A. Åkesson [ID](#)¹⁰⁰, A.V. Akimov [ID](#)³⁸, D. Akiyama [ID](#)¹⁷¹, N.N. Akolkar [ID](#)²⁵, S. Aktas [ID](#)^{22a}, K. Al Houry [ID](#)⁴², G.L. Alberghi [ID](#)^{24b}, J. Albert [ID](#)¹⁶⁸, P. Albicocco [ID](#)⁵⁴, G.L. Albouy [ID](#)⁶¹, S. Alderweireldt [ID](#)⁵³, Z.L. Alegria [ID](#)¹²⁴, M. Aleksa [ID](#)³⁷, I.N. Aleksandrov [ID](#)³⁹, C. Alexa [ID](#)^{28b}, T. Alexopoulos [ID](#)¹⁰, F. Alfonsi [ID](#)^{24b}, M. Algren [ID](#)⁵⁷, M. Alhroob [ID](#)¹⁷⁰, B. Ali [ID](#)¹³⁵, H.M.J. Ali [ID](#)⁹³, S. Ali [ID](#)³², S.W. Alibocus [ID](#)⁹⁴, M. Aliev [ID](#)^{34c}, G. Alimonti [ID](#)^{72a}, W. Alkahi [ID](#)⁵⁶, C. Allaire [ID](#)⁶⁷, B.M.M. Allbrooke [ID](#)¹⁴⁹, J.F. Allen [ID](#)⁵³, C.A. Allendes Flores [ID](#)^{140f}, P.P. Allport [ID](#)²¹, A. Aloisio [ID](#)^{73a,73b}, F. Alonso [ID](#)⁹², C. Alpigiani [ID](#)¹⁴¹, Z.M.K. Alsolami [ID](#)⁹³, M. Alvarez Estevez [ID](#)¹⁰¹, A. Alvarez Fernandez [ID](#)¹⁰², M. Alves Cardoso [ID](#)⁵⁷, M.G. Alvigi [ID](#)^{73a,73b}, M. Aly [ID](#)¹⁰³, Y. Amaral Coutinho [ID](#)^{84b}, A. Ambler [ID](#)¹⁰⁶, C. Amelung [ID](#)³⁷, M. Amerl [ID](#)¹⁰³, C.G. Ames [ID](#)¹¹¹, D. Amidei [ID](#)¹⁰⁸, B. Amini [ID](#)⁵⁵, K.J. Amirie [ID](#)¹⁵⁸, S.P. Amor Dos Santos [ID](#)^{133a}, K.R. Amos [ID](#)¹⁶⁶, S. An [ID](#)⁸⁵, V. Ananiev [ID](#)¹²⁸, C. Anastopoulos [ID](#)¹⁴², T. Andeen [ID](#)¹¹, J.K. Anders [ID](#)³⁷, A.C. Anderson [ID](#)⁶⁰, S.Y. Andrean [ID](#)^{48a,48b}, A. Andreazza [ID](#)^{72a,72b}, S. Angelidakis [ID](#)⁹, A. Angerami [ID](#)⁴², A.V. Anisenkov [ID](#)³⁸, A. Annovi [ID](#)^{75a}, C. Antel [ID](#)⁵⁷, E. Antipov [ID](#)¹⁴⁸, M. Antonelli [ID](#)⁵⁴, F. Anulli [ID](#)^{76a}, M. Aoki [ID](#)⁸⁵, T. Aoki [ID](#)¹⁵⁶, M.A. Aparo [ID](#)¹⁴⁹, L. Aperio Bella [ID](#)⁴⁹, C. Appelt [ID](#)¹⁹, A. Apyan [ID](#)²⁷, S.J. Arbiol Val [ID](#)⁸⁸, C. Arcangeletti [ID](#)⁵⁴, A.T.H. Arce [ID](#)⁵², J-F. Arguin [ID](#)¹¹⁰, S. Argyropoulos [ID](#)⁵⁵, J.-H. Arling [ID](#)⁴⁹, O. Arnaez [ID](#)⁴, H. Arnold [ID](#)¹⁴⁸, G. Artoni [ID](#)^{76a,76b}, H. Asada [ID](#)¹¹³, K. Asai [ID](#)¹²¹, S. Asai [ID](#)¹⁵⁶, N.A. Asbah [ID](#)³⁷, R.A. Ashby Pickering [ID](#)¹⁷⁰, K. Assamagan [ID](#)³⁰, R. Astalos [ID](#)^{29a}, K.S.V. Astrand [ID](#)¹⁰⁰, S. Atashi [ID](#)¹⁶², R.J. Atkin [ID](#)^{34a}, M. Atkinson [ID](#)¹⁶⁵, H. Atmani [ID](#)^{36f}, P.A. Atmasiddha [ID](#)¹³¹, K. Augsten [ID](#)¹³⁵, S. Auricchio [ID](#)^{73a,73b}, A.D. Auriol [ID](#)²¹, V.A. Austrup [ID](#)¹⁰³, G. Avolio [ID](#)³⁷, K. Axiotis [ID](#)⁵⁷, G. Azuelos [ID](#)^{110,ad}, D. Babal [ID](#)^{29b}, H. Bachacou [ID](#)¹³⁸, K. Bachas [ID](#)^{155,p}, A. Bachi [ID](#)³⁵, F. Backman [ID](#)^{48a,48b}, A. Badea [ID](#)⁴⁰, T.M. Baer [ID](#)¹⁰⁸, P. Bagnaia [ID](#)^{76a,76b}, M. Bahmani [ID](#)¹⁹, D. Bahner [ID](#)⁵⁵, K. Bai [ID](#)¹²⁶, J.T. Baines [ID](#)¹³⁷, L. Baines [ID](#)⁹⁶, O.K. Baker [ID](#)¹⁷⁵, E. Bakos [ID](#)¹⁶, D. Bakshi Gupta [ID](#)⁸, L.E. Balabram Filho [ID](#)^{84b}, V. Balakrishnan [ID](#)¹²³, R. Balasubramanian [ID](#)¹¹⁷, E.M. Baldin [ID](#)³⁸, P. Balek [ID](#)^{87a}, E. Ballabene [ID](#)^{24b,24a}, F. Balli [ID](#)¹³⁸, L.M. Baltes [ID](#)^{64a}, W.K. Balunas [ID](#)³³, J. Balz [ID](#)¹⁰², I. Bamwidhi [ID](#)^{119b}, E. Banas [ID](#)⁸⁸, M. Bandieramonte [ID](#)¹³², A. Bandyopadhyay [ID](#)²⁵, S. Bansal [ID](#)²⁵, L. Barak [ID](#)¹⁵⁴, M. Barakat [ID](#)⁴⁹, E.L. Barberio [ID](#)¹⁰⁷, D. Barberis [ID](#)^{58b,58a}, M. Barbero [ID](#)¹⁰⁴, M.Z. Barel [ID](#)¹¹⁷, T. Barillari [ID](#)¹¹², M-S. Barisits [ID](#)³⁷, T. Barklow [ID](#)¹⁴⁶, P. Baron [ID](#)¹²⁵, D.A. Baron Moreno [ID](#)¹⁰³, A. Baroncelli [ID](#)^{63a}, A.J. Barr [ID](#)¹²⁹, J.D. Barr [ID](#)⁹⁸, F. Barreiro [ID](#)¹⁰¹, J. Barreiro Guimarães da Costa [ID](#)¹⁴, U. Barron [ID](#)¹⁵⁴, M.G. Barros Teixeira [ID](#)^{133a}, S. Barsov [ID](#)³⁸, F. Bartels [ID](#)^{64a}, R. Bartoldus [ID](#)¹⁴⁶, A.E. Barton [ID](#)⁹³, P. Bartos [ID](#)^{29a}, A. Basan [ID](#)¹⁰², M. Baselga [ID](#)⁵⁰, A. Bassalat [ID](#)^{67,b}, M.J. Basso [ID](#)^{159a}, S. Bataju [ID](#)⁴⁵, R. Bate [ID](#)¹⁶⁷, R.L. Bates [ID](#)⁶⁰, S. Batlamous [ID](#)¹⁰¹, B. Batool [ID](#)¹⁴⁴, M. Battaglia [ID](#)¹³⁹, D. Battulga [ID](#)¹⁹, M. Baunce [ID](#)^{76a,76b}, M. Bauer [ID](#)⁸⁰, P. Bauer [ID](#)²⁵, L.T. Bazzano Hurrell [ID](#)³¹, J.B. Beacham [ID](#)⁵², T. Beau [ID](#)¹³⁰, J.Y. Beaucamp [ID](#)⁹², P.H. Beauchemin [ID](#)¹⁶¹, P. Bechtel [ID](#)²⁵, H.P. Beck [ID](#)^{20,o}, K. Becker [ID](#)¹⁷⁰, A.J. Beddall [ID](#)⁸³, V.A. Bednyakov [ID](#)³⁹, C.P. Bee [ID](#)¹⁴⁸, L.J. Beemster [ID](#)¹⁶, T.A. Beermann [ID](#)³⁷, M. Begalli [ID](#)^{84d}, M. Begel [ID](#)³⁰, A. Behera [ID](#)¹⁴⁸, J.K. Behr [ID](#)⁴⁹, J.F. Beirer [ID](#)³⁷, F. Beisiegel [ID](#)²⁵, M. Belfkir [ID](#)^{119b}, G. Bella [ID](#)¹⁵⁴, L. Bellagamba [ID](#)^{24b}, A. Bellerive [ID](#)³⁵, P. Bellos [ID](#)²¹, K. Beloborodov [ID](#)³⁸, D. Benckekroun [ID](#)^{36a}, F. Bendebba [ID](#)^{36a}, Y. Benhammou [ID](#)¹⁵⁴,

K.C. Benkendorfer ⁶², L. Beresford ⁴⁹, M. Beretta ⁵⁴, E. Bergeaas Kuutmann ¹⁶⁴, N. Berger ⁴,
 B. Bergmann ¹³⁵, J. Beringer ^{18a}, G. Bernardi ⁵, C. Bernius ¹⁴⁶, F.U. Bernlochner ²⁵,
 F. Bernon ^{37,104}, A. Berrocal Guardia ¹³, T. Berry ⁹⁷, P. Berta ¹³⁶, A. Berthold ⁵¹, S. Bethke ¹¹²,
 A. Betti ^{76a,76b}, A.J. Bevan ⁹⁶, N.K. Bhalla ⁵⁵, S. Bhatta ¹⁴⁸, D.S. Bhattacharya ¹⁶⁹,
 P. Bhattarai ¹⁴⁶, K.D. Bhide ⁵⁵, V.S. Bhopatkar ¹²⁴, R.M. Bianchi ¹³², G. Bianco ^{24b,24a},
 O. Biebel ¹¹¹, R. Bielski ¹²⁶, M. Biglietti ^{78a}, C.S. Billingsley ⁴⁵, Y. Bimgdi ^{36f}, M. Bindi ⁵⁶,
 A. Bingul ^{22b}, C. Bini ^{76a,76b}, G.A. Bird ³³, M. Birman ¹⁷², M. Biros ¹³⁶, S. Biryukov ¹⁴⁹,
 T. Bisanz ⁵⁰, E. Bisceglie ^{44b,44a}, J.P. Biswal ¹³⁷, D. Biswas ¹⁴⁴, I. Bloch ⁴⁹, A. Blue ⁶⁰,
 U. Blumenschein ⁹⁶, J. Blumenthal ¹⁰², V.S. Bobrovnikov ³⁸, M. Boehler ⁵⁵, B. Boehm ¹⁶⁹,
 D. Bogavac ³⁷, A.G. Bogdanchikov ³⁸, C. Bohm ^{48a}, V. Boisvert ⁹⁷, P. Bokan ³⁷, T. Bold ^{87a},
 M. Bomben ⁵, M. Bona ⁹⁶, M. Boonekamp ¹³⁸, C.D. Booth ⁹⁷, A.G. Borbély ⁶⁰,
 I.S. Bordulev ³⁸, G. Borissov ⁹³, D. Bortoletto ¹²⁹, D. Boscherini ^{24b}, M. Bosman ¹³,
 J.D. Bossio Sola ³⁷, K. Bouaouda ^{36a}, N. Bouchhar ¹⁶⁶, L. Boudet ⁴, J. Boudreau ¹³²,
 E.V. Bouhova-Thacker ⁹³, D. Boumediene ⁴¹, R. Bouquet ^{58b,58a}, A. Boveia ¹²², J. Boyd ³⁷,
 D. Boye ³⁰, I.R. Boyko ³⁹, L. Bozianu ⁵⁷, J. Bracinik ²¹, N. Brahimi ⁴, G. Brandt ¹⁷⁴,
 O. Brandt ³³, F. Braren ⁴⁹, B. Brau ¹⁰⁵, J.E. Brau ¹²⁶, R. Brenner ¹⁷², L. Brenner ¹¹⁷,
 R. Brenner ¹⁶⁴, S. Bressler ¹⁷², G. Brianti ^{79a,79b}, D. Britton ⁶⁰, D. Britzger ¹¹², I. Brock ²⁵,
 G. Brooijmans ⁴², E.M. Brooks ^{159b}, E. Brost ³⁰, L.M. Brown ¹⁶⁸, L.E. Bruce ⁶²,
 T.L. Bruckler ¹²⁹, P.A. Bruckman de Renstrom ⁸⁸, B. Brüers ⁴⁹, A. Bruni ^{24b}, G. Bruni ^{24b},
 M. Bruschi ^{24b}, N. Bruscinò ^{76a,76b}, T. Buanes ¹⁷, Q. Buat ¹⁴¹, D. Buchin ¹¹², A.G. Buckley ⁶⁰,
 O. Bulekov ³⁸, B.A. Bullard ¹⁴⁶, S. Burdin ⁹⁴, C.D. Burgard ⁵⁰, A.M. Burger ³⁷,
 B. Burghgrave ⁸, O. Burlayenko ⁵⁵, J. Burleson ¹⁶⁵, J.T.P. Burr ³³, J.C. Burzynski ¹⁴⁵,
 E.L. Busch ⁴², V. Büscher ¹⁰², P.J. Bussey ⁶⁰, J.M. Butler ²⁶, C.M. Buttar ⁶⁰,
 J.M. Butterworth ⁹⁸, W. Buttinger ¹³⁷, C.J. Buxo Vazquez ¹⁰⁹, A.R. Buzykaev ³⁸,
 S. Cabrera Urbán ¹⁶⁶, L. Cadamuro ⁶⁷, D. Caforio ⁵⁹, H. Cai ¹³², Y. Cai ^{14,114c}, Y. Cai ^{114a},
 V.M.M. Cairo ³⁷, O. Cakir ^{3a}, N. Calace ³⁷, P. Calafiura ^{18a}, G. Calderini ¹³⁰, P. Calfayan ⁶⁹,
 G. Callea ⁶⁰, L.P. Caloba ^{84b}, D. Calvet ⁴¹, S. Calvet ⁴¹, M. Calvetti ^{75a,75b}, R. Camacho Toro ¹³⁰,
 S. Camarda ³⁷, D. Camarero Munoz ²⁷, P. Camarri ^{77a,77b}, M.T. Camerlingo ^{73a,73b},
 D. Cameron ³⁷, C. Camincher ¹⁶⁸, M. Campanelli ⁹⁸, A. Camplani ⁴³, V. Canale ^{73a,73b},
 A.C. Canbay ^{3a}, E. Canonero ⁹⁷, J. Cantero ¹⁶⁶, Y. Cao ¹⁶⁵, F. Capocasa ²⁷, M. Capua ^{44b,44a},
 A. Carbone ^{72a,72b}, R. Cardarelli ^{77a}, J.C.J. Cardenas ⁸, G. Carducci ^{44b,44a}, T. Carli ³⁷,
 G. Carlino ^{73a}, J.I. Carlotto ¹³, B.T. Carlson ^{132,q}, E.M. Carlson ^{168,159a}, J. Carmignani ⁹⁴,
 L. Carminati ^{72a,72b}, A. Carnelli ¹³⁸, M. Carnesale ^{76a,76b}, S. Caron ¹¹⁶, E. Carquin ^{140f},
 S. Carrá ^{72a}, G. Carratta ^{24b,24a}, A.M. Carroll ¹²⁶, T.M. Carter ⁵³, M.P. Casado ^{13,i},
 M. Caspar ⁴⁹, F.L. Castillo ⁴, L. Castillo Garcia ¹³, V. Castillo Gimenez ¹⁶⁶, N.F. Castro ^{133a,133e},
 A. Catinaccio ³⁷, J.R. Catmore ¹²⁸, T. Cavaliere ⁴, V. Cavaliere ³⁰, N. Cavalli ^{24b,24a},
 L.J. Caviedes Betancourt ^{23b}, Y.C. Cekmecelioglu ⁴⁹, E. Celebi ⁸³, S. Cella ³⁷, F. Celli ¹²⁹,
 M.S. Centonze ^{71a,71b}, V. Cepaitis ⁵⁷, K. Cerny ¹²⁵, A.S. Cerqueira ^{84a}, A. Cerri ¹⁴⁹,
 L. Cerrito ^{77a,77b}, F. Cerutti ^{18a}, B. Cervato ¹⁴⁴, A. Cervelli ^{24b}, G. Cesarini ⁵⁴, S.A. Cetin ⁸³,
 D. Chakraborty ¹¹⁸, J. Chan ^{18a}, W.Y. Chan ¹⁵⁶, J.D. Chapman ³³, E. Chapon ¹³⁸,
 B. Chargeishvili ^{152b}, D.G. Charlton ²¹, M. Chatterjee ²⁰, C. Chauhan ¹³⁶, Y. Che ^{114a},
 S. Chekanov ⁶, S.V. Chekulaev ^{159a}, G.A. Chelkov ^{39,a}, A. Chen ¹⁰⁸, B. Chen ¹⁵⁴, B. Chen ¹⁶⁸,
 H. Chen ^{114a}, H. Chen ³⁰, J. Chen ^{63c}, J. Chen ¹⁴⁵, M. Chen ¹²⁹, S. Chen ¹⁵⁶, S.J. Chen ^{114a},
 X. Chen ^{63c}, X. Chen ^{15,ac}, Y. Chen ^{63a}, C.L. Cheng ¹⁷³, H.C. Cheng ^{65a}, S. Cheong ¹⁴⁶,
 A. Cheplakov ³⁹, E. Cheremushkina ⁴⁹, E. Cherepanova ¹¹⁷, R. Cherkaoui El Moursli ^{36e},
 E. Cheu ⁷, K. Cheung ⁶⁶, L. Chevalier ¹³⁸, V. Chiarella ⁵⁴, G. Chiarelli ^{75a}, N. Chiedde ¹⁰⁴,
 G. Chiodini ^{71a}, A.S. Chisholm ²¹, A. Chitan ^{28b}, M. Chitishvili ¹⁶⁶, M.V. Chizhov ³⁹,

K. Choi ¹¹, Y. Chou ¹⁴¹, E.Y.S. Chow ¹¹⁶, K.L. Chu ¹⁷², M.C. Chu ^{65a}, X. Chu ^{14,114c},
 Z. Chubinidze ⁵⁴, J. Chudoba ¹³⁴, J.J. Chwastowski ⁸⁸, D. Cieri ¹¹², K.M. Ciesla ^{87a},
 V. Cindro ⁹⁵, A. Ciocio ^{18a}, F. Cirotto ^{73a,73b}, Z.H. Citron ¹⁷², M. Citterio ^{72a}, D.A. Ciubotaru ^{28b},
 A. Clark ⁵⁷, P.J. Clark ⁵³, N. Clarke Hall ⁹⁸, C. Clarry ¹⁵⁸, J.M. Clavijo Columbie ⁴⁹,
 S.E. Clawson ⁴⁹, C. Clement ^{48a,48b}, Y. Coadou ¹⁰⁴, M. Cobal ^{70a,70c}, A. Coccaro ^{58b},
 R.F. Coelho Barrue ^{133a}, R. Coelho Lopes De Sa ¹⁰⁵, S. Coelli ^{72a}, B. Cole ⁴², J. Collot ⁶¹,
 P. Conde Muiño ^{133a,133g}, M.P. Connell ^{34c}, S.H. Connell ^{34c}, E.I. Conroy ¹²⁹, F. Conventi ^{73a,ae},
 H.G. Cooke ²¹, A.M. Cooper-Sarkar ¹²⁹, F.A. Corchia ^{24b,24a}, A. Cordeiro Oudot Choi ¹³⁰,
 L.D. Corpe ⁴¹, M. Corradi ^{76a,76b}, F. Corriveau ^{106,w}, A. Cortes-Gonzalez ¹⁹, M.J. Costa ¹⁶⁶,
 F. Costanza ⁴, D. Costanzo ¹⁴², B.M. Cote ¹²², J. Couthures ⁴, G. Cowan ⁹⁷, K. Cranmer ¹⁷³,
 D. Cremonini ^{24b,24a}, S. Crépe-Renaudin ⁶¹, F. Crescioli ¹³⁰, M. Cristinziani ¹⁴⁴,
 M. Cristoforetti ^{79a,79b}, V. Croft ¹¹⁷, J.E. Crosby ¹²⁴, G. Crosetti ^{44b,44a}, A. Cueto ¹⁰¹, H. Cui ⁹⁸,
 Z. Cui ⁷, W.R. Cunningham ⁶⁰, F. Curcio ¹⁶⁶, J.R. Curran ⁵³, P. Czodrowski ³⁷,
 M.J. Da Cunha Sargedas De Sousa ^{58b,58a}, J.V. Da Fonseca Pinto ^{84b}, C. Da Via ¹⁰³,
 W. Dabrowski ^{87a}, T. Dado ³⁷, S. Dahbi ¹⁵¹, T. Dai ¹⁰⁸, D. Dal Santo ²⁰, C. Dallapiccola ¹⁰⁵,
 M. Dam ⁴³, G. D'amen ³⁰, V. D'Amico ¹¹¹, J. Damp ¹⁰², J.R. Dandoy ³⁵, D. Dannheim ³⁷,
 M. Danninger ¹⁴⁵, V. Dao ¹⁴⁸, G. Darbo ^{58b}, S.J. Das ^{30,af}, F. Dattola ⁴⁹, S. D'Auria ^{72a,72b},
 A. D'avanzo ^{73a,73b}, C. David ^{34a}, T. Davidek ¹³⁶, I. Dawson ⁹⁶, H.A. Day-hall ¹³⁵, K. De ⁸,
 R. De Asmundis ^{73a}, N. De Biase ⁴⁹, S. De Castro ^{24b,24a}, N. De Groot ¹¹⁶, P. de Jong ¹¹⁷,
 H. De la Torre ¹¹⁸, A. De Maria ^{114a}, A. De Salvo ^{76a}, U. De Sanctis ^{77a,77b}, F. De Santis ^{71a,71b},
 A. De Santo ¹⁴⁹, J.B. De Vivie De Regie ⁶¹, D.V. Dedovich ³⁹, J. Degens ⁹⁴, A.M. Deiana ⁴⁵,
 F. Del Corso ^{24b,24a}, J. Del Peso ¹⁰¹, F. Del Rio ^{64a}, L. Delagrangé ¹³⁰, F. Deliot ¹³⁸,
 C.M. Delitzsch ⁵⁰, M. Della Pietra ^{73a,73b}, D. Della Volpe ⁵⁷, A. Dell'Acqua ³⁷,
 L. Dell'Asta ^{72a,72b}, M. Delmastro ⁴, P.A. Delsart ⁶¹, S. Demers ¹⁷⁵, M. Demichev ³⁹,
 S.P. Denisov ³⁸, L. D'Eramo ⁴¹, D. Derendarz ⁸⁸, F. Derue ¹³⁰, P. Dervan ⁹⁴, K. Desch ²⁵,
 C. Deutsch ²⁵, F.A. Di Bello ^{58b,58a}, A. Di Ciaccio ^{77a,77b}, L. Di Ciaccio ⁴,
 A. Di Domenico ^{76a,76b}, C. Di Donato ^{73a,73b}, A. Di Girolamo ³⁷, G. Di Gregorio ³⁷,
 A. Di Luca ^{79a,79b}, B. Di Micco ^{78a,78b}, R. Di Nardo ^{78a,78b}, K.F. Di Petrillo ⁴⁰,
 M. Diamantopoulou ³⁵, F.A. Dias ¹¹⁷, T. Dias Do Vale ¹⁴⁵, M.A. Diaz ^{140a,140b},
 F.G. Diaz Capriles ²⁵, A.R. Didenko ³⁹, M. Didenko ¹⁶⁶, E.B. Diehl ¹⁰⁸, S. Díez Cornell ⁴⁹,
 C. Díez Pardos ¹⁴⁴, C. Dimitriadi ¹⁶⁴, A. Dimitrievska ²¹, J. Dingfelder ²⁵, T. Dingley ¹²⁹,
 I-M. Dinu ^{28b}, S.J. Dittmeier ^{64b}, F. Dittus ³⁷, M. Divisek ¹³⁶, F. Djama ¹⁰⁴, T. Djobava ^{152b},
 C. Doglioni ^{103,100}, A. Dohnalova ^{29a}, J. Dolejsi ¹³⁶, Z. Dolezal ¹³⁶, K. Domijan ^{87a},
 K.M. Dona ⁴⁰, M. Donadelli ^{84d}, B. Dong ¹⁰⁹, J. Donini ⁴¹, A. D'Onofrio ^{73a,73b},
 M. D'Onofrio ⁹⁴, J. Dopke ¹³⁷, A. Doria ^{73a}, N. Dos Santos Fernandes ^{133a}, P. Dougan ¹⁰³,
 M.T. Dova ⁹², A.T. Doyle ⁶⁰, M.A. Dragnet ¹²⁹, E. Dreyer ¹⁷², I. Drivas-koulouris ¹⁰,
 M. Drnevich ¹²⁰, M. Drozdova ⁵⁷, D. Du ^{63a}, T.A. du Pree ¹¹⁷, F. Dubinin ³⁸, M. Dubovsky ^{29a},
 E. Duchovni ¹⁷², G. Duckeck ¹¹¹, O.A. Ducu ^{28b}, D. Duda ⁵³, A. Dudarev ³⁷, E.R. Duden ²⁷,
 M. D'uffizi ¹⁰³, L. Duflost ⁶⁷, M. Dührssen ³⁷, I. Duminica ^{28g}, A.E. Dumitriu ^{28b},
 M. Dunford ^{64a}, S. Dungs ⁵⁰, K. Dunne ^{48a,48b}, A. Duperrin ¹⁰⁴, H. Duran Yildiz ^{3a},
 M. Düren ⁵⁹, A. Durglishvili ^{152b}, B.L. Dwyer ¹¹⁸, G.I. Dyckes ^{18a}, M. Dyndal ^{87a},
 B.S. Dziedzic ³⁷, Z.O. Earnshaw ¹⁴⁹, G.H. Eberwein ¹²⁹, B. Eckerova ^{29a}, S. Eggebrecht ⁵⁶,
 E. Egidio Purcino De Souza ^{84e}, L.F. Ehrke ⁵⁷, G. Eigen ¹⁷, K. Einsweiler ^{18a}, T. Ekelof ¹⁶⁴,
 P.A. Ekman ¹⁰⁰, S. El Farkh ^{36b}, Y. El Ghazali ^{63a}, H. El Jarrari ³⁷, A. El Moussaouy ^{36a},
 V. Ellajosyula ¹⁶⁴, M. Ellert ¹⁶⁴, F. Ellinghaus ¹⁷⁴, N. Ellis ³⁷, J. Elmsheuser ³⁰, M. Elsayy ^{119a},
 M. Elsing ³⁷, D. Emelianov ¹³⁷, Y. Enari ⁸⁵, I. Ene ^{18a}, S. Epari ¹³, P.A. Erland ⁸⁸,
 D. Ernani Martins Neto ⁸⁸, M. Errenst ¹⁷⁴, M. Escalier ⁶⁷, C. Escobar ¹⁶⁶, E. Etzion ¹⁵⁴,

G. Evans [ID133a](#), H. Evans [ID69](#), L.S. Evans [ID97](#), A. Ezhilov [ID38](#), S. Ezzarqtouni [ID36a](#), F. Fabbri [ID24b,24a](#), L. Fabbri [ID24b,24a](#), G. Facini [ID98](#), V. Fadeyev [ID139](#), R.M. Fakhrutdinov [ID38](#), D. Fakoudis [ID102](#), S. Falciano [ID76a](#), L.F. Falda Ulhoa Coelho [ID37](#), F. Fallavollita [ID112](#), G. Falsetti [ID44b,44a](#), J. Faltova [ID136](#), C. Fan [ID165](#), Y. Fan [ID14](#), Y. Fang [ID14,114c](#), M. Fanti [ID72a,72b](#), M. Faraj [ID70a,70b](#), Z. Farazpay [ID99](#), A. Farbin [ID8](#), A. Farilla [ID78a](#), T. Farooque [ID109](#), S.M. Farrington [ID53](#), F. Fassi [ID36e](#), D. Fassouliotis [ID9](#), M. Faucci Giannelli [ID77a,77b](#), W.J. Fawcett [ID33](#), L. Fayard [ID67](#), P. Federic [ID136](#), P. Federicova [ID134](#), O.L. Fedin [ID38,a](#), M. Feickert [ID173](#), L. Feligioni [ID104](#), D.E. Fellers [ID126](#), C. Feng [ID63b](#), Z. Feng [ID117](#), M.J. Fenton [ID162](#), L. Ferencz [ID49](#), R.A.M. Ferguson [ID93](#), S.I. Fernandez Luengo [ID140f](#), P. Fernandez Martinez [ID13](#), M.J.V. Fernoux [ID104](#), J. Ferrando [ID93](#), A. Ferrari [ID164](#), P. Ferrari [ID117,116](#), R. Ferrari [ID74a](#), D. Ferrere [ID57](#), C. Ferretti [ID108](#), D. Fiacco [ID76a,76b](#), F. Fiedler [ID102](#), P. Fiedler [ID135](#), A. Filipčič [ID95](#), E.K. Filmer [ID1](#), F. Filthaut [ID116](#), M.C.N. Fiolhais [ID133a,133c,c](#), L. Fiorini [ID166](#), W.C. Fisher [ID109](#), T. Fitschen [ID103](#), P.M. Fitzhugh [ID138](#), I. Fleck [ID144](#), P. Fleischmann [ID108](#), T. Flick [ID174](#), M. Flores [ID34d,aa](#), L.R. Flores Castillo [ID65a](#), L. Flores Sanz De Acedo [ID37](#), F.M. Follega [ID79a,79b](#), N. Fomin [ID33](#), J.H. Foo [ID158](#), A. Formica [ID138](#), A.C. Forti [ID103](#), E. Fortin [ID37](#), A.W. Fortman [ID18a](#), M.G. Foti [ID18a](#), L. Fountas [ID9,j](#), D. Fournier [ID67](#), H. Fox [ID93](#), P. Francavilla [ID75a,75b](#), S. Francescato [ID62](#), S. Franchellucci [ID57](#), M. Franchini [ID24b,24a](#), S. Franchino [ID64a](#), D. Francis [ID37](#), L. Franco [ID116](#), V. Franco Lima [ID37](#), L. Franconi [ID49](#), M. Franklin [ID62](#), G. Frattari [ID27](#), Y.Y. Frid [ID154](#), J. Friend [ID60](#), N. Fritzsche [ID37](#), A. Froch [ID55](#), D. Froidevaux [ID37](#), J.A. Frost [ID129](#), Y. Fu [ID63a](#), S. Fuenzalida Garrido [ID140f](#), M. Fujimoto [ID104](#), K.Y. Fung [ID65a](#), E. Furtado De Simas Filho [ID84e](#), M. Furukawa [ID156](#), J. Fuster [ID166](#), A. Gaa [ID56](#), A. Gabrielli [ID24b,24a](#), A. Gabrielli [ID158](#), P. Gadow [ID37](#), G. Gagliardi [ID58b,58a](#), L.G. Gagnon [ID18a](#), S. Gaid [ID163](#), S. Galantzan [ID154](#), E.J. Gallas [ID129](#), B.J. Gallop [ID137](#), K.K. Gan [ID122](#), S. Ganguly [ID156](#), Y. Gao [ID53](#), F.M. Garay Walls [ID140a,140b](#), B. Garcia [ID30](#), C. García [ID166](#), A. Garcia Alonso [ID117](#), A.G. Garcia Caffaro [ID175](#), J.E. García Navarro [ID166](#), M. Garcia-Sciveres [ID18a](#), G.L. Gardner [ID131](#), R.W. Gardner [ID40](#), N. Garelli [ID161](#), D. Garg [ID81](#), R.B. Garg [ID146](#), J.M. Gargan [ID53](#), C.A. Garner [ID158](#), C.M. Garvey [ID34a](#), V.K. Gassmann [ID161](#), G. Gaudio [ID74a](#), V. Gautam [ID13](#), P. Gauzzi [ID76a,76b](#), J. Gavranovic [ID95](#), I.L. Gavrilenko [ID38](#), A. Gavriluk [ID38](#), C. Gay [ID167](#), G. Gaycken [ID126](#), E.N. Gazis [ID10](#), A.A. Geanta [ID28b](#), C.M. Gee [ID139](#), A. Gekow [ID122](#), C. Gemme [ID58b](#), M.H. Genest [ID61](#), A.D. Gentry [ID115](#), S. George [ID97](#), W.F. George [ID21](#), T. Geralis [ID47](#), P. Gessinger-Befurt [ID37](#), M.E. Geyik [ID174](#), M. Ghani [ID170](#), K. Ghorbanian [ID96](#), A. Ghosal [ID144](#), A. Ghosh [ID162](#), A. Ghosh [ID7](#), B. Giacobbe [ID24b](#), S. Giagu [ID76a,76b](#), T. Giani [ID117](#), A. Giannini [ID63a](#), S.M. Gibson [ID97](#), M. Gignac [ID139](#), D.T. Gil [ID87b](#), A.K. Gilbert [ID87a](#), B.J. Gilbert [ID42](#), D. Gillberg [ID35](#), G. Gilles [ID117](#), L. Ginabat [ID130](#), D.M. Gingrich [ID2,ad](#), M.P. Giordani [ID70a,70c](#), P.F. Giraud [ID138](#), G. Giugliarelli [ID70a,70c](#), D. Giugni [ID72a](#), F. Giuli [ID37](#), I. Gkialas [ID9,j](#), L.K. Gladilin [ID38](#), C. Glasman [ID101](#), G.R. Gledhill [ID126](#), G. Glemža [ID49](#), M. Glisic [ID126](#), I. Gnesi [ID44b,e](#), Y. Go [ID30](#), M. Goblirsch-Kolb [ID37](#), B. Gocke [ID50](#), D. Godin [ID110](#), B. Gokturk [ID22a](#), S. Goldfarb [ID107](#), T. Golling [ID57](#), M.G.D. Gololo [ID34g](#), D. Golubkov [ID38](#), J.P. Gombas [ID109](#), A. Gomes [ID133a,133b](#), G. Gomes Da Silva [ID144](#), A.J. Gomez Delegido [ID166](#), R. Gonçalves [ID133a](#), L. Gonella [ID21](#), A. Gongadze [ID152c](#), F. Gonnella [ID21](#), J.L. Gonski [ID146](#), R.Y. González Andana [ID53](#), S. González de la Hoz [ID166](#), R. Gonzalez Lopez [ID94](#), C. Gonzalez Renteria [ID18a](#), M.V. Gonzalez Rodrigues [ID49](#), R. Gonzalez Suarez [ID164](#), S. Gonzalez-Sevilla [ID57](#), L. Goossens [ID37](#), B. Gorini [ID37](#), E. Gorini [ID71a,71b](#), A. Gorišek [ID95](#), T.C. Gosart [ID131](#), A.T. Goshaw [ID52](#), M.I. Gostkin [ID39](#), S. Goswami [ID124](#), C.A. Gottardo [ID37](#), S.A. Gotz [ID111](#), M. Gouighri [ID36b](#), V. Goumarre [ID49](#), A.G. Goussiou [ID141](#), N. Govender [ID34c](#), R.P. Grabarczyk [ID129](#), I. Grabowska-Bold [ID87a](#), K. Graham [ID35](#), E. Gramstad [ID128](#), S. Grancagnolo [ID71a,71b](#), C.M. Grant [ID1,138](#), P.M. Gravila [ID28f](#), F.G. Gravili [ID71a,71b](#), H.M. Gray [ID18a](#), M. Greco [ID71a,71b](#), M.J. Green [ID1](#), C. Grefe [ID25](#), A.S. Grefsrud [ID17](#), I.M. Gregor [ID49](#), K.T. Greif [ID162](#), P. Grenier [ID146](#), S.G. Grewe [ID112](#), A.A. Grillo [ID139](#), K. Grimm [ID32](#), S. Grinstein [ID13,s](#), J.-F. Grivaz [ID67](#), E. Gross [ID172](#), J. Grosse-Knetter [ID56](#), J.C. Grundy [ID129](#), L. Guan [ID108](#), J.G.R. Guerrero Rojas [ID166](#),

G. Guerrieri ¹⁰², R. Gugel ¹⁰², J.A.M. Guhit ¹⁰⁸, A. Guida ¹⁹, E. Guilloton ¹⁷⁰, S. Guindon ³⁷, F. Guo ^{14,114c}, J. Guo ^{63c}, L. Guo ⁴⁹, Y. Guo ¹⁰⁸, R. Gupta ¹³², S. Gurbuz ²⁵, S.S. Gurdasani ⁵⁵, G. Gustavino ^{76a,76b}, P. Gutierrez ¹²³, L.F. Gutierrez Zagazeta ¹³¹, M. Gutsche ⁵¹, C. Gutschow ⁹⁸, C. Gwenlan ¹²⁹, C.B. Gwilliam ⁹⁴, E.S. Haaland ¹²⁸, A. Haas ¹²⁰, M. Habedank ⁴⁹, C. Haber ^{18a}, H.K. Hadavand ⁸, A. Hadeef ⁵¹, S. Hadzic ¹¹², A.I. Hagan ⁹³, J.J. Hahn ¹⁴⁴, E.H. Haines ⁹⁸, M. Haleem ¹⁶⁹, J. Haley ¹²⁴, J.J. Hall ¹⁴², G.D. Hallewell ¹⁰⁴, L. Halser ²⁰, K. Hamano ¹⁶⁸, M. Hamer ²⁵, G.N. Hamity ⁵³, E.J. Hampshire ⁹⁷, J. Han ^{63b}, K. Han ^{63a}, L. Han ^{114a}, L. Han ^{63a}, S. Han ^{18a}, Y.F. Han ¹⁵⁸, K. Hanagaki ⁸⁵, M. Hance ¹³⁹, D.A. Hangal ⁴², H. Hanif ¹⁴⁵, M.D. Hank ¹³¹, J.B. Hansen ⁴³, P.H. Hansen ⁴³, D. Harada ⁵⁷, T. Harenberg ¹⁷⁴, S. Harkusha ³⁸, M.L. Harris ¹⁰⁵, Y.T. Harris ¹²⁹, J. Harrison ¹³, N.M. Harrison ¹²², P.F. Harrison ¹⁷⁰, N.M. Hartman ¹¹², N.M. Hartmann ¹¹¹, R.Z. Hasan ^{97,137}, Y. Hasegawa ¹⁴³, F. Haslbeck ¹²⁹, S. Hassan ¹⁷, R. Hauser ¹⁰⁹, C.M. Hawkes ²¹, R.J. Hawkings ³⁷, Y. Hayashi ¹⁵⁶, D. Hayden ¹⁰⁹, C. Hayes ¹⁰⁸, R.L. Hayes ¹¹⁷, C.P. Hays ¹²⁹, J.M. Hays ⁹⁶, H.S. Hayward ⁹⁴, F. He ^{63a}, M. He ^{14,114c}, Y. He ⁴⁹, Y. He ⁹⁸, N.B. Heatley ⁹⁶, V. Hedberg ¹⁰⁰, A.L. Heggelund ¹²⁸, N.D. Hehir ^{96,*}, C. Heidegger ⁵⁵, K.K. Heidegger ⁵⁵, J. Heilman ³⁵, S. Heim ⁴⁹, T. Heim ^{18a}, J.G. Heinlein ¹³¹, J.J. Heinrich ¹²⁶, L. Heinrich ^{112,ab}, J. Hejbal ¹³⁴, A. Held ¹⁷³, S. Hellesund ¹⁷, C.M. Helling ¹⁶⁷, S. Hellman ^{48a,48b}, R.C.W. Henderson ⁹³, L. Henkelmann ³³, A.M. Henriques Correia ³⁷, H. Herde ¹⁰⁰, Y. Hernández Jiménez ¹⁴⁸, L.M. Herrmann ²⁵, T. Herrmann ⁵¹, G. Herten ⁵⁵, R. Hertenberger ¹¹¹, L. Hervas ³⁷, M.E. Hespings ¹⁰², N.P. Hessey ^{159a}, M. Hidaoui ^{36b}, N. Hidic ¹³⁶, E. Hill ¹⁵⁸, S.J. Hillier ²¹, J.R. Hinds ¹⁰⁹, F. Hinterkeuser ²⁵, M. Hirose ¹²⁷, S. Hirose ¹⁶⁰, D. Hirschbuehl ¹⁷⁴, T.G. Hitchings ¹⁰³, B. Hiti ⁹⁵, J. Hobbs ¹⁴⁸, R. Hobincu ^{28e}, N. Hod ¹⁷², M.C. Hodgkinson ¹⁴², B.H. Hodgkinson ¹²⁹, A. Hoecker ³⁷, D.D. Hofer ¹⁰⁸, J. Hofer ⁴⁹, T. Holm ²⁵, M. Holzbock ³⁷, L.B.A.H. Hommels ³³, B.P. Honan ¹⁰³, J.J. Hong ⁶⁹, J. Hong ^{63c}, T.M. Hong ¹³², B.H. Hooberman ¹⁶⁵, W.H. Hopkins ⁶, M.C. Hoppesch ¹⁶⁵, Y. Horii ¹¹³, S. Hou ¹⁵¹, A.S. Howard ⁹⁵, J. Howarth ⁶⁰, J. Hoya ⁶, M. Hrabovsky ¹²⁵, A. Hrynevich ⁴⁹, T. Hryn'ova ⁴, P.J. Hsu ⁶⁶, S.-C. Hsu ¹⁴¹, T. Hsu ⁶⁷, M. Hu ^{18a}, Q. Hu ^{63a}, S. Huang ^{65b}, X. Huang ^{14,114c}, Y. Huang ¹⁴², Y. Huang ¹⁰², Y. Huang ¹⁴, Z. Huang ¹⁰³, Z. Hubacek ¹³⁵, M. Huebner ²⁵, F. Huegging ²⁵, T.B. Huffman ¹²⁹, C.A. Hugli ⁴⁹, M. Huhtinen ³⁷, S.K. Huiberts ¹⁷, R. Hulsken ¹⁰⁶, N. Huseynov ^{12,g}, J. Huston ¹⁰⁹, J. Huth ⁶², R. Hyneman ¹⁴⁶, G. Iacobucci ⁵⁷, G. Iakovidis ³⁰, L. Iconomidou-Fayard ⁶⁷, J.P. Iddon ³⁷, P. Iengo ^{73a,73b}, R. Iguchi ¹⁵⁶, Y. Iiyama ¹⁵⁶, T. Iizawa ¹²⁹, Y. Ikegami ⁸⁵, N. Ilic ¹⁵⁸, H. Imam ^{84c}, M. Ince Lezki ⁵⁷, T. Ingebretsen Carlson ^{48a,48b}, J.M. Inglis ⁹⁶, G. Introzzi ^{74a,74b}, M. Iodice ^{78a}, V. Ippolito ^{76a,76b}, R.K. Irwin ⁹⁴, M. Ishino ¹⁵⁶, W. Islam ¹⁷³, C. Issever ^{19,49}, S. Istin ^{22a,ah}, H. Ito ¹⁷¹, R. Iuppa ^{79a,79b}, A. Ivina ¹⁷², J.M. Izen ⁴⁶, V. Izzo ^{73a}, P. Jacka ¹³⁴, P. Jackson ¹, C.S. Jagfeld ¹¹¹, G. Jain ^{159a}, P. Jain ⁴⁹, K. Jakobs ⁵⁵, T. Jakoubek ¹⁷², J. Jamieson ⁶⁰, W. Jang ¹⁵⁶, M. Javurkova ¹⁰⁵, P. Jawahar ¹⁰³, L. Jeanty ¹²⁶, J. Jejelava ^{152a,z}, P. Jenni ^{55,f}, C.E. Jessiman ³⁵, C. Jia ^{63b}, J. Jia ¹⁴⁸, X. Jia ⁶², X. Jia ^{14,114c}, Z. Jia ^{114a}, C. Jiang ⁵³, S. Jiggins ⁴⁹, J. Jimenez Pena ¹³, S. Jin ^{114a}, A. Jinaru ^{28b}, O. Jinnouchi ¹⁵⁷, P. Johansson ¹⁴², K.A. Johns ⁷, J.W. Johnson ¹³⁹, F.A. Jolly ⁴⁹, D.M. Jones ¹⁴⁹, E. Jones ⁴⁹, K.S. Jones ⁸, P. Jones ³³, R.W.L. Jones ⁹³, T.J. Jones ⁹⁴, H.L. Joos ^{56,37}, R. Joshi ¹²², J. Jovicevic ¹⁶, X. Ju ^{18a}, J.J. Junggeburth ¹⁰⁵, T. Junkermann ^{64a}, A. Juste Rozas ^{13,s}, M.K. Juzek ⁸⁸, S. Kabana ^{140e}, A. Kaczmarska ⁸⁸, M. Kado ¹¹², H. Kagan ¹²², M. Kagan ¹⁴⁶, A. Kahn ¹³¹, C. Kahra ¹⁰², T. Kaji ¹⁵⁶, E. Kajomovitz ¹⁵³, N. Kakati ¹⁷², I. Kalaitzidou ⁵⁵, C.W. Kalderon ³⁰, N.J. Kang ¹³⁹, D. Kar ^{34g}, K. Karava ¹²⁹, M.J. Kareem ^{159b}, E. Karentzos ⁵⁵, O. Karkout ¹¹⁷, S.N. Karpov ³⁹, Z.M. Karpova ³⁹, V. Kartvelishvili ⁹³, A.N. Karyukhin ³⁸, E. Kasimi ¹⁵⁵,







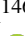

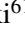

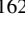






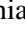


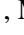


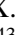


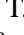



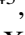
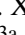

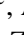


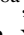

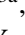
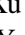
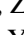




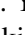
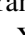

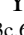


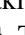





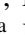


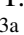











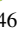


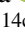

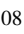
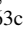
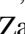
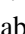
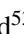


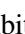


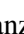











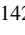
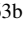



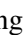
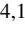
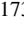
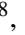

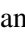

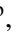
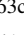

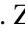
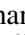

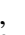
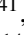
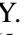
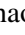


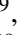
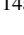
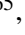
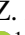
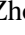

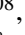
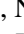
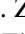



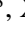
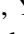
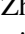












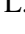



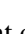


J. Katzy ⁴⁹, S. Kaur ³⁵, K. Kawade ¹⁴³, M.P. Kawale ¹²³, C. Kawamoto ⁸⁹, T. Kawamoto ^{63a}, E.F. Kay ³⁷, F.I. Kaya ¹⁶¹, S. Kazakos ¹⁰⁹, V.F. Kazanin ³⁸, Y. Ke ¹⁴⁸, J.M. Keaveney ^{34a}, R. Keeler ¹⁶⁸, G.V. Kehris ⁶², J.S. Keller ³⁵, A.S. Kelly ⁹⁸, J.J. Kempster ¹⁴⁹, P.D. Kennedy ¹⁰², O. Kepka ¹³⁴, B.P. Kerridge ¹³⁷, S. Kersten ¹⁷⁴, B.P. Kerševan ⁹⁵, L. Keszeghova ^{29a}, S. Ketabchi Haghighat ¹⁵⁸, R.A. Khan ¹³², A. Khanov ¹²⁴, A.G. Kharlamov ³⁸, T. Kharlamova ³⁸, E.E. Khoda ¹⁴¹, M. Kholodenko ^{133a}, T.J. Khoo ¹⁹, G. Khoriauli ¹⁶⁹, J. Khubua ^{152b}, Y.A.R. Khwaira ¹³⁰, B. Kibirige ^{34g}, D. Kim ⁶, D.W. Kim ^{48a,48b}, Y.K. Kim ⁴⁰, N. Kimura ⁹⁸, M.K. Kingston ⁵⁶, A. Kirchhoff ⁵⁶, C. Kirfel ²⁵, F. Kirfel ²⁵, J. Kirk ¹³⁷, A.E. Kiryunin ¹¹², C. Kitsaki ¹⁰, O. Kivernyk ²⁵, M. Klassen ¹⁶¹, C. Klein ³⁵, L. Klein ¹⁶⁹, M.H. Klein ⁴⁵, S.B. Klein ⁵⁷, U. Klein ⁹⁴, P. Klimek ³⁷, A. Klimentov ³⁰, T. Klioutchnikova ³⁷, P. Kluit ¹¹⁷, S. Kluth ¹¹², E. Kneringer ⁸⁰, T.M. Knight ¹⁵⁸, A. Knue ⁵⁰, D. Kobylanski ¹⁷², S.F. Koch ¹²⁹, M. Kocian ¹⁴⁶, P. Kodyš ¹³⁶, D.M. Koeck ¹²⁶, P.T. Koenig ²⁵, T. Koffas ³⁵, O. Kolay ⁵¹, I. Koletsou ⁴, T. Komarek ⁸⁸, K. Köneke ⁵⁵, A.X.Y. Kong ¹, T. Kono ¹²¹, N. Konstantinidis ⁹⁸, P. Kontaxakis ⁵⁷, B. Konya ¹⁰⁰, R. Kopeliansky ⁴², S. Koperny ^{87a}, K. Korcyl ⁸⁸, K. Kordas ^{155,d}, A. Korn ⁹⁸, S. Korn ⁵⁶, I. Korolkov ¹³, N. Korotkova ³⁸, B. Kortman ¹¹⁷, O. Kortner ¹¹², S. Kortner ¹¹², W.H. Kostecka ¹¹⁸, V.V. Kostyukhin ¹⁴⁴, A. Kotsokechagia ³⁷, A. Kotwal ⁵², A. Koulouris ³⁷, A. Kourkoumeli-Charalampidi ^{74a,74b}, C. Kourkoumelis ⁹, E. Kourlitis ^{112,ab}, O. Kovanda ¹²⁶, R. Kowalewski ¹⁶⁸, W. Kozanecki ¹³⁸, A.S. Kozhin ³⁸, V.A. Kramarenko ³⁸, G. Kramberger ⁹⁵, P. Kramer ¹⁰², M.W. Krasny ¹³⁰, A. Krasznahorkay ³⁷, A.C. Kraus ¹¹⁸, J.W. Kraus ¹⁷⁴, J.A. Kremer ⁴⁹, T. Kresse ⁵¹, L. Kretschmann ¹⁷⁴, J. Kretschmar ⁹⁴, K. Kreul ¹⁹, P. Krieger ¹⁵⁸, M. Krivos ¹³⁶, K. Krizka ²¹, K. Kroeninger ⁵⁰, H. Kroha ¹¹², J. Kroll ¹³⁴, J. Kroll ¹³¹, K.S. Krowpman ¹⁰⁹, U. Kruchonak ³⁹, H. Krüger ²⁵, N. Krumnack ⁸², M.C. Kruse ⁵², O. Kuchinskaja ³⁸, S. Kuday ^{3a}, S. Kuehn ³⁷, R. Kuesters ⁵⁵, T. Kuhl ⁴⁹, V. Kukhtin ³⁹, Y. Kulchitsky ^{38,a}, S. Kuleshov ^{140d,140b}, M. Kumar ^{34g}, N. Kumari ⁴⁹, P. Kumari ^{159b}, A. Kupco ¹³⁴, T. Kupfer ⁵⁰, A. Kupich ³⁸, O. Kuprash ⁵⁵, H. Kurashige ⁸⁶, L.L. Kurchaninov ^{159a}, O. Kurdysh ⁶⁷, Y.A. Kurochkin ³⁸, A. Kurova ³⁸, M. Kuze ¹⁵⁷, A.K. Kvam ¹⁰⁵, J. Kvita ¹²⁵, T. Kwan ¹⁰⁶, N.G. Kyriacou ¹⁰⁸, L.A.O. Laatu ¹⁰⁴, C. Lacasta ¹⁶⁶, F. Lacava ^{76a,76b}, H. Lacker ¹⁹, D. Lacour ¹³⁰, N.N. Lad ⁹⁸, E. Ladygin ³⁹, A. Lafarge ⁴¹, B. Laforge ¹³⁰, T. Lagouri ¹⁷⁵, F.Z. Lahbabi ^{36a}, S. Lai ⁵⁶, J.E. Lambert ¹⁶⁸, S. Lammers ⁶⁹, W. Lampl ⁷, C. Lampoudis ^{155,d}, G. Lamprinoudis ¹⁰², A.N. Lancaster ¹¹⁸, E. Lançon ³⁰, U. Landgraf ⁵⁵, M.P.J. Landon ⁹⁶, V.S. Lang ⁵⁵, O.K.B. Langrekken ¹²⁸, A.J. Lankford ¹⁶², F. Lanni ³⁷, K. Lantzsch ²⁵, A. Lanza ^{74a}, J.F. Laporte ¹³⁸, T. Lari ^{72a}, F. Lasagni Manghi ^{24b}, M. Lassnig ³⁷, V. Latonova ¹³⁴, A. Laurier ¹⁵³, S.D. Lawlor ¹⁴², Z. Lawrence ¹⁰³, R. Lazaridou ¹⁷⁰, M. Lazzaroni ^{72a,72b}, B. Le ¹⁰³, E.M. Le Boulicaut ⁵², L.T. Le Pottier ^{18a}, B. Leban ^{24b,24a}, A. Lebedev ⁸², M. LeBlanc ¹⁰³, F. Ledroit-Guillon ⁶¹, S.C. Lee ¹⁵¹, S. Lee ^{48a,48b}, T.F. Lee ⁹⁴, L.L. Leeuw ^{34c}, H.P. Lefebvre ⁹⁷, M. Lefebvre ¹⁶⁸, C. Leggett ^{18a}, G. Lehmann Miotto ³⁷, M. Leigh ⁵⁷, W.A. Leight ¹⁰⁵, W. Leinonen ¹¹⁶, A. Leisos ^{155,r}, M.A.L. Leite ^{84c}, C.E. Leitgeb ¹⁹, R. Leitner ¹³⁶, K.J.C. Leney ⁴⁵, T. Lenz ²⁵, S. Leone ^{75a}, C. Leonidopoulos ⁵³, A. Leopold ¹⁴⁷, R. Les ¹⁰⁹, C.G. Lester ³³, M. Levchenko ³⁸, J. Levêque ⁴, L.J. Levinson ¹⁷², G. Levrini ^{24b,24a}, M.P. Lewicki ⁸⁸, C. Lewis ¹⁴¹, D.J. Lewis ⁴, A. Li ⁵, B. Li ^{63b}, C. Li ^{63a}, C-Q. Li ¹¹², H. Li ^{63a}, H. Li ^{63b}, H. Li ^{114a}, H. Li ¹⁵, H. Li ^{63b}, J. Li ^{63c}, K. Li ¹⁴¹, L. Li ^{63c}, M. Li ^{14,114c}, S. Li ^{14,114c}, S. Li ^{63d,63c}, T. Li ⁵, X. Li ¹⁰⁶, Z. Li ¹²⁹, Z. Li ¹⁵⁶, Z. Li ^{14,114c}, Z. Li ^{63a}, S. Liang ^{14,114c}, Z. Liang ¹⁴, M. Liberatore ¹³⁸, B. Liberti ^{77a}, K. Lie ^{65c}, J. Lieber Marin ^{84e}, H. Lien ⁶⁹, H. Lin ¹⁰⁸, K. Lin ¹⁰⁹, R.E. Lindley ⁷, J.H. Lindon ², J. Ling ⁶², E. Lipeles ¹³¹, A. Lipniacka ¹⁷, A. Lister ¹⁶⁷, J.D. Little ⁶⁹, B. Liu ¹⁴, B.X. Liu ^{114b}, D. Liu ^{63d,63c}, E.H.L. Liu ²¹, J.B. Liu ^{63a}, J.K.K. Liu ³³, K. Liu ^{63d}, K. Liu ^{63d,63c}, M. Liu ^{63a}, M.Y. Liu ^{63a},

P. Liu ¹⁴, Q. Liu ^{63d,141,63c}, X. Liu ^{63a}, X. Liu ^{63b}, Y. Liu ^{114b,114c}, Y.L. Liu ^{63b}, Y.W. Liu ^{63a},
 S.L. Lloyd ⁹⁶, E.M. Lobodzinska ⁴⁹, P. Loch ⁷, T. Lohse ¹⁹, K. Lohwasser ¹⁴², E. Loiacono ⁴⁹,
 M. Lokajicek ^{134,*}, J.D. Lomas ²¹, J.D. Long ¹⁶⁵, I. Longarini ¹⁶², R. Longo ¹⁶⁵,
 I. Lopez Paz ⁶⁸, A. Lopez Solis ⁴⁹, N.A. Lopez-canelas ⁷, N. Lorenzo Martinez ⁴, A.M. Lory ¹¹¹,
 M. Losada ^{119a}, G. Löschke Centeno ¹⁴⁹, O. Loseva ³⁸, X. Lou ^{48a,48b}, X. Lou ^{14,114c},
 A. Lounis ⁶⁷, P.A. Love ⁹³, G. Lu ^{14,114c}, M. Lu ⁶⁷, S. Lu ¹³¹, Y.J. Lu ⁶⁶, H.J. Lubatti ¹⁴¹,
 C. Luci ^{76a,76b}, F.L. Lucio Alves ^{114a}, F. Luehring ⁶⁹, I. Luise ¹⁴⁸, O. Lukianchuk ⁶⁷,
 O. Lundberg ¹⁴⁷, B. Lund-Jensen ^{147,*}, N.A. Luongo ⁶, M.S. Lutz ³⁷, A.B. Lux ²⁶, D. Lynn ³⁰,
 R. Lysak ¹³⁴, E. Lytken ¹⁰⁰, V. Lyubushkin ³⁹, T. Lyubushkina ³⁹, M.M. Lyukova ¹⁴⁸,
 M.Firdaus M. Soberi ⁵³, H. Ma ³⁰, K. Ma ^{63a}, L.L. Ma ^{63b}, W. Ma ^{63a}, Y. Ma ¹²⁴,
 J.C. MacDonald ¹⁰², P.C. Machado De Abreu Farias ^{84e}, R. Madar ⁴¹, T. Madula ⁹⁸, J. Maeda ⁸⁶,
 T. Maeno ³⁰, H. Maguire ¹⁴², V. Maiboroda ¹³⁸, A. Maio ^{133a,133b,133d}, K. Maj ^{87a},
 O. Majersky ⁴⁹, S. Majewski ¹²⁶, N. Makovec ⁶⁷, V. Maksimovic ¹⁶, B. Malaescu ¹³⁰,
 Pa. Malecki ⁸⁸, V.P. Maleev ³⁸, F. Malek ^{61,n}, M. Mali ⁹⁵, D. Malito ⁹⁷, U. Mallik ⁸¹,
 S. Maltezos¹⁰, S. Malyukov³⁹, J. Mamuzic ¹³, G. Mancini ⁵⁴, M.N. Mancini ²⁷, G. Manco ^{74a,74b},
 J.P. Mandalia ⁹⁶, S.S. Mandarray ¹⁴⁹, I. Mandić ⁹⁵, L. Manhaes de Andrade Filho ^{84a},
 I.M. Maniatis ¹⁷², J. Manjarres Ramos ⁹¹, D.C. Mankad ¹⁷², A. Mann ¹¹¹, S. Manzoni ³⁷,
 L. Mao ^{63c}, X. Mapekula ^{34c}, A. Marantis ^{155,r}, G. Marchiori ⁵, M. Marcisovsky ¹³⁴,
 C. Marcon ^{72a}, M. Marinescu ²¹, S. Marium ⁴⁹, M. Marjanovic ¹²³, A. Markhoos ⁵⁵,
 M. Markovitch ⁶⁷, E.J. Marshall ⁹³, Z. Marshall ^{18a}, S. Marti-Garcia ¹⁶⁶, J. Martin ⁹⁸,
 T.A. Martin ¹³⁷, V.J. Martin ⁵³, B. Martin dit Latour ¹⁷, L. Martinelli ^{76a,76b}, M. Martinez ^{13,s},
 P. Martinez Agullo ¹⁶⁶, V.I. Martinez Outschoorn ¹⁰⁵, P. Martinez Suarez ¹³, S. Martin-Haugh ¹³⁷,
 G. Martinovicova ¹³⁶, V.S. Martoiu ^{28b}, A.C. Martyniuk ⁹⁸, A. Marzin ³⁷, D. Mascione ^{79a,79b},
 L. Masetti ¹⁰², J. Masik ¹⁰³, A.L. Maslennikov ³⁸, P. Massarotti ^{73a,73b}, P. Mastrandrea ^{75a,75b},
 A. Mastroberardino ^{44b,44a}, T. Masubuchi ¹²⁷, T. Mathisen ¹⁶⁴, J. Matousek ¹³⁶, J. Maurer ^{28b},
 A.J. Maury ⁶⁷, B. Maček ⁹⁵, D.A. Maximov ³⁸, A.E. May ¹⁰³, R. Mazini ¹⁵¹, I. Maznas ¹¹⁸,
 M. Mazza ¹⁰⁹, S.M. Mazza ¹³⁹, E. Mazzeo ^{72a,72b}, C. Mc Ginn ³⁰, J.P. Mc Gowan ¹⁶⁸,
 S.P. Mc Kee ¹⁰⁸, C.C. McCracken ¹⁶⁷, E.F. McDonald ¹⁰⁷, A.E. McDougall ¹¹⁷,
 J.A. Mcfayden ¹⁴⁹, R.P. McGovern ¹³¹, R.P. McKenzie ^{34g}, T.C. McLachlan ⁴⁹, D.J. McLaughlin ⁹⁸,
 S.J. McMahon ¹³⁷, C.M. Mcpartland ⁹⁴, R.A. McPherson ^{168,w}, S. Mehlhase ¹¹¹, A. Mehta ⁹⁴,
 D. Melini ¹⁶⁶, B.R. Mellado Garcia ^{34g}, A.H. Melo ⁵⁶, F. Meloni ⁴⁹,
 A.M. Mendes Jacques Da Costa ¹⁰³, H.Y. Meng ¹⁵⁸, L. Meng ⁹³, S. Menke ¹¹², M. Mentink ³⁷,
 E. Meoni ^{44b,44a}, G. Mercado ¹¹⁸, S. Merianos ¹⁵⁵, C. Merlassino ^{70a,70c}, L. Merola ^{73a,73b},
 C. Meroni ^{72a,72b}, J. Metcalfe ⁶, A.S. Mete ⁶, E. Meuser ¹⁰², C. Meyer ⁶⁹, J-P. Meyer ¹³⁸,
 R.P. Middleton ¹³⁷, L. Mijović ⁵³, G. Mikenberg ¹⁷², M. Mikestikova ¹³⁴, M. Mikuž ⁹⁵,
 H. Mildner ¹⁰², A. Milic ³⁷, D.W. Miller ⁴⁰, E.H. Miller ¹⁴⁶, L.S. Miller ³⁵, A. Milov ¹⁷²,
 D.A. Milstead^{48a,48b}, T. Min^{114a}, A.A. Minaenko ³⁸, I.A. Minashvili ^{152b}, L. Mince ⁶⁰,
 A.I. Mincer ¹²⁰, B. Mindur ^{37a}, M. Mineev ³⁹, Y. Mino ⁸⁹, L.M. Mir ¹³, M. Miralles Lopez ⁶⁰,
 M. Mironova ^{18a}, M.C. Missio ¹¹⁶, A. Mitra ¹⁷⁰, V.A. Mitsou ¹⁶⁶, Y. Mitsumori ¹¹³, O. Miu ¹⁵⁸,
 P.S. Miyagawa ⁹⁶, T. Mkrtchyan ^{64a}, M. Mlinarevic ⁹⁸, T. Mlinarevic ⁹⁸, M. Mlynarikova ³⁷,
 S. Mobius ²⁰, P. Mogg ¹¹¹, M.H. Mohamed Farook ¹¹⁵, A.F. Mohammed ^{14,114c}, S. Mohapatra ⁴²,
 G. Mokgatitwane ^{34g}, L. Moleri ¹⁷², B. Mondal ¹⁴⁴, S. Mondal ¹³⁵, K. Mönig ⁴⁹,
 E. Monnier ¹⁰⁴, L. Monsonis Romero¹⁶⁶, J. Montejo Berlingen ¹³, A. Montella ^{48a,48b},
 M. Montella ¹²², F. Montekali ^{78a,78b}, F. Monticelli ⁹², S. Monzani ^{70a,70c}, A. Morancho Tarda ⁴³,
 N. Morange ⁶⁷, A.L. Moreira De Carvalho ⁴⁹, M. Moreno Llácer ¹⁶⁶, C. Moreno Martinez ⁵⁷,
 P. Morettini ^{58b}, S. Morgenstern ³⁷, M. Morii ⁶², M. Morinaga ¹⁵⁶, F. Morodei ^{76a,76b},
 L. Morvaj ³⁷, P. Moschovakos ³⁷, B. Moser ¹²⁹, M. Mosidze ^{152b}, T. Moskalets ⁴⁵,

P. Moskvitina ¹¹⁶, J. Moss ^{32,k}, P. Moszkowicz ^{87a}, A. Moussa ^{36d}, E.J.W. Moyses ¹⁰⁵,
 O. Mtintsilana ^{34g}, S. Muanza ¹⁰⁴, J. Mueller ¹³², D. Muenstermann ⁹³, R. Müller ³⁷,
 G.A. Mullier ¹⁶⁴, A.J. Mullin³³, J.J. Mullin¹³¹, D.P. Mungo ¹⁵⁸, D. Munoz Perez ¹⁶⁶,
 F.J. Munoz Sanchez ¹⁰³, M. Murin ¹⁰³, W.J. Murray ^{170,137}, M. Muškinja ⁹⁵, C. Mwewa ³⁰,
 A.G. Myagkov ^{38,a}, A.J. Myers ⁸, G. Myers ¹⁰⁸, M. Myska ¹³⁵, B.P. Nachman ^{18a},
 O. Nackenhorst ⁵⁰, K. Nagai ¹²⁹, K. Nagano ⁸⁵, J.L. Nagle ^{30,af}, E. Nagy ¹⁰⁴, A.M. Nairz ³⁷,
 Y. Nakahama ⁸⁵, K. Nakamura ⁸⁵, K. Nakkalil ⁵, H. Nanjo ¹²⁷, E.A. Narayanan ¹¹⁵,
 I. Naryshkin ³⁸, L. Nasella ^{72a,72b}, M. Naseri ³⁵, S. Nasri ^{119b}, C. Nass ²⁵, G. Navarro ^{23a},
 J. Navarro-Gonzalez ¹⁶⁶, R. Nayak ¹⁵⁴, A. Nayaz ¹⁹, P.Y. Nechaeva ³⁸, S. Nechaeva ^{24b,24a},
 F. Nechansky ⁴⁹, L. Nedic ¹²⁹, T.J. Neep ²¹, A. Negri ^{74a,74b}, M. Negrini ^{24b}, C. Nellist ¹¹⁷,
 C. Nelson ¹⁰⁶, K. Nelson ¹⁰⁸, S. Nemecek ¹³⁴, M. Nessi ^{37,h}, M.S. Neubauer ¹⁶⁵, F. Neuhaus ¹⁰²,
 J. Neundorf ⁴⁹, P.R. Newman ²¹, C.W. Ng ¹³², Y.W.Y. Ng ⁴⁹, B. Ngair ^{119a}, H.D.N. Nguyen ¹¹⁰,
 R.B. Nickerson ¹²⁹, R. Nicolaidou ¹³⁸, J. Nielsen ¹³⁹, M. Niemeyer ⁵⁶, J. Niermann ⁵⁶,
 N. Nikiforou ³⁷, V. Nikolaenko ^{38,a}, I. Nikolic-Audit ¹³⁰, K. Nikolopoulos ²¹, P. Nilsson ³⁰,
 I. Ninca ⁴⁹, G. Ninio ¹⁵⁴, A. Nisati ^{76a}, N. Nishu ², R. Nisius ¹¹², J-E. Nitschke ⁵¹,
 E.K. Nkadimeng ^{34g}, T. Nobe ¹⁵⁶, T. Nommensen ¹⁵⁰, M.B. Norfolk ¹⁴², B.J. Norman ³⁵,
 M. Noury ^{36a}, J. Novak ⁹⁵, T. Novak ⁹⁵, L. Novotny ¹³⁵, R. Novotny ¹¹⁵, L. Nozka ¹²⁵,
 K. Ntekas ¹⁶², N.M.J. Nunes De Moura Junior ^{84b}, J. Ocariz ¹³⁰, A. Ochi ⁸⁶, I. Ochoa ^{133a},
 S. Oerde ^{49,t}, J.T. Offermann ⁴⁰, A. Ogrodnik ¹³⁶, A. Oh ¹⁰³, C.C. Ohm ¹⁴⁷, H. Oide ⁸⁵,
 R. Oishi ¹⁵⁶, M.L. Ojeda ⁴⁹, Y. Okumura ¹⁵⁶, L.F. Oleiro Seabra ^{133a}, I. Oleksiyuk ⁵⁷,
 S.A. Olivares Pino ^{140d}, G. Oliveira Correa ¹³, D. Oliveira Damazio ³⁰, J.L. Oliver ¹⁶²,
 Ö.O. Öncel ⁵⁵, A.P. O'Neill ²⁰, A. Onofre ^{133a,133e}, P.U.E. Onyisi ¹¹, M.J. Oreglia ⁴⁰,
 G.E. Orellana ⁹², D. Orestano ^{78a,78b}, N. Orlando ¹³, R.S. Orr ¹⁵⁸, L.M. Osojnak ¹³¹,
 R. Ospanov ^{63a}, G. Otero y Garzon ³¹, H. Otono ⁹⁰, P.S. Ott ^{64a}, G.J. Ottino ^{18a}, M. Ouchrif ^{36d},
 F. Ould-Saada ¹²⁸, T. Ovsiannikova ¹⁴¹, M. Owen ⁶⁰, R.E. Owen ¹³⁷, V.E. Ozcan ^{22a},
 F. Ozturk ⁸⁸, N. Ozturk ⁸, S. Ozturk ⁸³, H.A. Pacey ¹²⁹, A. Pacheco Pages ¹³,
 C. Padilla Aranda ¹³, G. Padovano ^{76a,76b}, S. Pagan Griso ^{18a}, G. Palacino ⁶⁹, A. Palazzo ^{71a,71b},
 J. Pampel ²⁵, J. Pan ¹⁷⁵, T. Pan ^{65a}, D.K. Panchal ¹¹, C.E. Pandini ¹¹⁷, J.G. Panduro Vazquez ¹³⁷,
 H.D. Pandya ¹, H. Pang ¹⁵, P. Pani ⁴⁹, G. Panizzo ^{70a,70c}, L. Panwar ¹³⁰, L. Paolozzi ⁵⁷,
 S. Parajuli ¹⁶⁵, A. Paramonov ⁶, C. Paraskevopoulos ⁵⁴, D. Paredes Hernandez ^{65b},
 A. Pareti ^{74a,74b}, K.R. Park ⁴², T.H. Park ¹⁵⁸, M.A. Parker ³³, F. Parodi ^{58b,58a}, E.W. Parrish ¹¹⁸,
 V.A. Parrish ⁵³, J.A. Parsons ⁴², U. Parzefall ⁵⁵, B. Pascual Dias ¹¹⁰, L. Pascual Dominguez ¹⁰¹,
 E. Pasqualucci ^{76a}, S. Passaggio ^{58b}, F. Pastore ⁹⁷, P. Patel ⁸⁸, U.M. Patel ⁵², J.R. Pater ¹⁰³,
 T. Pauly ³⁷, C.I. Pazos ¹⁶¹, J. Pearkes ¹⁴⁶, M. Pedersen ¹²⁸, R. Pedro ^{133a}, S.V. Peleganchuk ³⁸,
 O. Penc ³⁷, E.A. Pender ⁵³, G.D. Penn ¹⁷⁵, K.E. Penski ¹¹¹, M. Penzin ³⁸, B.S. Peralva ^{84d},
 A.P. Pereira Peixoto ¹⁴¹, L. Pereira Sanchez ¹⁴⁶, D.V. Perepelitsa ^{30,af}, G. Perera ¹⁰⁵,
 E. Perez Codina ^{159a}, M. Perganti ¹⁰, H. Pernegger ³⁷, S. Perrella ^{76a,76b}, O. Perrin ⁴¹,
 K. Peters ⁴⁹, R.F.Y. Peters ¹⁰³, B.A. Petersen ³⁷, T.C. Petersen ⁴³, E. Petit ¹⁰⁴, V. Petousis ¹³⁵,
 C. Petridou ^{155,d}, T. Petru ¹³⁶, A. Petrukhin ¹⁴⁴, M. Pettee ^{18a}, A. Petukhov ³⁸, K. Petukhova ³⁷,
 R. Pezoa ^{140f}, L. Pezzotti ³⁷, G. Pezzullo ¹⁷⁵, T.M. Pham ¹⁷³, T. Pham ¹⁰⁷, P.W. Phillips ¹³⁷,
 G. Piacquadio ¹⁴⁸, E. Pianori ^{18a}, F. Piazza ¹²⁶, R. Piegai ³¹, D. Pietreanu ^{28b},
 A.D. Pilkington ¹⁰³, M. Pinamonti ^{70a,70c}, J.L. Pinfeld ², B.C. Pinheiro Pereira ^{133a},
 A.E. Pinto Pinoargote ^{138,138}, L. Pintucci ^{70a,70c}, K.M. Piper ¹⁴⁹, A. Pirttikoski ⁵⁷, D.A. Pizzi ³⁵,
 L. Pizzimento ^{65b}, A. Pizzini ¹¹⁷, M.-A. Pleier ³⁰, V. Pleskot ¹³⁶, E. Plotnikova³⁹, G. Poddar ⁹⁶,
 R. Poettgen ¹⁰⁰, L. Poggioli ¹³⁰, I. Pokharel ⁵⁶, S. Polacek ¹³⁶, G. Polesello ^{74a},
 A. Poley ^{145,159a}, A. Polini ^{24b}, C.S. Pollard ¹⁷⁰, Z.B. Pollock ¹²², E. Pompa Pacchi ^{76a,76b},
 N.I. Pond ⁹⁸, D. Ponomarenko ¹¹⁶, L. Pontecorvo ³⁷, S. Popa ^{28a}, G.A. Popeneciu ^{28d},

A. Poreba ³⁷, D.M. Portillo Quintero ^{159a}, S. Pospisil ¹³⁵, M.A. Postill ¹⁴², P. Postolache ^{28c},
 K. Potamianos ¹⁷⁰, P.A. Potepa ^{87a}, I.N. Potrap ³⁹, C.J. Potter ³³, H. Potti ¹⁵⁰, J. Poveda ¹⁶⁶,
 M.E. Pozo Astigarraga ³⁷, A. Prades Ibanez ^{77a,77b}, J. Pretel ¹⁶⁸, D. Price ¹⁰³, M. Primavera ^{71a},
 L. Primomo ^{70a,70c}, M.A. Principe Martin ¹⁰¹, R. Privara ¹²⁵, T. Procter ⁶⁰, M.L. Proffitt ¹⁴¹,
 N. Proklova ¹³¹, K. Prokofiev ^{65c}, G. Proto ¹¹², J. Proudfoot ⁶, M. Przybycien ^{87a},
 W.W. Przygoda ^{87b}, A. Psallidas ⁴⁷, J.E. Puddefoot ¹⁴², D. Pudzha ⁵⁵, D. Pyatiizbyantseva ³⁸,
 J. Qian ¹⁰⁸, D. Qichen ¹⁰³, Y. Qin ¹³, T. Qiu ⁵³, A. Quadt ⁵⁶, M. Queitsch-Maitland ¹⁰³,
 G. Quetant ⁵⁷, R.P. Quinn ¹⁶⁷, G. Rabanal Bolanos ⁶², D. Rafanoharana ⁵⁵, F. Raffaelli ^{77a,77b},
 F. Ragusa ^{72a,72b}, J.L. Rainbolt ⁴⁰, J.A. Raine ⁵⁷, S. Rajagopalan ³⁰, E. Ramakoti ³⁸,
 L. Rambelli ^{58b,58a}, I.A. Ramirez-Berend ³⁵, K. Ran ^{49,114c}, D.S. Rankin ¹³¹, N.P. Rapheeha ^{34g},
 H. Rasheed ^{28b}, V. Raskina ¹³⁰, D.F. Rassloff ^{64a}, A. Rastogi ^{18a}, S. Rave ¹⁰², S. Ravera ^{58b,58a},
 B. Ravina ⁵⁶, I. Ravinovich ¹⁷², M. Raymond ³⁷, A.L. Read ¹²⁸, N.P. Readioff ¹⁴²,
 D.M. Rebuzzi ^{74a,74b}, G. Redlinger ³⁰, A.S. Reed ¹¹², K. Reeves ²⁷, J.A. Reidelsturz ¹⁷⁴,
 D. Reikher ¹²⁶, A. Rej ⁵⁰, C. Rembser ³⁷, M. Renda ^{28b}, F. Renner ⁴⁹, A.G. Rennie ¹⁶²,
 A.L. Rescia ⁴⁹, S. Resconi ^{72a}, M. Ressegotti ^{58b,58a}, S. Rettie ³⁷, J.G. Reyes Rivera ¹⁰⁹,
 E. Reynolds ^{18a}, O.L. Rezanova ³⁸, P. Reznicek ¹³⁶, H. Riani ^{36d}, N. Ribaric ⁹³, E. Ricci ^{79a,79b},
 R. Richter ¹¹², S. Richter ^{48a,48b}, E. Richter-Was ^{87b}, M. Ridel ¹³⁰, S. Ridouani ^{36d}, P. Rieck ¹²⁰,
 P. Riedler ³⁷, E.M. Riefel ^{48a,48b}, J.O. Rieger ¹¹⁷, M. Rijssenbeek ¹⁴⁸, M. Rimoldi ³⁷,
 L. Rinaldi ^{24b,24a}, P. Rincke ^{56,164}, T.T. Rinn ³⁰, M.P. Rinnagel ¹¹¹, G. Ripellino ¹⁶⁴, I. Riu ¹³,
 J.C. Rivera Vergara ¹⁶⁸, F. Rizatdinova ¹²⁴, E. Rizvi ⁹⁶, B.R. Roberts ^{18a}, S.S. Roberts ¹³⁹,
 S.H. Robertson ^{106,w}, D. Robinson ³³, M. Robles Manzano ¹⁰², A. Robson ⁶⁰, A. Rocchi ^{77a,77b},
 C. Roda ^{75a,75b}, S. Rodriguez Bosca ³⁷, Y. Rodriguez Garcia ^{23a}, A. Rodriguez Rodriguez ⁵⁵,
 A.M. Rodríguez Vera ¹¹⁸, S. Roe ³⁷, J.T. Roemer ³⁷, A.R. Roepe-Gier ¹³⁹, O. Røhne ¹²⁸,
 R.A. Rojas ¹⁰⁵, C.P.A. Roland ¹³⁰, J. Roloff ³⁰, A. Romaniouk ³⁸, E. Romano ^{74a,74b},
 M. Romano ^{24b}, A.C. Romero Hernandez ¹⁶⁵, N. Rompotis ⁹⁴, L. Roos ¹³⁰, S. Rosati ^{76a},
 B.J. Rosser ⁴⁰, E. Rossi ¹²⁹, E. Rossi ^{73a,73b}, L.P. Rossi ⁶², L. Rossini ⁵⁵, R. Rosten ¹²²,
 M. Rotaru ^{28b}, B. Rottler ⁵⁵, C. Rougier ⁹¹, D. Rousseau ⁶⁷, D. Rousso ⁴⁹, A. Roy ¹⁶⁵,
 S. Roy-Garand ¹⁵⁸, A. Rozanov ¹⁰⁴, Z.M.A. Rozario ⁶⁰, Y. Rozen ¹⁵³, A. Rubio Jimenez ¹⁶⁶,
 A.J. Ruby ⁹⁴, V.H. Ruelas Rivera ¹⁹, T.A. Ruggeri ¹, A. Ruggiero ¹²⁹, A. Ruiz-Martinez ¹⁶⁶,
 A. Rummler ³⁷, Z. Rurikova ⁵⁵, N.A. Rusakovich ³⁹, H.L. Russell ¹⁶⁸, G. Russo ^{76a,76b},
 J.P. Rutherford ⁷, S. Rutherford Colmenares ³³, M. Rybar ¹³⁶, E.B. Rye ¹²⁸, A. Ryzhov ⁴⁵,
 J.A. Sabater Iglesias ⁵⁷, H.F.W. Sadrozinski ¹³⁹, F. Safai Tehrani ^{76a}, B. Safarzadeh Samani ¹³⁷,
 S. Saha ¹, M. Sahinsoy ⁸³, A. Saibel ¹⁶⁶, M. Saimpert ¹³⁸, M. Saito ¹⁵⁶, T. Saito ¹⁵⁶,
 A. Sala ^{72a,72b}, D. Salamani ³⁷, A. Salnikov ¹⁴⁶, J. Salt ¹⁶⁶, A. Salvador Salas ¹⁵⁴,
 D. Salvatore ^{44b,44a}, F. Salvatore ¹⁴⁹, A. Salzburger ³⁷, D. Sammel ⁵⁵, E. Sampson ⁹³,
 D. Sampsonidis ^{155,d}, D. Sampsonidou ¹²⁶, J. Sánchez ¹⁶⁶, V. Sanchez Sebastian ¹⁶⁶,
 H. Sandaker ¹²⁸, C.O. Sander ⁴⁹, J.A. Sandesara ¹⁰⁵, M. Sandhoff ¹⁷⁴, C. Sandoval ^{23b},
 L. Sanfilippo ^{64a}, D.P.C. Sankey ¹³⁷, T. Sano ⁸⁹, A. Sansoni ⁵⁴, L. Santi ^{37,76b}, C. Santoni ⁴¹,
 H. Santos ^{133a,133b}, A. Santra ¹⁷², E. Sanzani ^{24b,24a}, K.A. Saoucha ¹⁶³, J.G. Saraiva ^{133a,133d},
 J. Sardain ⁷, O. Sasaki ⁸⁵, K. Sato ¹⁶⁰, C. Sauer ^{64b}, E. Sauvan ⁴, P. Savard ^{158,ad}, R. Sawada ¹⁵⁶,
 C. Sawyer ¹³⁷, L. Sawyer ⁹⁹, C. Sbarra ^{24b}, A. Sbrizzi ^{24b,24a}, T. Scanlon ⁹⁸,
 J. Schaarschmidt ¹⁴¹, U. Schäfer ¹⁰², A.C. Schaffer ^{67,45}, D. Schaile ¹¹¹, R.D. Schamberger ¹⁴⁸,
 C. Scharf ¹⁹, M.M. Schefer ²⁰, V.A. Schegelsky ³⁸, D. Scheirich ¹³⁶, M. Schernau ¹⁶²,
 C. Scheulen ⁵⁶, C. Schiavi ^{58b,58a}, M. Schioppa ^{44b,44a}, B. Schlag ^{146,m}, K.E. Schleicher ⁵⁵,
 S. Schlenker ³⁷, J. Schmeing ¹⁷⁴, M.A. Schmidt ¹⁷⁴, K. Schmieden ¹⁰², C. Schmitt ¹⁰²,
 N. Schmitt ¹⁰², S. Schmitt ⁴⁹, L. Schoeffel ¹³⁸, A. Schoening ^{64b}, P.G. Scholer ³⁵, E. Schopf ¹²⁹,
 M. Schott ²⁵, J. Schovancova ³⁷, S. Schramm ⁵⁷, T. Schroer ⁵⁷, H-C. Schultz-Coulon ^{64a},

M. Schumacher ^{id55}, B.A. Schumm ^{id139}, Ph. Schune ^{id138}, A.J. Schuy ^{id141}, H.R. Schwartz ^{id139},
A. Schwartzman ^{id146}, T.A. Schwarz ^{id108}, Ph. Schwemling ^{id138}, R. Schwienhorst ^{id109},
F.G. Sciacca ^{id20}, A. Sciandra ^{id30}, G. Sciolla ^{id27}, F. Scuri ^{id75a}, C.D. Sebastiani ^{id94}, K. Sedlaczek ^{id118},
S.C. Seidel ^{id115}, A. Seiden ^{id139}, B.D. Seidlitz ^{id42}, C. Seitz ^{id49}, J.M. Seixas ^{id84b}, G. Sekhniaidze ^{id73a},
L. Selem ^{id61}, N. Semprini-Cesari ^{id24b,24a}, D. Sengupta ^{id57}, V. Senthilkumar ^{id166}, L. Serin ^{id67},
M. Sessa ^{id77a,77b}, H. Severini ^{id123}, F. Sforza ^{id58b,58a}, A. Sfyrla ^{id57}, Q. Sha ^{id14}, E. Shabalina ^{id56},
A.H. Shah ^{id33}, R. Shaheen ^{id147}, J.D. Shahinian ^{id131}, D. Shaked Renous ^{id172}, L.Y. Shan ^{id14},
M. Shapiro ^{id18a}, A. Sharma ^{id37}, A.S. Sharma ^{id167}, P. Sharma ^{id81}, P.B. Shatalov ^{id38}, K. Shaw ^{id149},
S.M. Shaw ^{id103}, Q. Shen ^{id63c}, D.J. Sheppard ^{id145}, P. Sherwood ^{id98}, L. Shi ^{id98}, X. Shi ^{id14},
S. Shimizu ^{id85}, C.O. Shimmin ^{id175}, J.D. Shinner ^{id97}, I.P.J. Shipsey ^{id129}, S. Shirabe ^{id90},
M. Shiyakova ^{id39,u}, M.J. Shochet ^{id40}, D.R. Shope ^{id128}, B. Shrestha ^{id123}, S. Shrestha ^{id122,ag},
M.J. Shroff ^{id168}, P. Sicho ^{id134}, A.M. Sickles ^{id165}, E. Sideras Haddad ^{id34g}, A.C. Sidley ^{id117},
A. Sidoti ^{id24b}, F. Siegert ^{id51}, Dj. Sijacki ^{id16}, F. Sili ^{id92}, J.M. Silva ^{id53}, I. Silva Ferreira ^{id84b},
M.V. Silva Oliveira ^{id30}, S.B. Silverstein ^{id48a}, S. Simion ^{id67}, R. Simoniello ^{id37}, E.L. Simpson ^{id103},
H. Simpson ^{id149}, L.R. Simpson ^{id108}, N.D. Simpson ^{id100}, S. Simsek ^{id83}, S. Sindhu ^{id56}, P. Sinervo ^{id158},
S. Singh ^{id158}, S. Sinha ^{id49}, S. Sinha ^{id103}, M. Sioli ^{id24b,24a}, I. Siral ^{id37}, E. Sitnikova ^{id49},
J. Sjölin ^{id48a,48b}, A. Skaf ^{id56}, E. Skorda ^{id21}, P. Skubic ^{id123}, M. Slawinska ^{id88}, V. Smakhtin ^{id172},
B.H. Smart ^{id137}, S.Yu. Smirnov ^{id38}, Y. Smirnov ^{id38}, L.N. Smirnova ^{id38,a}, O. Smirnova ^{id100},
A.C. Smith ^{id42}, D.R. Smith ^{id162}, E.A. Smith ^{id40}, H.A. Smith ^{id129}, J.L. Smith ^{id103}, R. Smith ^{id146},
M. Smizanska ^{id93}, K. Smolek ^{id135}, A.A. Snesev ^{id38}, S.R. Snider ^{id158}, H.L. Snoek ^{id117},
S. Snyder ^{id30}, R. Sobie ^{id168,w}, A. Soffer ^{id154}, C.A. Solans Sanchez ^{id37}, E.Yu. Soldatov ^{id38},
U. Soldevila ^{id166}, A.A. Solodkov ^{id38}, S. Solomon ^{id27}, A. Soloshenko ^{id39}, K. Solovieva ^{id55},
O.V. Solovyanov ^{id41}, P. Sommer ^{id51}, A. Sonay ^{id13}, W.Y. Song ^{id159b}, A. Sopczak ^{id135}, A.L. Soppio ^{id98},
F. Sopkova ^{id29b}, J.D. Sorenson ^{id115}, I.R. Sotarriva Alvarez ^{id157}, V. Sothilingam ^{id64a},
O.J. Soto Sandoval ^{id140c,140b}, S. Sottocornola ^{id69}, R. Soualah ^{id163}, Z. Soumami ^{id36e}, D. South ^{id49},
N. Soybelman ^{id172}, S. Spagnolo ^{id71a,71b}, M. Spalla ^{id112}, D. Sperlich ^{id55}, G. Spigo ^{id37},
B. Spisso ^{id73a,73b}, D.P. Spiteri ^{id60}, M. Spousta ^{id136}, E.J. Staats ^{id35}, R. Stamen ^{id64a}, A. Stampekis ^{id21},
M. Standke ^{id25}, E. Stanecka ^{id88}, W. Stanek-Maslouska ^{id49}, M.V. Stange ^{id51}, B. Stanislaus ^{id18a},
M.M. Stanitzki ^{id49}, B. Stapf ^{id49}, E.A. Starchenko ^{id38}, G.H. Stark ^{id139}, J. Stark ^{id91}, P. Staroba ^{id134},
P. Starovoitov ^{id64a}, S. Stärz ^{id106}, R. Staszewski ^{id88}, G. Stavropoulos ^{id47}, P. Steinberg ^{id30},
B. Stelzer ^{id145,159a}, H.J. Stelzer ^{id132}, O. Stelzer-Chilton ^{id159a}, H. Stenzel ^{id59}, T.J. Stevenson ^{id149},
G.A. Stewart ^{id37}, J.R. Stewart ^{id124}, M.C. Stockton ^{id37}, G. Stoicea ^{id28b}, M. Stolarski ^{id133a},
S. Stonjek ^{id112}, A. Straessner ^{id51}, J. Strandberg ^{id147}, S. Strandberg ^{id48a,48b}, M. Stratmann ^{id174},
M. Strauss ^{id123}, T. Strebler ^{id104}, P. Strizenc ^{id29b}, R. Ströhmer ^{id169}, D.M. Strom ^{id126},
R. Stroynowski ^{id45}, A. Strubig ^{id48a,48b}, S.A. Stucci ^{id30}, B. Stugu ^{id17}, J. Stupak ^{id123}, N.A. Styles ^{id49},
D. Su ^{id146}, S. Su ^{id63a}, W. Su ^{id63d}, X. Su ^{id63a}, D. Suchy ^{id29a}, K. Sugizaki ^{id156}, V.V. Sulin ^{id38},
M.J. Sullivan ^{id94}, D.M.S. Sultan ^{id129}, L. Sultanaliyeva ^{id38}, S. Sultansoy ^{id3b}, T. Sumida ^{id89},
S. Sun ^{id173}, O. Sunneborn Gudnadottir ^{id164}, N. Sur ^{id104}, M.R. Sutton ^{id149}, H. Suzuki ^{id160},
M. Svatos ^{id134}, M. Swiatlowski ^{id159a}, T. Swirski ^{id169}, I. Sykora ^{id29a}, M. Sykora ^{id136}, T. Sykora ^{id136},
D. Ta ^{id102}, K. Tackmann ^{id49,t}, A. Taffard ^{id162}, R. Tafirout ^{id159a}, J.S. Tafoya Vargas ^{id67}, Y. Takubo ^{id85},
M. Talby ^{id104}, A.A. Talyshv ^{id38}, K.C. Tam ^{id65b}, N.M. Tamir ^{id154}, A. Tanaka ^{id156}, J. Tanaka ^{id156},
R. Tanaka ^{id67}, M. Tanasini ^{id148}, Z. Tao ^{id167}, S. Tapia Araya ^{id140f}, S. Tapprogge ^{id102},
A. Tarek Abouelfadl Mohamed ^{id109}, S. Tarem ^{id153}, K. Tariq ^{id14}, G. Tarna ^{id28b}, G.F. Tartarelli ^{id72a},
M.J. Tartarin ^{id91}, P. Tas ^{id136}, M. Tasevsky ^{id134}, E. Tassi ^{id44b,44a}, A.C. Tate ^{id165}, G. Tateno ^{id156},
Y. Tayalati ^{id36e,v}, G.N. Taylor ^{id107}, W. Taylor ^{id159b}, R. Teixeira De Lima ^{id146}, P. Teixeira-Dias ^{id97},
J.J. Teoh ^{id158}, K. Terashi ^{id156}, J. Terron ^{id101}, S. Terzo ^{id13}, M. Testa ^{id54}, R.J. Teuscher ^{id158,w},
A. Thaler ^{id80}, O. Theiner ^{id57}, N. Themistokleous ^{id53}, T. Theveneaux-Pelzer ^{id104}, O. Thielmann ^{id174},

B.J. Wilson , P.J. Windischhofer , F.I. Winkel , F. Winklmeier , B.T. Winter , J.K. Winter , M. Wittgen , M. Wobisch , T. Wojtkowski , Z. Wolffs , J. Wollrath , M.W. Wolter , H. Wolters , M.C. Wong , E.L. Woodward , S.D. Worm , B.K. Wosiek , K.W. Woźniak , S. Wozniowski , K. Wraight , C. Wu , M. Wu , M. Wu , S.L. Wu , X. Wu , Y. Wu , Z. Wu , J. Wuerzinger , T.R. Wyatt , B.M. Wynne , S. Xella , L. Xia , M. Xia , M. Xie , S. Xin , A. Xiong , J. Xiong , D. Xu , H. Xu , L. Xu , R. Xu , T. Xu , Y. Xu , Z. Xu , Z. Xu , B. Yabsley , S. Yacoob , Y. Yamaguchi , E. Yamashita , H. Yamauchi , T. Yamazaki , Y. Yamazaki , J. Yan , S. Yan , Z. Yan , H.J. Yang , H.T. Yang , S. Yang , T. Yang , X. Yang , X. Yang , Y. Yang , Y. Yang , Z. Yang , W.-M. Yao , H. Ye , H. Ye , J. Ye , S. Ye , X. Ye , Y. Yeh , I. Yeletsikh , B.K. Yeo , M.R. Yexley , T.P. Yildirim , P. Yin , K. Yorita , S. Younas , C.J.S. Young , C. Young , C. Yu , Y. Yu , J. Yuan , M. Yuan , R. Yuan , L. Yue , M. Zaazoua , B. Zabinski , E. Zaid , Z.K. Zak , T. Zakareishvili , S. Zambito , J.A. Zamora Saa , J. Zang , D. Zanzi , O. Zaplatilek , C. Zeitnitz , H. Zeng , J.C. Zeng , D.T. Zenger Jr , O. Zenin , T. Ženiš , S. Zenz , S. Zerradi , D. Zerwas , M. Zhai , D.F. Zhang , J. Zhang , J. Zhang , K. Zhang , L. Zhang , L. Zhang , P. Zhang , R. Zhang , S. Zhang , S. Zhang , T. Zhang , X. Zhang , X. Zhang , Y. Zhang , Y. Zhang , Y. Zhang , Z. Zhang , Z. Zhang , Z. Zhang , H. Zhao , T. Zhao , Y. Zhao , Z. Zhao , Z. Zhao , A. Zhemchugov , J. Zheng , K. Zheng , X. Zheng , Z. Zheng , D. Zhong , B. Zhou , H. Zhou , N. Zhou , Y. Zhou , Y. Zhou , C.G. Zhu , J. Zhu , X. Zhu , Y. Zhu , Y. Zhu , X. Zhuang , K. Zhukov , N.I. Zimine , J. Zinsser , M. Ziolkowski , L. Živković , A. Zoccoli , K. Zoch , T.G. Zorbas , O. Zormpa , W. Zou , L. Zwalinski .

¹Department of Physics, University of Adelaide, Adelaide; Australia.

²Department of Physics, University of Alberta, Edmonton AB; Canada.

³(^a)Department of Physics, Ankara University, Ankara; (^b)Division of Physics, TOBB University of Economics and Technology, Ankara; Türkiye.

⁴LAPP, Université Savoie Mont Blanc, CNRS/IN2P3, Annecy; France.

⁵APC, Université Paris Cité, CNRS/IN2P3, Paris; France.

⁶High Energy Physics Division, Argonne National Laboratory, Argonne IL; United States of America.

⁷Department of Physics, University of Arizona, Tucson AZ; United States of America.

⁸Department of Physics, University of Texas at Arlington, Arlington TX; United States of America.

⁹Physics Department, National and Kapodistrian University of Athens, Athens; Greece.

¹⁰Physics Department, National Technical University of Athens, Zografou; Greece.

¹¹Department of Physics, University of Texas at Austin, Austin TX; United States of America.

¹²Institute of Physics, Azerbaijan Academy of Sciences, Baku; Azerbaijan.

¹³Institut de Física d'Altes Energies (IFAE), Barcelona Institute of Science and Technology, Barcelona; Spain.

¹⁴Institute of High Energy Physics, Chinese Academy of Sciences, Beijing; China.

¹⁵Physics Department, Tsinghua University, Beijing; China.

¹⁶Institute of Physics, University of Belgrade, Belgrade; Serbia.

¹⁷Department for Physics and Technology, University of Bergen, Bergen; Norway.

¹⁸(^a)Physics Division, Lawrence Berkeley National Laboratory, Berkeley CA; (^b)University of California,

Berkeley CA; United States of America.

¹⁹Institut für Physik, Humboldt Universität zu Berlin, Berlin; Germany.

²⁰Albert Einstein Center for Fundamental Physics and Laboratory for High Energy Physics, University of Bern, Bern; Switzerland.

²¹School of Physics and Astronomy, University of Birmingham, Birmingham; United Kingdom.

²²(^a)Department of Physics, Bogazici University, Istanbul; (^b)Department of Physics Engineering, Gaziantep University, Gaziantep; (^c)Department of Physics, Istanbul University, Istanbul; Türkiye.

²³(^a)Facultad de Ciencias y Centro de Investigaciones, Universidad Antonio Nariño,

Bogotá; (^b)Departamento de Física, Universidad Nacional de Colombia, Bogotá; Colombia.

²⁴(^a)Dipartimento di Fisica e Astronomia A. Righi, Università di Bologna, Bologna; (^b)INFN Sezione di Bologna; Italy.

²⁵Physikalisches Institut, Universität Bonn, Bonn; Germany.

²⁶Department of Physics, Boston University, Boston MA; United States of America.

²⁷Department of Physics, Brandeis University, Waltham MA; United States of America.

²⁸(^a)Transilvania University of Brasov, Brasov; (^b)Horia Hulubei National Institute of Physics and Nuclear Engineering, Bucharest; (^c)Department of Physics, Alexandru Ioan Cuza University of Iasi, Iasi; (^d)National Institute for Research and Development of Isotopic and Molecular Technologies, Physics Department, Cluj-Napoca; (^e)National University of Science and Technology Politehnica, Bucharest; (^f)West University in Timisoara, Timisoara; (^g)Faculty of Physics, University of Bucharest, Bucharest; Romania.

²⁹(^a)Faculty of Mathematics, Physics and Informatics, Comenius University, Bratislava; (^b)Department of Subnuclear Physics, Institute of Experimental Physics of the Slovak Academy of Sciences, Kosice; Slovak Republic.

³⁰Physics Department, Brookhaven National Laboratory, Upton NY; United States of America.

³¹Universidad de Buenos Aires, Facultad de Ciencias Exactas y Naturales, Departamento de Física, y CONICET, Instituto de Física de Buenos Aires (IFIBA), Buenos Aires; Argentina.

³²California State University, CA; United States of America.

³³Cavendish Laboratory, University of Cambridge, Cambridge; United Kingdom.

³⁴(^a)Department of Physics, University of Cape Town, Cape Town; (^b)iThemba Labs, Western

Cape; (^c)Department of Mechanical Engineering Science, University of Johannesburg,

Johannesburg; (^d)National Institute of Physics, University of the Philippines Diliman

(Philippines); (^e)University of South Africa, Department of Physics, Pretoria; (^f)University of Zululand,

KwaDlangezwa; (^g)School of Physics, University of the Witwatersrand, Johannesburg; South Africa.

³⁵Department of Physics, Carleton University, Ottawa ON; Canada.

³⁶(^a)Faculté des Sciences Ain Chock, Réseau Universitaire de Physique des Hautes Energies - Université Hassan II, Casablanca; (^b)Faculté des Sciences, Université Ibn-Tofail, Kénitra; (^c)Faculté des Sciences Semlalia, Université Cadi Ayyad, LPHEA-Marrakech; (^d)LPMR, Faculté des Sciences, Université Mohamed Premier, Oujda; (^e)Faculté des sciences, Université Mohammed V, Rabat; (^f)Institute of Applied Physics, Mohammed VI Polytechnic University, Ben Guerir; Morocco.

³⁷CERN, Geneva; Switzerland.

³⁸Affiliated with an institute covered by a cooperation agreement with CERN.

³⁹Affiliated with an international laboratory covered by a cooperation agreement with CERN.

⁴⁰Enrico Fermi Institute, University of Chicago, Chicago IL; United States of America.

⁴¹LPC, Université Clermont Auvergne, CNRS/IN2P3, Clermont-Ferrand; France.

⁴²Nevis Laboratory, Columbia University, Irvington NY; United States of America.

⁴³Niels Bohr Institute, University of Copenhagen, Copenhagen; Denmark.

⁴⁴(^a)Dipartimento di Fisica, Università della Calabria, Rende; (^b)INFN Gruppo Collegato di Cosenza, Laboratori Nazionali di Frascati; Italy.

- ⁴⁵Physics Department, Southern Methodist University, Dallas TX; United States of America.
- ⁴⁶Physics Department, University of Texas at Dallas, Richardson TX; United States of America.
- ⁴⁷National Centre for Scientific Research "Demokritos", Agia Paraskevi; Greece.
- ⁴⁸(^a) Department of Physics, Stockholm University; (^b) Oskar Klein Centre, Stockholm; Sweden.
- ⁴⁹Deutsches Elektronen-Synchrotron DESY, Hamburg and Zeuthen; Germany.
- ⁵⁰Fakultät Physik, Technische Universität Dortmund, Dortmund; Germany.
- ⁵¹Institut für Kern- und Teilchenphysik, Technische Universität Dresden, Dresden; Germany.
- ⁵²Department of Physics, Duke University, Durham NC; United States of America.
- ⁵³SUPA - School of Physics and Astronomy, University of Edinburgh, Edinburgh; United Kingdom.
- ⁵⁴INFN e Laboratori Nazionali di Frascati, Frascati; Italy.
- ⁵⁵Physikalisches Institut, Albert-Ludwigs-Universität Freiburg, Freiburg; Germany.
- ⁵⁶II. Physikalisches Institut, Georg-August-Universität Göttingen, Göttingen; Germany.
- ⁵⁷Département de Physique Nucléaire et Corpusculaire, Université de Genève, Genève; Switzerland.
- ⁵⁸(^a) Dipartimento di Fisica, Università di Genova, Genova; (^b) INFN Sezione di Genova; Italy.
- ⁵⁹II. Physikalisches Institut, Justus-Liebig-Universität Giessen, Giessen; Germany.
- ⁶⁰SUPA - School of Physics and Astronomy, University of Glasgow, Glasgow; United Kingdom.
- ⁶¹LPSC, Université Grenoble Alpes, CNRS/IN2P3, Grenoble INP, Grenoble; France.
- ⁶²Laboratory for Particle Physics and Cosmology, Harvard University, Cambridge MA; United States of America.
- ⁶³(^a) Department of Modern Physics and State Key Laboratory of Particle Detection and Electronics, University of Science and Technology of China, Hefei; (^b) Institute of Frontier and Interdisciplinary Science and Key Laboratory of Particle Physics and Particle Irradiation (MOE), Shandong University, Qingdao; (^c) School of Physics and Astronomy, Shanghai Jiao Tong University, Key Laboratory for Particle Astrophysics and Cosmology (MOE), SKLPPC, Shanghai; (^d) Tsung-Dao Lee Institute, Shanghai; (^e) School of Physics and Microelectronics, Zhengzhou University; China.
- ⁶⁴(^a) Kirchhoff-Institut für Physik, Ruprecht-Karls-Universität Heidelberg, Heidelberg; (^b) Physikalisches Institut, Ruprecht-Karls-Universität Heidelberg, Heidelberg; Germany.
- ⁶⁵(^a) Department of Physics, Chinese University of Hong Kong, Shatin, N.T., Hong Kong; (^b) Department of Physics, University of Hong Kong, Hong Kong; (^c) Department of Physics and Institute for Advanced Study, Hong Kong University of Science and Technology, Clear Water Bay, Kowloon, Hong Kong; China.
- ⁶⁶Department of Physics, National Tsing Hua University, Hsinchu; Taiwan.
- ⁶⁷IJCLab, Université Paris-Saclay, CNRS/IN2P3, 91405, Orsay; France.
- ⁶⁸Centro Nacional de Microelectrónica (IMB-CNM-CSIC), Barcelona; Spain.
- ⁶⁹Department of Physics, Indiana University, Bloomington IN; United States of America.
- ⁷⁰(^a) INFN Gruppo Collegato di Udine, Sezione di Trieste, Udine; (^b) ICTP, Trieste; (^c) Dipartimento Politecnico di Ingegneria e Architettura, Università di Udine, Udine; Italy.
- ⁷¹(^a) INFN Sezione di Lecce; (^b) Dipartimento di Matematica e Fisica, Università del Salento, Lecce; Italy.
- ⁷²(^a) INFN Sezione di Milano; (^b) Dipartimento di Fisica, Università di Milano, Milano; Italy.
- ⁷³(^a) INFN Sezione di Napoli; (^b) Dipartimento di Fisica, Università di Napoli, Napoli; Italy.
- ⁷⁴(^a) INFN Sezione di Pavia; (^b) Dipartimento di Fisica, Università di Pavia, Pavia; Italy.
- ⁷⁵(^a) INFN Sezione di Pisa; (^b) Dipartimento di Fisica E. Fermi, Università di Pisa, Pisa; Italy.
- ⁷⁶(^a) INFN Sezione di Roma; (^b) Dipartimento di Fisica, Sapienza Università di Roma, Roma; Italy.
- ⁷⁷(^a) INFN Sezione di Roma Tor Vergata; (^b) Dipartimento di Fisica, Università di Roma Tor Vergata, Roma; Italy.
- ⁷⁸(^a) INFN Sezione di Roma Tre; (^b) Dipartimento di Matematica e Fisica, Università Roma Tre, Roma; Italy.
- ⁷⁹(^a) INFN-TIFPA; (^b) Università degli Studi di Trento, Trento; Italy.

- ⁸⁰Universität Innsbruck, Department of Astro and Particle Physics, Innsbruck; Austria.
- ⁸¹University of Iowa, Iowa City IA; United States of America.
- ⁸²Department of Physics and Astronomy, Iowa State University, Ames IA; United States of America.
- ⁸³Istinye University, Sariyer, Istanbul; Türkiye.
- ⁸⁴(^a) Departamento de Engenharia Elétrica, Universidade Federal de Juiz de Fora (UFJF), Juiz de Fora; (^b) Universidade Federal do Rio De Janeiro COPPE/EE/IF, Rio de Janeiro; (^c) Instituto de Física, Universidade de São Paulo, São Paulo; (^d) Rio de Janeiro State University, Rio de Janeiro; (^e) Federal University of Bahia, Bahia; Brazil.
- ⁸⁵KEK, High Energy Accelerator Research Organization, Tsukuba; Japan.
- ⁸⁶Graduate School of Science, Kobe University, Kobe; Japan.
- ⁸⁷(^a) AGH University of Krakow, Faculty of Physics and Applied Computer Science, Krakow; (^b) Marian Smoluchowski Institute of Physics, Jagiellonian University, Krakow; Poland.
- ⁸⁸Institute of Nuclear Physics Polish Academy of Sciences, Krakow; Poland.
- ⁸⁹Faculty of Science, Kyoto University, Kyoto; Japan.
- ⁹⁰Research Center for Advanced Particle Physics and Department of Physics, Kyushu University, Fukuoka ; Japan.
- ⁹¹L2IT, Université de Toulouse, CNRS/IN2P3, UPS, Toulouse; France.
- ⁹²Instituto de Física La Plata, Universidad Nacional de La Plata and CONICET, La Plata; Argentina.
- ⁹³Physics Department, Lancaster University, Lancaster; United Kingdom.
- ⁹⁴Oliver Lodge Laboratory, University of Liverpool, Liverpool; United Kingdom.
- ⁹⁵Department of Experimental Particle Physics, Jožef Stefan Institute and Department of Physics, University of Ljubljana, Ljubljana; Slovenia.
- ⁹⁶School of Physics and Astronomy, Queen Mary University of London, London; United Kingdom.
- ⁹⁷Department of Physics, Royal Holloway University of London, Egham; United Kingdom.
- ⁹⁸Department of Physics and Astronomy, University College London, London; United Kingdom.
- ⁹⁹Louisiana Tech University, Ruston LA; United States of America.
- ¹⁰⁰Fysiska institutionen, Lunds universitet, Lund; Sweden.
- ¹⁰¹Departamento de Física Teórica C-15 and CIAFF, Universidad Autónoma de Madrid, Madrid; Spain.
- ¹⁰²Institut für Physik, Universität Mainz, Mainz; Germany.
- ¹⁰³School of Physics and Astronomy, University of Manchester, Manchester; United Kingdom.
- ¹⁰⁴CPPM, Aix-Marseille Université, CNRS/IN2P3, Marseille; France.
- ¹⁰⁵Department of Physics, University of Massachusetts, Amherst MA; United States of America.
- ¹⁰⁶Department of Physics, McGill University, Montreal QC; Canada.
- ¹⁰⁷School of Physics, University of Melbourne, Victoria; Australia.
- ¹⁰⁸Department of Physics, University of Michigan, Ann Arbor MI; United States of America.
- ¹⁰⁹Department of Physics and Astronomy, Michigan State University, East Lansing MI; United States of America.
- ¹¹⁰Group of Particle Physics, University of Montreal, Montreal QC; Canada.
- ¹¹¹Fakultät für Physik, Ludwig-Maximilians-Universität München, München; Germany.
- ¹¹²Max-Planck-Institut für Physik (Werner-Heisenberg-Institut), München; Germany.
- ¹¹³Graduate School of Science and Kobayashi-Maskawa Institute, Nagoya University, Nagoya; Japan.
- ¹¹⁴(^a) Department of Physics, Nanjing University, Nanjing; (^b) School of Science, Shenzhen Campus of Sun Yat-sen University; (^c) University of Chinese Academy of Science (UCAS), Beijing; China.
- ¹¹⁵Department of Physics and Astronomy, University of New Mexico, Albuquerque NM; United States of America.
- ¹¹⁶Institute for Mathematics, Astrophysics and Particle Physics, Radboud University/Nikhef, Nijmegen; Netherlands.

- ¹¹⁷Nikhef National Institute for Subatomic Physics and University of Amsterdam, Amsterdam; Netherlands.
- ¹¹⁸Department of Physics, Northern Illinois University, DeKalb IL; United States of America.
- ¹¹⁹(^a)New York University Abu Dhabi, Abu Dhabi;(^b)United Arab Emirates University, Al Ain; United Arab Emirates.
- ¹²⁰Department of Physics, New York University, New York NY; United States of America.
- ¹²¹Ochanomizu University, Otsuka, Bunkyo-ku, Tokyo; Japan.
- ¹²²Ohio State University, Columbus OH; United States of America.
- ¹²³Homer L. Dodge Department of Physics and Astronomy, University of Oklahoma, Norman OK; United States of America.
- ¹²⁴Department of Physics, Oklahoma State University, Stillwater OK; United States of America.
- ¹²⁵Palacký University, Joint Laboratory of Optics, Olomouc; Czech Republic.
- ¹²⁶Institute for Fundamental Science, University of Oregon, Eugene, OR; United States of America.
- ¹²⁷Graduate School of Science, Osaka University, Osaka; Japan.
- ¹²⁸Department of Physics, University of Oslo, Oslo; Norway.
- ¹²⁹Department of Physics, Oxford University, Oxford; United Kingdom.
- ¹³⁰LPNHE, Sorbonne Université, Université Paris Cité, CNRS/IN2P3, Paris; France.
- ¹³¹Department of Physics, University of Pennsylvania, Philadelphia PA; United States of America.
- ¹³²Department of Physics and Astronomy, University of Pittsburgh, Pittsburgh PA; United States of America.
- ¹³³(^a)Laboratório de Instrumentação e Física Experimental de Partículas - LIP, Lisboa;(^b)Departamento de Física, Faculdade de Ciências, Universidade de Lisboa, Lisboa;(^c)Departamento de Física, Universidade de Coimbra, Coimbra;(^d)Centro de Física Nuclear da Universidade de Lisboa, Lisboa;(^e)Departamento de Física, Universidade do Minho, Braga;(^f)Departamento de Física Teórica y del Cosmos, Universidad de Granada, Granada (Spain);(^g)Departamento de Física, Instituto Superior Técnico, Universidade de Lisboa, Lisboa; Portugal.
- ¹³⁴Institute of Physics of the Czech Academy of Sciences, Prague; Czech Republic.
- ¹³⁵Czech Technical University in Prague, Prague; Czech Republic.
- ¹³⁶Charles University, Faculty of Mathematics and Physics, Prague; Czech Republic.
- ¹³⁷Particle Physics Department, Rutherford Appleton Laboratory, Didcot; United Kingdom.
- ¹³⁸IRFU, CEA, Université Paris-Saclay, Gif-sur-Yvette; France.
- ¹³⁹Santa Cruz Institute for Particle Physics, University of California Santa Cruz, Santa Cruz CA; United States of America.
- ¹⁴⁰(^a)Departamento de Física, Pontificia Universidad Católica de Chile, Santiago;(^b)Millennium Institute for Subatomic physics at high energy frontier (SAPHIR), Santiago;(^c)Instituto de Investigación Multidisciplinario en Ciencia y Tecnología, y Departamento de Física, Universidad de La Serena;(^d)Universidad Andres Bello, Department of Physics, Santiago;(^e)Instituto de Alta Investigación, Universidad de Tarapacá, Arica;(^f)Departamento de Física, Universidad Técnica Federico Santa María, Valparaíso; Chile.
- ¹⁴¹Department of Physics, University of Washington, Seattle WA; United States of America.
- ¹⁴²Department of Physics and Astronomy, University of Sheffield, Sheffield; United Kingdom.
- ¹⁴³Department of Physics, Shinshu University, Nagano; Japan.
- ¹⁴⁴Department Physik, Universität Siegen, Siegen; Germany.
- ¹⁴⁵Department of Physics, Simon Fraser University, Burnaby BC; Canada.
- ¹⁴⁶SLAC National Accelerator Laboratory, Stanford CA; United States of America.
- ¹⁴⁷Department of Physics, Royal Institute of Technology, Stockholm; Sweden.
- ¹⁴⁸Departments of Physics and Astronomy, Stony Brook University, Stony Brook NY; United States of

America.

¹⁴⁹Department of Physics and Astronomy, University of Sussex, Brighton; United Kingdom.

¹⁵⁰School of Physics, University of Sydney, Sydney; Australia.

¹⁵¹Institute of Physics, Academia Sinica, Taipei; Taiwan.

¹⁵²(^a) E. Andronikashvili Institute of Physics, Iv. Javakhishvili Tbilisi State University, Tbilisi; (^b) High Energy Physics Institute, Tbilisi State University, Tbilisi; (^c) University of Georgia, Tbilisi; Georgia.

¹⁵³Department of Physics, Technion, Israel Institute of Technology, Haifa; Israel.

¹⁵⁴Raymond and Beverly Sackler School of Physics and Astronomy, Tel Aviv University, Tel Aviv; Israel.

¹⁵⁵Department of Physics, Aristotle University of Thessaloniki, Thessaloniki; Greece.

¹⁵⁶International Center for Elementary Particle Physics and Department of Physics, University of Tokyo, Tokyo; Japan.

¹⁵⁷Department of Physics, Tokyo Institute of Technology, Tokyo; Japan.

¹⁵⁸Department of Physics, University of Toronto, Toronto ON; Canada.

¹⁵⁹(^a) TRIUMF, Vancouver BC; (^b) Department of Physics and Astronomy, York University, Toronto ON; Canada.

¹⁶⁰Division of Physics and Tomonaga Center for the History of the Universe, Faculty of Pure and Applied Sciences, University of Tsukuba, Tsukuba; Japan.

¹⁶¹Department of Physics and Astronomy, Tufts University, Medford MA; United States of America.

¹⁶²Department of Physics and Astronomy, University of California Irvine, Irvine CA; United States of America.

¹⁶³University of Sharjah, Sharjah; United Arab Emirates.

¹⁶⁴Department of Physics and Astronomy, University of Uppsala, Uppsala; Sweden.

¹⁶⁵Department of Physics, University of Illinois, Urbana IL; United States of America.

¹⁶⁶Instituto de Física Corpuscular (IFIC), Centro Mixto Universidad de Valencia - CSIC, Valencia; Spain.

¹⁶⁷Department of Physics, University of British Columbia, Vancouver BC; Canada.

¹⁶⁸Department of Physics and Astronomy, University of Victoria, Victoria BC; Canada.

¹⁶⁹Fakultät für Physik und Astronomie, Julius-Maximilians-Universität Würzburg, Würzburg; Germany.

¹⁷⁰Department of Physics, University of Warwick, Coventry; United Kingdom.

¹⁷¹Waseda University, Tokyo; Japan.

¹⁷²Department of Particle Physics and Astrophysics, Weizmann Institute of Science, Rehovot; Israel.

¹⁷³Department of Physics, University of Wisconsin, Madison WI; United States of America.

¹⁷⁴Fakultät für Mathematik und Naturwissenschaften, Fachgruppe Physik, Bergische Universität Wuppertal, Wuppertal; Germany.

¹⁷⁵Department of Physics, Yale University, New Haven CT; United States of America.

^a Also Affiliated with an institute covered by a cooperation agreement with CERN.

^b Also at An-Najah National University, Nablus; Palestine.

^c Also at Borough of Manhattan Community College, City University of New York, New York NY; United States of America.

^d Also at Center for Interdisciplinary Research and Innovation (CIRI-AUTH), Thessaloniki; Greece.

^e Also at Centro Studi e Ricerche Enrico Fermi; Italy.

^f Also at CERN, Geneva; Switzerland.

^g Also at CMD-AC UNEC Research Center, Azerbaijan State University of Economics (UNEC); Azerbaijan.

^h Also at Département de Physique Nucléaire et Corpusculaire, Université de Genève, Genève; Switzerland.

ⁱ Also at Departament de Física de la Universitat Autònoma de Barcelona, Barcelona; Spain.

^j Also at Department of Financial and Management Engineering, University of the Aegean, Chios; Greece.

- k* Also at Department of Physics, California State University, Sacramento; United States of America.
- l* Also at Department of Physics, King's College London, London; United Kingdom.
- m* Also at Department of Physics, Stanford University, Stanford CA; United States of America.
- n* Also at Department of Physics, Stellenbosch University; South Africa.
- o* Also at Department of Physics, University of Fribourg, Fribourg; Switzerland.
- p* Also at Department of Physics, University of Thessaly; Greece.
- q* Also at Department of Physics, Westmont College, Santa Barbara; United States of America.
- r* Also at Hellenic Open University, Patras; Greece.
- s* Also at Institutio Catalana de Recerca i Estudis Avancats, ICREA, Barcelona; Spain.
- t* Also at Institut für Experimentalphysik, Universität Hamburg, Hamburg; Germany.
- u* Also at Institute for Nuclear Research and Nuclear Energy (INRNE) of the Bulgarian Academy of Sciences, Sofia; Bulgaria.
- v* Also at Institute of Applied Physics, Mohammed VI Polytechnic University, Ben Guerir; Morocco.
- w* Also at Institute of Particle Physics (IPP); Canada.
- x* Also at Institute of Physics and Technology, Mongolian Academy of Sciences, Ulaanbaatar; Mongolia.
- y* Also at Institute of Physics, Azerbaijan Academy of Sciences, Baku; Azerbaijan.
- z* Also at Institute of Theoretical Physics, Ilia State University, Tbilisi; Georgia.
- aa* Also at National Institute of Physics, University of the Philippines Diliman (Philippines); Philippines.
- ab* Also at Technical University of Munich, Munich; Germany.
- ac* Also at The Collaborative Innovation Center of Quantum Matter (CICQM), Beijing; China.
- ad* Also at TRIUMF, Vancouver BC; Canada.
- ae* Also at Università di Napoli Parthenope, Napoli; Italy.
- af* Also at University of Colorado Boulder, Department of Physics, Colorado; United States of America.
- ag* Also at Washington College, Chestertown, MD; United States of America.
- ah* Also at Yeditepe University, Physics Department, Istanbul; Türkiye.
- * Deceased